UNIVERSIDADE DA BEIRA INTERIOR
Ciências

Preparation, characterization and environmental applications of SnO_2-Sb_2O_x films

Dália Sofia Chasqueira dos Santos

Thesis for obtaining Ph.D. Degree in

Chemistry

(3º cycle of studies)

Supervisor: Ana Maria Carreira Lopes
Co-Supervisor: Maria de Lurdes Franco Ciríaco

Covilhã, November 2016

Dedicatory

To my family, especially to my daughter!

Acknowledgements

Financial support from ICIUBI-Santander Totta Investigação is gratefully acknowledged.

I would like to acknowledge the opportunity to develop this study in the University of Beira Interior, integrated in the Research Unit FibEnTech/MTP, which provided all the resources needed for the development of this work.

I would like to thank my supervisors Prof. Doctor Ana Maria Carreira Lopes and Prof. Doctor Maria de Lurdes Franco Ciríaco for their friendship and invaluable scientific support. I am also grateful for their continuous guidance and help, for the immense expertise and constructive discussions that were crucial for the success of this work.

I also would like to thank Prof. Doctor Maria José Pacheco for her availability and support. Her collaboration was decisive for this work.

To my laboratory colleagues, Annabel, Paulo, who shared with me my daily life along this postgraduate period, I would like to express my gratitude for their friendship, presence, patience and support.

To my grandparents, José and Maria José, without yours efforts this would not have been possible.

To my mom, my acknowledgment for making this day possible.

Finally, I am deeply grateful to Alexandre for all his love, patience and support over the past years.

Resumo alargado

O sucesso do tratamento eletroquímico de águas residuais depende de um grande número de fatores; em particular, da natureza do material do elétrodo, que influencia fortemente a eficiência do processo.

Os materiais de elétrodo são claramente um dos parâmetros mais importantes na otimização dos processos eletroquímicos. A opção por um determinado material de elétrodo é feita em função da sua zona útil de potencial na solução a utilizar. Esta zona de potenciais está limitada por diversos fatores, como a estabilidade estrutural, mecânica, química e eletroquímica do material de elétrodo, a formação na sua superfície de uma camada de uma substância isoladora (passivação), a decomposição do eletrólito suporte, etc. A durabilidade do elétrodo nas condições de trabalho, assim como o seu custo, são igualmente parâmetros a ter em conta. O material de elétrodo ideal para a degradação de poluentes orgânicos deve exibir alta atividade para a oxidação e baixa atividade perante as reações secundárias (por exemplo, evolução de oxigénio).

Este trabalho consistiu na preparação de filmes de SnO_2-SbO_x que sejam estrutural, química, mecânica e electroquimicamente estáveis; estes materiais devem ainda ter tempos de vida útil prolongados, de modo a que possam vir a ser utilizados exaustivamente na degradação de contaminantes, reduzindo assim o seu custo.

Ao longo deste trabalho, foram preparados diferentes filmes de óxidos mistos de estanho e antimónio. Um dos métodos utilizado foi a eletrodeposição em camadas alternadas de estanho e antimónio sobre um substrato. Foram testadas deposições diretas sobre o substrato de titânio ou sobre uma camada intermédia de platina ou de cobre. Estas deposições intermédias têm como objetivo otimizar o tempo de vida útil do filme de óxidos.

De seguida, e com o objetivo de obter filmes mais finos e uniformes, testou-se a eletrodeposição simultânea de Sn e Sb, tendo utilizado substratos idênticos: Ti; Ti/Pt; Ti/Cu.

Deste modo, foram preparadas vários materiais de elétrodos com base em filmes de óxidos de estanho e antimónio, usando os dois métodos de eletrodeposição diferentes e com diferentes camadas intermédias. Para todos os materiais preparados foi realizada a caracterização estrutural, morfológica e eletroquímica do elétrodo, recorrendo-se a várias técnicas, como difração de raios X, microscopia eletrónica de varrimento e voltametria cíclica.

Com estes filmes de óxidos, após a caracterização usual, foi efetuado um estudo sobre a reação de evolução de oxigénio, tendo-se determinado a energia de ativação aparente da oxidação da água em cada um dos diferentes materiais. Conclui-se ainda que o fator de rugosidade influencia profundamente a reação de evolução de oxigénio, pois o material com fator de rugosidade superior apresenta menor energia de ativação aparente para a evolução do oxigénio.

Os materiais preparados sobre substratos contendo uma camada intermédia de cobre mostraram ter apetência para a evolução do oxigénio, não podendo contudo ser usados na

degradação de poluentes orgânicos, pois este processo requer potenciais mais elevados, onde se dá a oxidação do cobre e a desativação do elétrodo.

O elétrodo Ti/Pt/SnO_2-Sb que apresentava boas características para ser utilizado em eletro-oxidação, foi utilizado na degradação de soluções de 100 mg L^{-1} de diclofenac, tendo-se obtido remoções de carga poluente de cerca de 50% ao fim de 6 h de ensaio. Para além disso, o material manteve-se e com resultados reprodutíveis ao fim de 200 h de ensaios.

O material que ao longo de todos os estudos já descritos mostrou apresentar uma maior estabilidade mecânica, química e eletroquímica, o Ti/Pt/SnO_2-Sb_2O_4, foi usado na degradação de lixiviados de aterros sanitários, que são efluentes com cargas orgânicas e inorgânicas muito elevadas. Este material foi ainda usado em amostras de efluentes simulados contendo ácido húmico e sais inorgânicos. Embora os resultados obtidos para este material em termos de remoção de carga orgânica sejam, em geral, ligeiramente inferiores aos obtidos com outros materiais de ânodo, como o diamante dopado com boro (BDD) e o Ti/Pt/PbO_2, os elétrodos de Ti/Pt/SnO_2-Sb_2O_4 provaram ser uma excelente alternativa àqueles dois materiais. Em particular, para a remoção de azoto total verifica-se que o ânodo Ti/Pt/SnO_2-Sb_2O_4 é mais eficiente do que o ânodo de BDD.

Palavras-chave

Filmes de SnO_2-Sb_2O_x; eletrodeposição; evolução de oxigénio; eletrodegradação de fármacos; diclofenac; degradação anódica; lixiviados de aterros sanitários; ácido húmico.

Abstract

In this work, SnO_2-SbO_x films were prepared over different substrates and utilizing different electrodeposition techniques for the deposition of the tin and antimony layers over the substrates, namely alternate and simultaneous depositions. All the mixed oxides prepared were structural, morphological and electrochemically characterized by, respectively, X-ray diffraction, scanning electron microscopy and cyclic voltammetry.

To obtain thinner and uniform films, Sn-Sb oxide materials were prepared using the simultaneous and alternate deposition of the metals over several different substrates, namely Ti; Ti/Pt; Ti/Cu. All these materials were fully characterized and used in a thermodynamic study to find the material most suitable for oxygen evolution. It was observed that: Materials roughness depends mainly on the substrates roughness, being Ti/Pt/SnO_2-Sb the material with higher roughness; Oxides grown on Ti/Cu substrate presented the lowest potential for oxygen evolution, particularly the material prepared by simultaneous electrodeposition of Sn and Sb; The roughness deeply influences the oxygen evolution potential.

Ti/Pt/SnO_2-Sb material, prepared by simultaneous Sn Sb electrodepositions, was utilized in a degradation study, using as model pollutant diclofenac. It was observed a good degradation rate of the diclofenac, with the electrode material presenting good mechanical, chemical and electrochemical stabilities.

From all the prepared materials, the Ti/Pt/SnO_2-Sb_2O_4 was the anode that presented more stability towards anodic oxidation, as well as the highest lifetime. For this reason, it was chosen to be used in the degradation of very complex real effluents, sanitary landfill leachates, and in the degradation of humic acid. Results were compared with other anode materials, boron-doped diamond (BDD) and Ti/Pt/PbO_2. Ti/Pt/SnO_2-Sb_2O_4 electrodes proved to be an excellent alternative to the other materials, although they were not so efficient in the removal of the organic matter. On the other hand, they were more efficient than BDD in the removal of the total nitrogen.

The exhaustive utilization of the Ti/Pt/SnO_2-Sb_2O_4 anode, even with sanitary landfill leachates at 700 A m^{-2}, has been showing that it is an excellent option to other electrode materials. However, the use of the platinization step increases its price and an alternative solution should be further attempted.

Keywords

SnO_2-Sb_2O_x films; electrodeposition; oxygen evolution; anodic degradation; electrodegradation of pharmaceutical drugs; diclofenac; sanitary landfill leachates; humic acid.

Index

List of figures

List of tables

List of symbols and acronyms

$[Cl^-]_0$	Initial chloride concentration
A	Electrode area
Abs	Absorbance
AN	Ammonia nitrogen
AO	Anodic oxidation
AOPs	Advanced oxidation processes
BDD	Boron-doped diamond
BOD_{20}	Twenty-day biochemical oxygen demand
BOD_5	Five-day biochemical oxygen demand
C	Double-layer capacitance
COD	Chemical oxygen demand
Cond.	Conductivity
CV	Ciclic voltammetry
CVD	Chemical Vapor deposition
DC	Dissolved carbon
DIC	Dissolved inorganic carbon
DOC	Dissolved organic carbon
DS	Dissolved solids
E	Potential
EAOPs	Electrochemical advanced oxidation processes
EDS	Dispersive energy spectroscopy
EO	Electrochemical oxidation
F	Faraday constant
HPLC	High-performance liquid chromatography
I	Applied current intensity
j	Current density
j_0	Exchange current density
j_{lim}	Limiting current density
MMO	Mixed metal oxide
NDIR	Non-dispersive infrared
OER	Oxygen evolution reaction
R_f	Relative roughness factor
SEM	Scanning electron microscopy
SS	Suspended solids
TKN	Total Kjeldahl nitrogen
TN	Total nitrogen
TOC	Total organic carbon
UV-vis	Ultraviolet-visible

V	Sample volume
υ	Scanning rate
XRD	X-ray powder diffraction
ΔG	Apparent activation energy
η	Overpotential

1. Introduction

This chapter presents an overview on the motivation to develop the studies involving the preparation, the characterization and the environmental applications of stannous and antimony mixed oxides. It defines also the main objectives and the strategy implemented to attain the objectives.

1.1 Environmental context

Dyes, toxic organic molecules, inorganic salts, adsorbable organohalogens, aromatic pesticide residues, drugs, and surfactants are the major components of the wastewaters released from textile, leather, pulp and paper, printing, photograph, cosmetic, pharmaceutical, and food industries [Rao *et al.*, 2014]. Wastewaters containing these chemicals are refractory and are often toxic to microorganisms involved in the biological treatment processes. Other major environmental concern are the leachates formed by the percolation of rainwater through the solid waste deposited on sanitary landfills [Fernandes *et al.*, 2015].

In order to solve the environmental problems posed by the presence of all the cited toxic substances, several methods, besides the biological processes, have been endeavoured [Sirés *et al.*, 2014]. Electrochemical degradation processes are being developed as an attempt to solve the environmental challenge posed by the effluents containing refractory substances, since they are attractive processes due to their environmental compatibility, simplicity, robustness in structure, and easy operation. Especially, electrolysis can be used as a pretreatment technology to detoxify ahead of biotreatment, rather than mineralizing completely the effluent to be treated, with high cost [Comninellis and Chen, 2010].

Although organic wastes can, in general, be oxidized at numerous electrode materials, the electrochemical efficacy depends on the kind and on the structure of the anode materials [Comninellis and Chen, 2010].

Long service lifetime, large surface area, wide operating potential window between hydrogen and oxygen evolution reaction (OER) overpotentials, high catalytic activity, physical stability, resistance to corrosion, low price, and easy to fabricate are the prerequisites to be fulfilled by the anodes employed in the electrochemical wastewater treatment [Rao *et al.*, 2014].

The use of metallic oxide electrodes (MMO) for electrocatalytic oxidation of organic pollutants is very promising. These electrodes generally consist of a titanium substrate covered with metallic oxide films, whose composition strongly affects their electrochemical behaviour. Among the metallic oxide electrodes, tin and antimony mixed oxide electrodes are one of the best candidates to be utilized as anodes for the electrochemical combustion of organic pollutants, since, in general, they present higher oxygen overpotential than other metallic

oxide electrodes, particularly when the appropriate preparation techniques are employed [Huang *et al.*, 2007]. Nevertheless, there are very few studies in the literature where this material was utilized as anode for the degradation of complex mixtures [Cossu *et al.*, 1998; Fernandes *et al.*, 2014; Fernandes *et al.*, 2016].

1.2 Global aims

The main goal of this thesis was to search for an efficient tin and antimony metal oxides material to be utilized as anode, to find suitable and low-cost electrochemical solutions for the degradation of organic pollutants and refractory wastewaters, such as pharmaceutical compounds, and refractory wastewaters, such as sanitary landfill leachates and synthetic wastewaters containing humic acid.

In this context, the objectives of this study are:

1. To prepare Sb-doped SnO_2 materials that are structural, chemical, mechanical and electrochemically stables.

2. To obtain Sb-doped SnO_2 materials with extended lifetime, suitable to be used in the degradation of organic pollutants or in the oxygen evolution reactions.

3. To find correlations between the preparation method and the abilities of the prepared material for the different possible applications, namely degradation of organic pollutants or oxygen evolution reactions.

4. To find, among all the prepared materials which is the most appropriate to be used as anode in the degradation of different types of pollutants.

1.3 Strategy

To attain the objectives defined in the previous point, the following strategy was implemented:

1. To make Sb-doped SnO_2 oxides using different preparation methods, namely alternate or simultaneously electrochemical depositions of tin and antimony layers, in order to obtain thin films with uniform surfaces, thus avoiding the interaction between the solution and the substrate or any existent interlayer.

2. To test different substrates, besides titanium, to avoid the formation of the TiO_2 passivating film. A platinum interlayer was deposited over the titanium substrate and other substrates, such as copper, were also tested.

3. To perform the structural, morphological, chemical and electrochemically characterization of the oxides, for all the new materials prepared, to assess the influence of utilizing different deposition techniques or the deposition over different substrates.

4. To perform a thermodynamic study, to evaluate some of the properties of the new materials and understand the influence of the metals deposition technique and of the substrate on that properties.

5. To utilize the prepared materials that presented the most favourable properties for the degradation of different pollutants/wastewaters.

1.4 Thesis overview

This thesis is divided into five chapters. This first chapter presents the context in which this thesis is inserted and the overall goals to attain with the studies performed. It also gives a description of the strategy to achieve the proposed objectives.

The second chapter contains a literature review on the preparation methods of tin and antimony mixed oxides and their environmental applications.

Chapter 3 presents a description of the preparation methods employed to obtain the different tin and antimony oxide materials, utilizing different metal deposition strategies and different substrates. This chapter also contains the structural and morphological characterization of the prepared materials, as well as the assessment of the relative roughness of the prepared materials, utilizing electrochemical techniques.

In Chapter 4, a thermodynamic study of the oxygen evolution reaction at the oxide anodes described in the previous chapter is presented. Chapter 4 also contains one environmental application of Ti/Pt/SnO_2-Sb anode, in the degradation of diclofenac, and two environmental studies with Ti/Pt/SnO_2-Sb_2O_4 anodes, using complex effluents, such as real leachate from sanitary landfills and simulated wastewaters, containing humic acid. At the end of both studies, the degradation efficiency of this material is compared with other reference anode materials, namely, Ti/Pt/PbO_2, and commercial boron-doped diamond (BDD) anodes.

Finally, Chapter 5 presents the main conclusions obtained in this work, as well as some proposals for future work.

2. SnO_2-Sb_2O_x films - Literature review

SnO_2 in its pure form is an n-type semiconductor, with a band gap of about 3.5 eV, which cannot be used directly as electrode material due to its high resistivity at room temperature. The conductivity, the electro-catalytic properties and the stability of the SnO_2 films can be deeply increased by the introduction of dopant ions.

Antimony is one of the most commonly used dopants in SnO_2 films, because it can reduce the band gap and increase the conductivity and the electro-catalytic activity [Comninellis and Chen, 2010]. When doped with Sb, SnO_2 electrodes present high overpotential for the oxygen evolution and electro-catalytic characteristics suitable for the oxidation of organic pollutants [Kong *et al.*, 2007].

In this chapter, a literature review on the different preparation methods of the stannous oxides, and the influence of the preparation method on the oxides properties will be first discussed. The influence of the SnO_2 doping agent on the applications of the oxides will be also assessed.

2.1 Films preparation methods

The mixed metal oxide anodes are cheap and easy to fabricate [Rao *et al.*, 2014]. Various preparation methods have been attempted to produce SnO_2-Sb_2O_x anodes. In general, these methods fall into two main groups: chemical methods, such as, thermochemical decomposition, electrodeposition, sol–gel method, spin coating, Chemical Vapor Deposition (CVD), spray pyrolysis; and physical methods, like magnetron sputtering [Chen *et al.*, 2010a; Zhang *et al.*, 2014]. However, when the objective is to prepare metal oxide anodes, the most common procedure is the layer by layer synthesis techniques, including thermochemical degradation of the support layer and electrodeposition of the active layer. This usually results in good anti-corrosion characteristics of the inner layer and good electro-catalytic of the outer layer [Wu *et al.*, 2014]. To ensure the stability of the oxides layer, it is necessary to ensure a good adhesion of this layer on the substrate. Thus, it is important to perform a pretreatment to remove grease or oxides from the surface of metal substrate, which might influence the layer adherence [Comninellis and Chen, 2010].

One of the most used substrates is titanium and many of the variations in the preparation of SnO_2 electrodes are meant to extend the lifetime of the electrode, a problem associated with the performance of the Ti/SnO_2 electrodes.

The interaction of the electrode material with the substrate may also influence the chemical adsorption and the catalytic properties of the deposited metal oxides. Several studies have concluded that Ti/SnO_2-Sb_2O_4 anodes have a short lifetime due to the formation of an intermediate layer of TiO_2 with high resistivity [Berenguer *et al.*, 2009]. This layer can be formed during the electrode preparation or during its use as anode because oxide films have a

considerable porosity. In both cases, the formation of a TiO_2 interlayer is inevitable [Chen *et al.*, 2005; Cossu *et al.*, 1998 and Stucki *et al.*, 1991a]. To avoid the formation of the TiO_2 interlayer, various attempts have been made, such as pre-platinization of the substrate, addition of an IrO_2 layer and deposition of a Cu film over the substrate [Chen *et al.*, 2005; Comninellis, 1992; Cossu *et al.*, 1998; Johnson *et al.*, 2000; Rodgers *et al.*, 1999].

In the following paragraphs, the main methods described in the literature for the preparation of metal oxide films will be discussed, giving a special emphasis to those utilized in the preparation of antimony-doped tin oxides. The influence of the preparation methods on the characteristics of the films will be considered.

2.1.1 Thermochemical decomposition

Thermochemical decomposition, or pyrolysis, is the most widely applied method for the fabrication of Sb-SnO_2-based MMO anodes or Ir- and Ru-based MMO anodes. The main advantage of this synthesis method is its easy operation. In a typical thermochemical decomposition procedure, the metal salts, in general metal chlorides, are directly dissolved. The solvent used may be isopropanol, ethanol, butanol or their mixtures. In order to avoid the hydrolysis of the metal salts, it is necessary to acidify the precursor solution by adding hydrochloric acid. The calcination temperature is also a very important factor and it plays a critical role in the electrocatalytic performance of MMO anodes [Feng, 2010; Wu *et al.*, 2014].

The MMO properties, such as, chemical composition, crystallinity and crystal grain size, surface morphology, electrical conductance, electrocatalysis performance, and electrode stability, are affected by the precursor composition, solvents and loadings, substrate pretreatment, and thermal decomposition parameters, especially the temperature and the duration of the preparation and calcinations processes [Comninellis and Chen, 2010].

In general, the Sb-SnO_2 films have a "cracked-mud" morphology, being formed by small uniform particles, and the electrode surface presents low roughness /porosity [Wu, 2014].

2.1.2 Electrodeposition

Electrodeposition is a simple and cheap method for the preparation of metal oxides, even for large-scale production [Chen *et al.*, 2010 b]. This method allows the direct deposition of the metal layer over the substrate, with a good control of the deposited amount and without needing adhesive substances to join the metal layer to the substrate [Bartlett, 2002; Chen *et al.*, 2010 b; Comninellis and Chen, 2010; Musiani, 1997].

Electrodeposition is analogous to a galvanic cell acting in reverse. To deposit a metal, the substrate can be used as anode or cathode, and both electrodes must be immersed in an electrolytic solution containing one or more dissolved metal salts. When the substrate is used as anode, the application of a direct current to the anode can oxidize the metal atoms, forming

the metal oxide. If the substrate is utilized as cathode, the dissolved metal ions in the electrolyte solution are reduced and deposited over the cathode [Musiani, 1997].

Electrochemical deposition is rather used to prepare metals and conducting metal oxide films because it presents several interesting features: the thickness and morphology of the metal oxide layer can be controlled by varying the experimental parameters and the films are uniformly deposited at good deposition rates [Comninellis and Chen, 2010; Chen, 2010b]. This film layer uniformity is very important if the films are to be used in electrodegradation studies. Other advantages of the electrodeposition technique is that it can be performed at low temperature, with trivial equipment [Comninellis and Chen, 2010].

The preparation of mixed metal oxides, like Sb-doped Sn oxides, can be prepared either by co-electrodeposition together or by a sequencing electrodeposition [Comninellis and Chen, 2010]. In general, the films obtained by electrodeposition present granular surface structure and high electrocatalytic activity [Wu *et al.*, 2014].

2.1.3 Other preparation methods

- **Sol-Gel method**

The sol-gel process is, in general, used to produce solid materials from small molecules. It can be utilized to prepare metal oxides by the conversion of monomers into a colloidal solution (sol) that acts as the precursor for an integrated network (or gel) of discrete particles or network polymers. Metal alkoxides can be used as typical precursors [Sakka, 2005; Wu *et al.*, 2014].

In general, the precursor salts are hydrolyzed, by dispersion, in appropriate media, followed by vigorous stirring. The formation of solid phase particles from hydrolyzed precursor is time dependent [Rao *et al.*, 2014; Wu *et al.*, 2014].

The sol-gel process presents several advantages, such as: it allows deposition of thin films over substrates of different shapes or areas, and the films composition can be easily controlled by controlling the homogeneity and the concentration of the solutions, without using expensive equipment [Canevari, 2011; Sakka, 2005].

The doped tin oxide films formed by sol-gel technique present heterogeneous cracked morphology. They have low impedance and very good electrocatalytic activity [Wu *et al.*, 2014].

- **Spin Coating**

The spin coating technique is the most indicated for flat substrates because it leads to very uniform coatings. For uneven substrates, dip coating or painting is preferred. In the spin coating technique, a small amount of the coating material is deposited at the center of the substrate that is rotated at high speed to spread the coating material, due to the centrifugal force. The material is then dried and the process of coating and drying is repeated until a desired thickness of the coat is obtained. Finally, the coated substrate is annealed to obtain the desired thickness

that will give the material the wanted morphological characteristics and wear resistance [Rao *et al.*, 2014].

- **Chemical Vapor Deposition**

In Chemical Vapor Deposition, generally the reactant (precursors) gases are pumped into the reaction chamber, maintained at optimum temperature and pressure, where these reactive gases are adsorbed and react with the substrate to form a thin film. Metal organic chemical vapor deposition utilizes organometallic compounds as precursors. Using this technique, thin films with high uniformity can be reproduced. However, it involves complex processes, high temperature, and toxic gases. Amjoud *et al*. (1998), Duverneuil *et al*. (2002), Yusta *et al*. (1997) and Watts *et al*. (2008) have used gas phase methods for the preparation of thin film metal oxide-coated electrodes.

CVD appears to be the least attempted chemical method for preparing MMO anodes, due to its high operation cost and the difficulty in introducing several metal precursors in the furnace [Rao *et al.*, 2014; Wu *et al.*, 2014].

The films prepared by this technique present dense, homogeneous surface with high roughness [Wu *et al.*, 2014].

Recently, Ti/SnO_2 anodes were prepared by chemical vapor deposition without O_2 as a precursor, H_20 as a precursor was used, avoiding the formation of the TiO_2 passivation layer. These electrodes presented a compact microstructure with high overpotential for oxygen evolution and a superior activity for pollutant oxidation. Although a higher surface area should lead to improved catalytic properties in this electrode (as in BDD) prepared by CVD, the surface area was smaller than when prepared by conventional methods, but the catalytic properties were still improved.

- **Spray Pyrolysis**

Spray pyrolysis is an aerosol process, relatively simple and cost effective. It involves the atomization of the precursors in the form of droplets and the conversion of these droplets into solid particles by heating. The nature of the deposit obtained on the substrate is dependent on the transformations suffered by the droplets. There are several parameters influencing the transformations experienced by the droplets, namely, the temperature gradient between the spraying nozzle and the substrate, the carrier gas and precursor solution flow velocity, and shape and nature of the substrate [Rao *et al.*, 2014].

- **Magnetron Sputtering**

In the basic sputtering process, a target (or cathode) plate is bombarded by energetic ions generated in a glow discharge plasma, located in front of the target. The bombardment process causes the removal, i.e., “sputtering”, of target atoms, which may then condense on a substrate as a thin film.

Secondary electrons are also emitted from the target surface as a result of the ion bombardment, and these electrons play an important role in maintaining the plasma. The basic sputtering process has been known for many years and many materials have been successfully deposited using this technique [Kelly and Arnell, 2000].

The sputtering method presents several advantages, namely high adhesion of films, facility of sputtering any metal, alloy or compound, high-purity films, ability to coat heat-sensitive substrates, and excellent uniformity on large-area substrates, which explains the numerous applications of the sputtered films [Barrocas *et al.*, 2013].

2.2 Applications of SnO_2-Sb_2O_x films

There are a multitude of examples in the literature about possible applications of antimony-doped tin oxides [Lan *et al.*, 2015; Mueller *et al.*, 2015]. However, as this study was mainly focused on environmental applications and water oxidation using SbSn mixed oxides, a literature review on these subjects will be presented below.

2.2.1 Environmental applications

Pollution by recalcitrant organic compounds is a significant environmental problem mainly because the most spread wastewater treatments are based on biological processes that fail in their degradation. To prevent the release of these compounds to the environment new treatment techniques to complement or even substitute the biological processes must be developed. In particular, advanced oxidation processes (AOPs), processes where there is production of OH radicals, are being under intensive study, since they can operate in an efficient and sustainable way [Chaplin, 2014; Sirés *et al.*, 2014].

Among AOPs, electrochemical advanced oxidation processes (EAOPs) have emerged as a promising technologies for the destruction of recalcitrant compounds and complex wastewaters [Chaplin, 2014; Sirés *et al.*, 2014].

The electrochemical treatment effectiveness depends on many factors, namely, on the electrode material, because its nature is determinant for the type of mechanism involved in the pollutants degradation process and strongly influences its selectivity and efficiency [Comninellis and Chen, 2010; Panizza and Cerisola, 2005].

There are several electrochemical techniques for the pollutants removal or degradation, such as electrocoagulation/flocculation, electro-Fenton, cathodic reduction, and anodic oxidation. Since the anodic oxidation was the technique utilized in this thesis for the degradation of several types of polluted wastewaters, the following paragraphs will be mainly focused on the application of this process using MMOs.

The ideal electrode material for the electro-oxidation of organic pollutants should be stable as anode in the electrolytic medium and present high activity for the oxidation of the organic matter and low activity towards secondary reactions. It should also be cheap and environmental compactible [Chen *et al.*, 2010b; Comninellis and Chen, 2010; Maharana *et al.*, 2015].

Comninellis (1994) has investigated different anode materials, namely Pt, Ti/IrO_2, and Ti/SnO_2, in the electrochemical conversion/combustion of several organic pollutants. Simplified mechanisms for electrochemical oxidation and combustion were presented, being the first step of the mechanism the discharge of water molecules to form •OH radicals:

$$MO_x + H_2O \rightarrow MO_x(\bullet OH) + H^+ + e^- \quad (1)$$

Depending on the nature of the electrode material (MO_x), selective oxidation (for ''active'' electrodes) or combustion (for ''non-active'' electrode) can occur. The Ti/SnO_2 has been considered "non-active" electrode since Sn(IV) is the highest oxidation state. This anode has high overvoltage for oxygen evolution reaction and can promote the oxidation of organic compounds by highly reactive OH radicals, generated at the electrode surface [Comninellis, 1994].

The performance of doped SnO_2 electrodes is believed to be superior to Pt, graphite, PbO_2, and many other common electrodes, due to its higher current efficiency and because the oxidation reactions on the SnO_2 electrode are very unselective, which gave to this electrode the possibility of being applied to a multitude of different wastewaters [Chen *et al.*, 2005; Comninellis and Pulgarin, 1993; Stucki *et al.*, 1991a; Stucki *et al.*, 1991b].

The anodic oxidation of phenol was performed on different electrode materials and a SnO_2–Sb_2O_5 electrode showed the highest ability to completely oxidize phenol among PbO_2, IrO_2, RuO_2, and Pt, and with a current efficiency over three times higher than for the other electrodes [Rodgers *et al.*, 1999]. In addition, the behavior of a Ti/SnO_2–Sb_2O_5 electrode in the electrodegradation of phenol in the presence of NaCl was studied and compared with that of a Ti/IrO_2 electrode, but the indirect oxidation process attributed to ClO^- was only verified with the Ti/IrO_2 electrode [Comninellis and Nerini, 1995].

Ti/SnO_2 and Ti/IrO_2 anodes were also used in the oxidation of 1,4-benzoquinone [Pulgarin *et al.*, 1994]. With Ti/IrO_2, non-toxic carboxylic acids were obtained as final products, while these carboxylic acids were oxidized to CO_2 with Ti/SnO_2.

Polcaro *et al.* in 1999 compared the performance of Sb-doped Ti/SnO_2 and Ti/PbO_2 anodes in the electrochemical degradation of 2-chlorophenol and concluded that Ti/SnO_2 presented a better ability to oxidize toxic compounds. These two electrode materials were also used in the electrochemical treatment of landfill leachate, but did not show substantial differences under the experimental conditions used, achieving a COD removal of 50% from a leachate with an initial COD of 1200 mg/L [Cossu *et al.*, 1998]. A Ti–SnO_2–Sb_2O_5 electrode, prepared by the thermal method, and a BDD electrode were used in the anodic oxidation of acetic acid, maleic acid, and phenol [Chen *et al.*, 2003]. Interestingly, the BDD electrode presented a higher

current efficiency and service-life. Furthermore, a mixed oxide electrode of Ti/SnO_2–Sb_2O_3–Nb_2O_5/PbO_2 was applied to the oxidation of phenol with good performance [Yang *et al.,* 2009]. The SnO_2–Sb_2O_3 layer was obtained by dipping and annealing at 450 ºC under an influx of oxygen, followed by Nb_2O_5/PbO_2 electrodeposition. Recently, the anodic oxidation of 4-chloro-3-methylphenol in aqueous solution using Ti/SnO_2–Sb/PbO_2 electrodes was investigated [Song *et al.*, 2010]. PbO_2 was used because it is a cheap material, easy to prepare and has low resistivity, good chemical stability and, with a SnO_2 + Sb_2O_3 interlayer, increased lifetime and electrocatalytic activity.

In another recent report in this area, Sb-doped SnO_2 electrodes were prepared by two different methods, electrodeposition followed by thermal oxidation, which gave a nanocoated material, and by a dip-coating method, where a non-nanocoated material was obtained [Liu and Feng, 2009]. When comparing the performance of both these electrodes, the nanocoated electrode gave a faster and higher phenol and TOC removals, probably due to the larger specific surface area and oxygen adsorption.

The various studies found in the literature have shown that doped Ti/SnO_2 is a very promising material for the electrodegradation of organics, due to its unselective character toward anodic oxidation and also because of its low price, especially when compared to BDD.

2.2.2 Oxygen Evolution

The anodic activity of an electrode material depends on the overpotential for oxygen evolution reaction. If the material is to be used in the production of oxygen from the water electrooxidation reaction, there are advantages in choosing materials with a low overpotential for oxygen evolution so that the energy consumption becomes lower. Additionally, at these materials, the direct anodic oxidation of pollutants occurs with high efficiency for low current densities [Armenta-Armenta and Diaz, 2005] because if the current density is high, a significant decrease in the current efficiency is expected due to oxygen evolution. However, it was observed that the electrochemical combustion of most of the organic compounds only occurs without the loss of electrode activity at anode materials presenting high overpotential for oxygen evolution [Comninellis, 1994]. According to a compilation of values for oxygen evolution overpotentials at different anode materials presented by Chen [2004] in a review paper, SnO_2 and PbO_2 anodes have similar oxygen evolution overpotentials, which are higher than that of platinum and lower than that of BDD. Thus, regarding current efficiency, SnO_2 or PbO_2 anodes are more advantageous than BDD. The anodic oxidation of pollutants is more efficient in the oxygen evolution region because, in addition to avoiding polarization of the electrode's surface, hydroxyl radicals can be produced and promote pollutant oxidation by indirect processes, although with a decrease in the current efficiency due to the competition between water/pollutant oxidation.

Although anodic oxidation is an effective technique for producing oxygen or oxidizing organic pollutants, to achieve good oxidation rates, the choice of the appropriate anode material is of

great importance, and it must possess suitable oxygen overpotential, good electrical conductivity and electrochemical and mechanical stabilities [Martínez-Huitle *et al.*, 2004; Martínez-Huitle and Andrade, 2011; Sirés and Brillas, 2012; Wu *et al.*, 2011; Zheng *et al.*, 2011]. Various electrode materials, such as platinum, carbon, BDD and metal oxides, namely PbO_2, SnO_2, RuO_2 and IrO_2, have already been studied [Ciríaco *et al.*, 2009; Panizza and Cerisola, 2004; Sirés and Brillas, 2012]. Among them, SnO_2 has been extensively tested due to its low preparation cost.

Although the increasing concern over environmental pollution brought renewed attention to research for suitable anode materials, the interest in the kinetics and mechanism of the oxygen evolution reaction in the process of the water electrolysis still remains of great importance [Villullas *et al.*, 2003]. The study of the electrocatalytic properties of electrodes coated with films of metal oxides is of fundamental importance for the understanding of their electrochemical behavior, including the Tafel slope, exchange current density, the effect of the temperature on the kinetic parameters and the apparent activation energy [Lassali *et al.*, 1999; Suffredini *et al.*, 2004; Wu *et al.*, 2011].

3. Preparation and characterization of tin and antimony mixed oxides

This chapter presents the preparation method and the results from the characterization of the Sb-doped SnO_2 films, prepared by different techniques and utilizing different substrates:

- Ti/Pt/SnO_2-Sb_2O_4, prepared by alternate electrodeposition over a platinized titanium foil;
- Ti/Cu/SnO_2-Sb_2O_3, prepared by alternate electrodeposition over a titanium foil previously recovered with a copper layer;
- Ti/SnO_2-Sb, prepared by simultaneous electrodeposition over a titanium foil;
- Ti/Pt/SnO_2-Sb, prepared by simultaneous electrodeposition over a platinized titanium foil;
- Ti/Cu/SnO_2-Sb, prepared by simultaneous electrodeposition over a titanium foil previously recovered with a copper layer.

The studies presented in this chapter were already published in specialized journals [Santos *et al.*, 2013; Santos *et al.*, 2014a].

3.1 Materials and methods

3.1.1 Reagents

In the preparation of the electrodes, the following reagents were used: titanium foil, 0.25 mm thick, 99.7%, Sigma-Aldrich; sodium hydroxide, 96.8%, Pronalab; oxalic acid, 99%, Merck; chloridric acid, 37%, Pronalab; $H_2PtCl_6.xH_2O$, 99.9%, Sigma-Aldrich; tin (II) chloride, 98%, Sigma-Aldrich; antimony (III) chloride, 99%, Fluka; citric acid, 100%, Pronalab; copper sulfate, 99%, Merck; tartaric Acid, 99.5%, Sigma-Aldrich; $Na_4P_2O_7.10H_2O$, 99%, Sigma-Aldrich; Gelatine, Merck and Sulfuric Acid, 95 to 98%, Sigma-Aldrich.

3.1.2 Characterization techniques

The electrodes were structurally characterized by X-ray powder diffraction (XRD) at room temperature using a Rigaku DMAXIII/C diffractometer with Cu Kα radiation (λ= 0.15406 nm) at 30 kV/40 mA. The diffraction patterns were collected in the range of 2θ = 10–90º with a 0.028 step and an acquisition time of 2 s per step.

The morphologies were evaluated by scanning electron microscopy (SEM) and microanalysis was performed by dispersive energy spectroscopy (EDS), in a Hitachi (S-2700)/Oxford (60–74) system, operating at 20 keV.

The electrochemical behavior was evaluated by voltammetric studies. The cyclic voltammetric measurements were performed using a potentiostat/galvanostat VoltaLab PGZ 301, in a one-compartment cell, with a 10 cm^2 doped-Sb SnO_2 electrode as the working electrode, a 5 cm^2

(per side) platinum plate as the counter electrode and a commercial saturated $Ag/AgCl,KCl_{sat}$ electrode as the reference electrode.

The relative roughness factor, R_f, of the electrodes' coating was estimated by running cyclic voltammetric curves with the prepared metal oxides as the working electrode. Because the electrodes are made of conductive oxides, the double-layer charging current, I, which is closely related to the double-layer capacitance, C, of the electrode/solution interface, is linearly dependent on the scanning rate, υ. Thus, running cyclic voltammetries at different scan rates in the potential region where only double-layer charging currents are observed, different I values can be obtained for the different scan rates, at a constant E value that is the point at which an approximate symmetry for the anodic and cathodic currents is observed. From the plot of I versus υ a linear correlation can be obtained. The slope of the obtained equation divided by the geometric area of the electrode yields the normalized capacitance of the oxide/solution interface ($C = dq/dE = dI/dυ$). To estimate the relative roughness factor of the films, the normalized capacitance is compared with that of an oxide with a smooth surface, which is assumed to be 60 $\mu F\ cm^{-2}$.

3.2 $Ti/Pt/SnO_2$-Sb_2O_4

3.2.1 Electrode preparation

Ti substrates, with dimensions of 2 cm x 2.5 cm x 0.25 mm, were pre-treated by mechanical polishing followed by etching with 40 % NaOH (w/w) at 80 ºC for 2 h and 15 % oxalic acid (w/w) at 98 ºC for 1 h. The substrates were then washed with double-distilled water. Substrate platinization was performed in a one-compartment double-walled cell connected to a thermostatic water bath, which enabled the recirculation of water at 65 ºC. The cell contained a chloroplatinic acid solution, and a current density of 250 $mA\ cm^{-2}$ was applied using the Ti substrate as the cathode and two platinum plates (8 cm^2) as anodes.

After platinization, alternate Sn and Sb electrodepositions on the Ti substrate were carried out in the same cell. For the Sn deposition, 100 mL of an aqueous solution with 0.948 g of $SnCl_2$ and 2 mL of concentrated chloridric acid was used with a current density of 10 $mA\ cm^{-2}$ maintained for 30 min at 35 ºC. For the Sb deposition, 100 mL of an aqueous solution with 1.329 g of $SbCl_3$ and 3.842 g of citric acid was used with a current density of 10 $mA\ cm^{-2}$ maintained for 10 min at 35 ºC. These two procedures were repeated 4 times.

After this treatment, the electrodes were heated in a tubular furnace at 550 ºC for 6 h, to obtain the respective oxides. The geometric area of the prepared electrodes was 10 cm^2 (both sides).

3.2.2 Characterization

- Structural Characterization by DRX

After calcination at 550 ºC, an X-ray diffractogram of the Ti/Pt/SnO_2-Sb_2O_4 electrode was obtained (Figure 1) and compared with those from the JCPDS ICDS database. The presence of the Sb_2O_4 (file PDF#11-0694, relative to an orthorhombic structure with a = 5.436 Å, b = 4.81 Å and c = 11.76 Å) and SnO_2 (file PDF # 41-1445, tetragonal structure with a = b = 4.7382 Å and c = 3.1871 Å) phases were confirmed. A platinum phase was also identified (PDF # 04-0802), probably detected due to the porosity and thickness of the material.

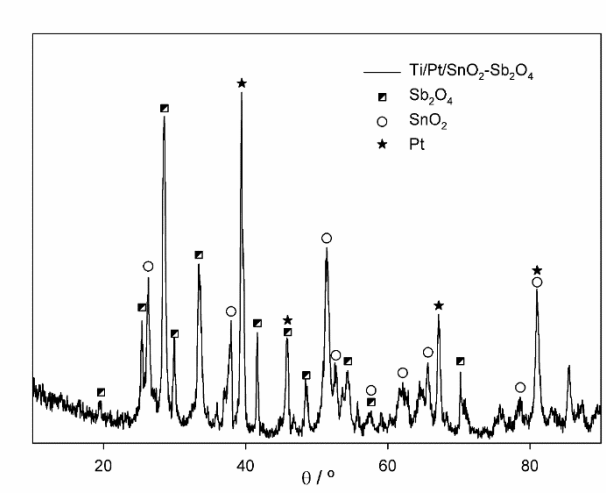

Figure 1. X-ray diffractogram of the Ti/Pt/SnO_2-Sb_2O_4 composite oxide electrode in their final form after calcination at 550 ºC.

- Morphological characterization by SEM

Morphology views of the Ti substrate (Figure 2 a), platinized (Figure 2 b) and covered with the oxides Ti/Pt/SnO_2-Sb_2O_4 electrode (Figure 3), are presented. The appearance of the Ti substrate platinized is similar to cauliflower. The morphology of the Ti/Pt/SnO_2-Sb_2O_4 electrode is quite different from that of the Ti/SnO_2-Sb_2O_4 electrodes prepared in a similar way but without platinization, which presented the characteristics of cracked mud [Andrade *et al.*, 2004; Ciríaco *et al.*, 2011; Zanta *et al.*, 2003]. In fact, the morphology views of Figure 3 show a granular morphology.

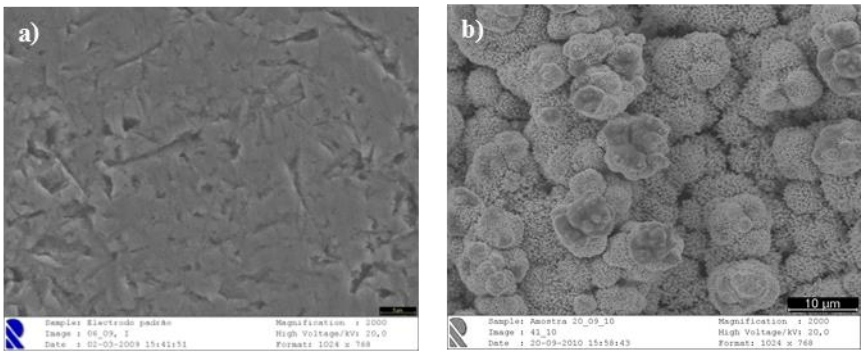

Figure 2. - Micrographs of the (a) Ti plate covered with (b) Pt. Magnifications of 2000 x top view.

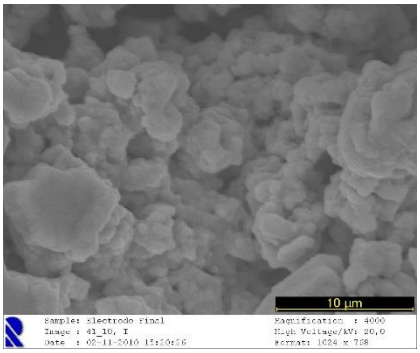

Figure 3. Micrograph of the surface of the Ti/Pt/SnO_2-Sb_2O_4: magnification 4000 x top view.

- Chemical Characterization by EDS

The results from the EDS analysis of the final stage of the Ti/Pt/SnO_2-Sb_2O_4 electrodes, in atomic molar percentages, were as follows: O - 74%, Sn - 9% and Sb - 17%. The Sb content was higher than expected, possibly because the final electrodeposited layer consists of antimony, which is more easily detected by EDS.

- Relative roughness

Figure 4 presents several cyclic voltammograms recorded at different scan rates between 2 and 50 mV s^{-1} in 0.035 M Na_2SO_4 aqueous solution from 0.6 to 0.8 V versus Ag/AgCl,KCl_{sat}. The I values for the different scan rates were obtained at E = 0.7 V versus Ag/AgCl,KCl_{sat}, the point at which an approximate symmetry for the anodic and cathodic currents was observed. From the plot of I versus υ for the Ti/Pt/SnO_2-Sb_2O_4 electrode (Figure 4 and inset), the following linear equation was obtained:

$$I\ (A) = 0.0245\ \upsilon\ (V\ s^{-1}) + 0.000068, \text{ with } r^2 = 0.997 \qquad (2)$$

Dividing the slope value by the geometric area of the electrode yields the normalized capacitance of the oxide/solution interface, $C_{Ti/Pt/SnO2\text{-}Sb2O4}$=0.00245 F cm^{-2}.

To estimate the relative roughness factor of the Ti/Pt/SnO_2–Sb_2O_4 film, its capacitance was divided by 60 μF cm^{-2}, providing an R_f of 41 for the prepared material.

In a previous work with these electrodes [Ciríaco *et al.*, 2011], which were not platinized and with 4 alternate depositions of each metal, a normalized capacitance of 0.0466 F cm^{-2} and a roughness factor of 777 were obtained; however, the deposition time for each metal was 4 times longer. The roughness factors were lower for the platinized electrode prepared in this work, likely due to the lower metal deposition time used in this case, which prevents the growth of surface imperfections and decreases the roughness factor of the films. The metal deposition time was reduced to avoid excessive imperfections, which fall into the solution and increase electrode preparation costs.

Wu and co-workers in 2008 have prepared amorphous tin oxide (SnO_x) films by cathodic deposition on graphite, achieving a specific capacitance of 0.255 F cm^{-2} and a roughness factor of 4167, which is much higher than that obtained in this work. This order-of-magnitude discrepancy between roughness factors is not unusual; the literature includes roughness factors for metal oxide films that vary by factors of several thousand.

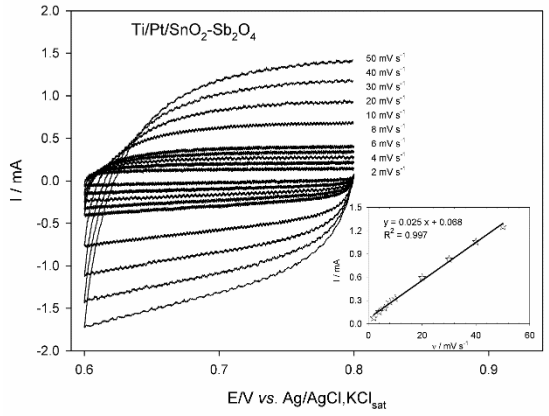

Figure 4. Cyclic voltammograms for Ti/Pt/SnO_2-Sb_2O_4 (10 cm^2) obtained at the double-layer region for scan rates from 2 to 50 mV s^{-1} in a 0.035 M Na_2SO_4 solution. Inset: Linear regression of I *vs.* υ measured at E= 0.7 V.

3.3 Ti/Cu/SnO_2-Sb_2O_3

3.3.1 Electrode preparation

In the first step of the Ti/Cu/SnO_2-Sb_2O_3 electrode preparation, the Ti substrate was pre-treated as previously described in preparation of Ti/Pt/SnO_2-Sb_2O_4. The copper deposition on the Ti substrate, pretreated, was performed in a one-compartment double-wall cell connected to a thermostatic water-bath, which enabled the recirculation of water at 44ºC. The cell contained a copper sulfate aqueous solution and a current density of 50 mA cm^{-2} was applied

for 0.5 h using Ti substrate as the cathode and two platinum plates as anodes [Martínez-Huitle and Andrade, 2011]. After copper deposition, alternate Sn and Sb electrodepositions on the Ti substrate were carried out in the same cell and in the same method of section 3.2.1.
After this treatment, the electrodes were heated in a tubular furnace at 550 ºC, as for the Ti/Pt/SnO_2-Sb_2O_4

3.3.2 Characterization

- Structural Characterization by DRX

After calcination at 550 ºC, an X-ray diffractogram of the Ti/Cu/SnO_2-Sb_2O_3 electrode was obtained (Figure 5) and compared with those from the JCPDS ICDS database. The presence of the SnO_2 (file PDF#41-1445) and Sb_2O_3 (file PDF#43-1071) phases were confirmed. A SbSn intermetallic phase (PDF#33-0118) can also be detected.

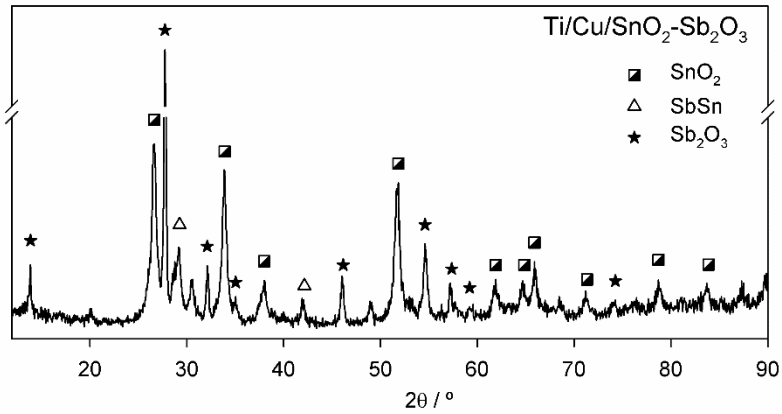

Figure 5. X-ray diffractogram of the Ti/Cu/SnO_2-Sb_2O_3 composite oxide electrode in its final form after calcination at 550 ºC.

- Morphological characterization by SEM

Figure 6 presents the micrograph of the titanium substrate covered with the copper interlayer. The morphology of the electrode is similar to several parallelepiped, the surface is fairly uniform. In Figure 7 (a and b), micrographs of the Ti/Cu/SnO_2-Sb_2O_3 surface, with two different magnifications, are shown. The electrodes presents homogeneous Sn-Sb oxide crystallites with a globular form consisting of 5-10 μm agglomerates of smaller crystallites. The structure is highly porous.

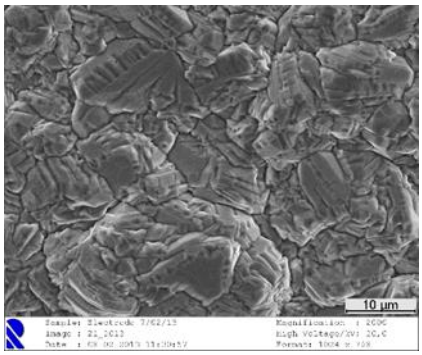

Figure 6. Micrograph of the Ti plate covered with Cu. Magnifications of 2000 x top view.

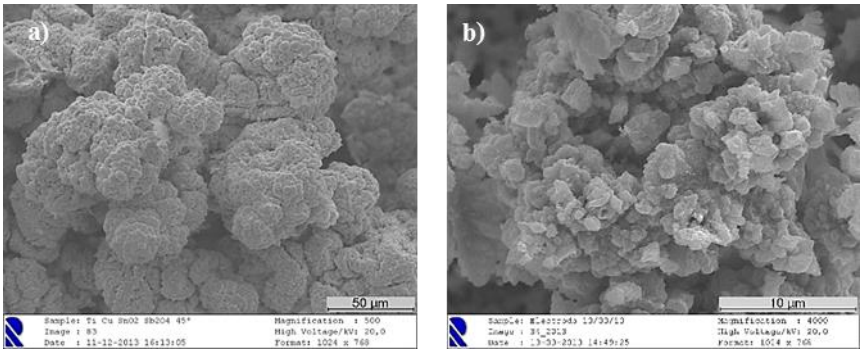

Figure 7. Micrographs of the surface of the Ti/Cu/SnO_2-Sb_2O_3: magnifications a) of 500 x. 45º inclination and b) 4000 x top view.

- Relative roughness

To determine the oxides' capacitance, cyclic voltammetric curves were run at scanning rates varying from 2 to 50 mV s^{-1}, in 0.035 M Na_2SO_4 aqueous solution, in a one-compartment electrochemical cell, using the prepared oxide as working electrode. Figure 8 presents the cyclic voltammograms recorded in the potential range where only double-layer charging currents were observed. From the plot of I values vs scan rates (inset of Figure 8), at E=-0.18 V, a R_f of 70 was obtained for the Ti/Cu/SnO_2-Sb_2O_3 material.

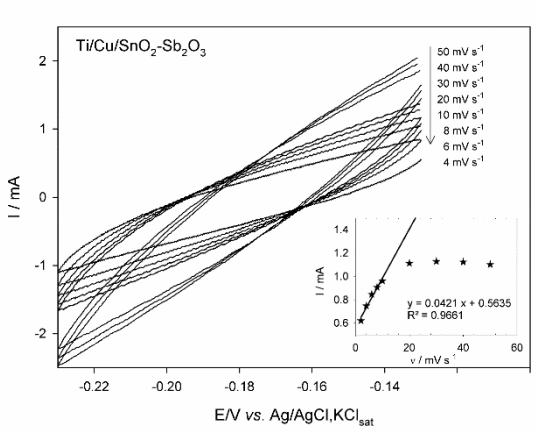

Figure 8. Cyclic voltammograms for Ti/Cu/SnO_2-Sb_2O_3 electrode material (10 cm^2) obtained at the double-layer region for scan rates from 2 to 50 mV s^{-1} in a 0.035 M Na_2SO_4 solution. Inset: Linear regression of I *vs.* υ with theoretical equations adjusted to the linear zone, with I measured at: -0.18 V.

3.4 Ti/SnO_2-Sb

3.4.1 Electrode preparation

To achieve more uniform films than those prepared by alternate deposition of tin and antimony, a different deposition method was tested, where tin and antimony were electrodeposited simultaneously [Martínez-Huitle and Andrade, 2011].

The Ti substrate was first pretreated, and the pretreatment consisted of a mechanical polishing of the substrate followed by its immersion in a concentrated chloridric acid boiling bath for 1 minute. For the Ti/SnO_2-Sb anode preparation, simultaneous deposition of tin and antimony on the Ti substrate was performed using a one-compartment double-wall cell connected to a thermostatic water-bath, which enabled the recirculation of water at 44ºC. The cell contained a tin and antimony solution and a current density of 2.5 mA cm^{-2} was applied for 1 h using Ti substrate as the cathode between two Pt plate anodes. The molar ratios of the components of the electrodeposition solutions were 16:1:54.8:5.9 of $SnCl_2$:$SbCl_3$:$Na_4P_2O_7$.$10H_2O$:$C_4H_6O_6$, with the $SnCl_2$ concentration of 0.13 mol L^{-1}. A 0.4 g L^{-1} solution of gelatine was also added. After this treatment, the electrodes were heated in a tubular furnace at 500 ºC for 2 h to obtain the respective oxides.

3.4.2 Characterization

- Structural Characterization by DRX

In Figure 9, the diffractogram of the prepared Ti/SnO_2-Sb electrode is presented. When Sn and Sb electrodepositions were carried out simultaneously the predominant phase was the SnO_2, assigned according to the file PDF#41-1445 from the JCPDS ICDS database. A SbSn intermetallic phase (PDF#33-0118) can also be detected in the diffractogram. In this films prepared by the simultaneous electrodeposition method, some diffraction lines, not assigned to the previous discussed phases, can be assigned to the Sn,Sb-P_2O_7 phases [Chernaya *et al.*, 2005; Xu *et al.*, 2012 Hibino and Kobayashi, 2013] because pyrophosphate is used in the simultaneous electrodeposition preparation method.

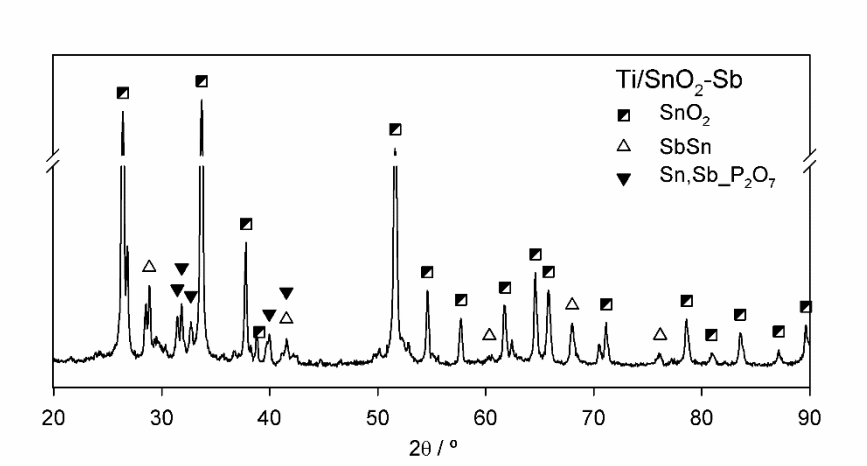

Figure 9. X-Ray diffractogram for Ti/SnO_2-Sb electrode material in its final form after calcination at 500 ºC.

- Morphological characterization by SEM

In Figure 10, micrographs of the electrodes' surface, with two different magnifications, are presented. Ti/SnO_2-Sb (Figure 10, a and b) presents homogeneous Sn-Sb oxide crystallites with a globular form consisting of 5-10 µm agglomerates of smaller crystallites. The structure is highly porous.

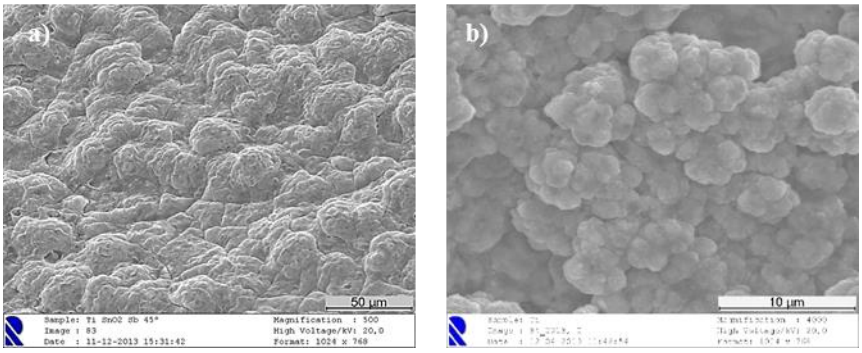

Figure 10. Micrographs of the Ti/SnO_2-Sb electrode material: magnifications of a) 500 x. 45º inclination and b) 4000 x top view.

- Relative roughness

Figure 11 presents the cyclic voltammograms recorded in the potential range where only double-layer charging currents were observed. Plots of the I values (E=-0.15 V) *vs.* scan rate are also presented in Figure 11, as inset, where the equation of the fitted line are also shown. The R_f determined for the Ti/SnO_2-Sb material was 34.

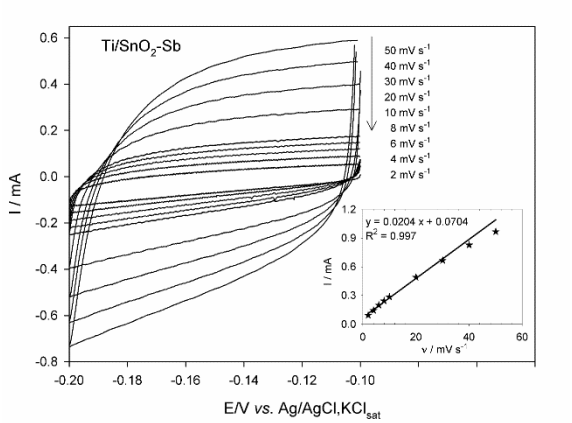

Figure 11. Cyclic voltammograms for Ti/SnO_2-Sb electrode material (10 cm^2) obtained at the double-layer region for scan rates from 2 to 50 mV s^{-1} in a 0.035 M Na_2SO_4 solution. Inset: Linear regression of I *vs.* υ, with theoretical equation adjusted to the linear zone, with I measured at: -0.15 V.

3.5 Ti/Pt/SnO_2-Sb

3.5.1 Electrode preparation

The Ti/Pt/SnO_2-Sb electrode preparation comprised the substrate pretreatment, the electrodeposition of the platinum intermediate layer, the simultaneously deposition of tin and antimony and finally the heating of the electrode in a tubular furnace at 500 ºC for 2 h to obtain the respective oxides.

The pretreatment consisted of a mechanical polishing of the titanium substrate followed by its immersion in a concentrated chloridric acid boiling bath for 1 minute. The Pt deposition on the Ti pretreated substrate was performed as described elsewhere [Andrade *et al.*, 2007].

For the Ti/Pt/SnO_2-Sb anode, simultaneous deposition of tin and antimony on the Ti substrate was performed using a one-compartment double-wall cell connected to a thermostatic water-bath, which enabled the recirculation of water at 44ºC. The solutions' composition is described in section 3.4.1.

3.5.2 Characterization

- Structural Characterization by DRX

In Figure 12, the diffractogram of the prepared Ti/Pt/SnO_2-Sb electrode material is presented. When Sn and Sb electrodepositions were carried out simultaneously the predominant phase was the SnO_2, assigned according to the file PDF#41-1445 from the JCPDS ICDS database. In this materials prepared with a Pt electrodeposited interlayer, Pt diffraction lines were identified.

In this films prepared by the simultaneous electrodeposition method, some diffraction lines, not assigned to the previous discussed phases when the alternate deposition were performed, can be assigned to the Sn,Sb-P_2O_7 phases [Chernaya *et al.*, 2005; Hibino and Kobayashi, 2013; Xu *et al.*, 2012] because pyrophosphate is used in the simultaneous electrodeposition preparation method.

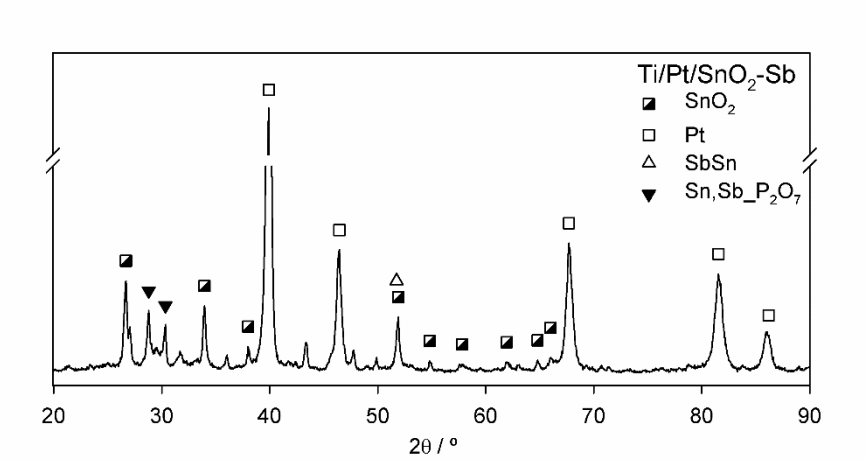

Figure 12. X-Ray diffractogram for Ti/Pt/SnO_2-Sb electrode material in its final form after calcination at 500 ºC

- Morphological characterization by SEM

In Figure 13, micrographs of the electrodes' surfaces, with two different magnifications, are presented. Ti/Pt/SnO_2-Sb presents homogeneous Sn-Sb oxide crystallites. The structure is highly porous. The introduction of a Pt metallic interlayer reduces the porosity of the film and presents a more compact coating similar to cauliflower. However, the number of agglomerates is higher and presents lower dimensions, leading to a higher surface area.

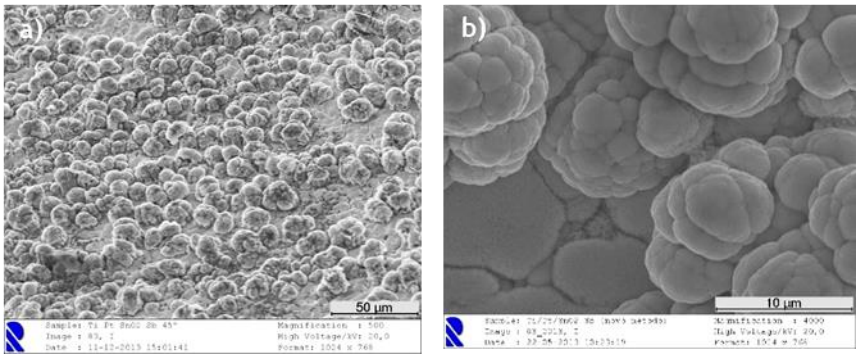

Figure 13. Micrographs of the Ti/Pt/SnO_2-Sb electrode material: magnifications of a) 500 x. 45º inclination and b) 4000 x top view.

- Relative roughness

Figure 14 presents the cyclic voltammograms recorded in the potential range where only double-layer charging currents were observed. Plot of I values for the different scan rates,

obtained at E=0.7 V, where anodic and cathodic currents presented higher symmetry, is depicted in the inset of Figure 14. From the fitted equation, a R_f for the Ti/Pt/SnO_2-Sb material of 201 was obtained.

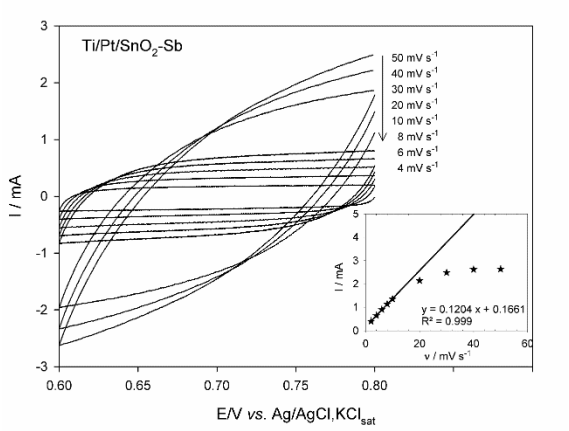

Figure 14. Cyclic voltammograms for Ti/Pt/SnO_2-Sb electrode material (10 cm^2) obtained at the double-layer region for scan rates from 2 to 50 mV s^{-1} in a 0.035 M Na_2SO_4 solution. Inset: Linear regression of I *vs.* υ, with theoretical equation adjusted to the linear zone, with I measured at: 0.7 V.

3.6 Ti/Cu/SnO_2-Sb

3.6.1 Electrode preparation

The electrodes preparation comprised the substrate pretreatment, the electrodeposition of the copper intermediate layer, the simultaneously deposition of tin and antimony and finally the heating of the electrode in a tubular furnace at 500 ºC for 2 h to obtain the respective oxides. The pretreatement was similar to that already described (3.4.1). The copper deposition on the Ti substrate, pretreated, was performed as in section 3.3.1

For the Ti/Cu/SnO_2-Sb anode, simultaneous deposition of tin and antimony on the Ti substrate was performed as previously described (3.4.1).

3.6.2 Characterization

- Structural Characterization by DRX

In Figure 15, the diffractogram of the prepared Ti/Cu/SnO_2-Sb electrode is presented. When Sn and Sb electrodepositions were carried out simultaneously the predominant phase was the SnO_2, assigned according to the file PDF#41-1445 from the JCPDS ICDS database. In this materials prepared with a Cu electrodeposited interlayer, Cu diffraction lines were, also, identified. A SbSn intermetallic phase (PDF#33-0118) can be detected too.

In this films prepared by the simultaneous electrodeposition method, some diffraction lines, not assigned to the previous discussed phases, can be assigned to the Sn,Sb-P_2O_7 phases [Chernaya *et al.*, 2005; Xu *et al.*, 2012; Hibino and Kobayashi, 2013] because pyrophosphate is used in the simultaneous electrodeposition preparation method.

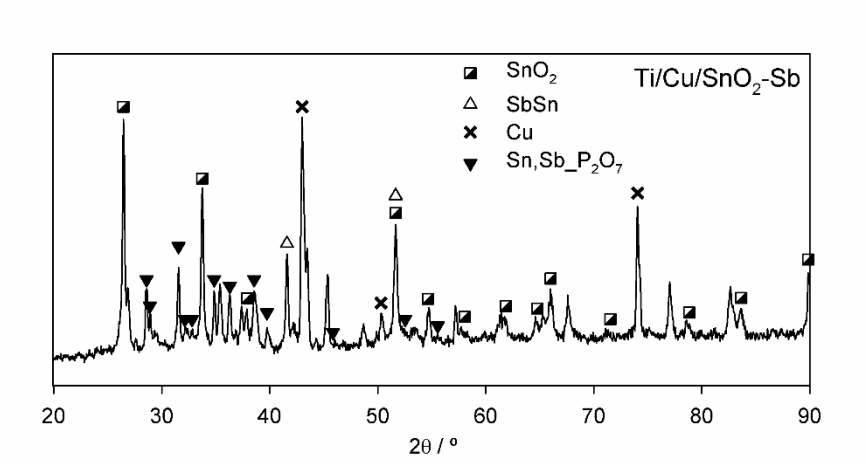

Figure 15. X-Ray diffractogram for Ti/Cu/SnO_2-Sb electrode material in its final form after calcination at 500 ºC.

- Morphological characterization by SEM

In Figure 16, micrographs of the electrodes' surfaces, with two different magnifications, are presented. Ti/Cu/SnO_2-Sb surface presents homogeneous Sn-Sb oxide crystallites with a globular form consisting of 5-10 μm agglomerates of smaller crystallites. The structure is highly porous.

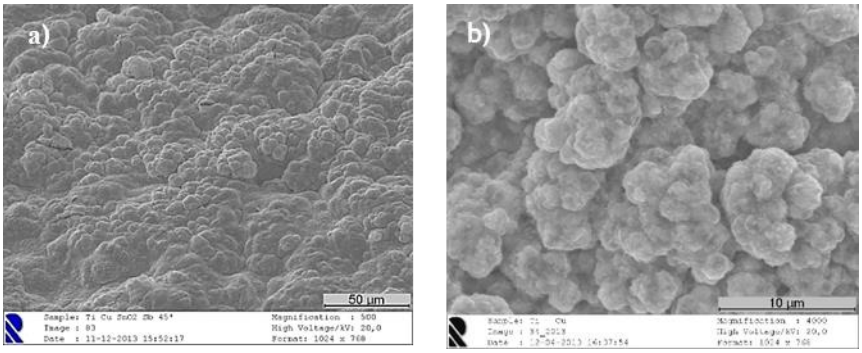

Figure 16. Micrographs of Ti/Cu/SnO_2-Sb electrode material: magnifications of a) 500 x. 45º inclination and b) 4000 x top view.

- Relative roughness

Figure 17 presents the cyclic voltammograms recorded in the potential range where only double-layer charging currents were observed. I values for the different scan rates, obtained at E=0.07 V, were plotted as a function of scan rate (inset of Figure 17), providing a R_f of 7 for the Ti/Cu/SnO_2-Sb material.

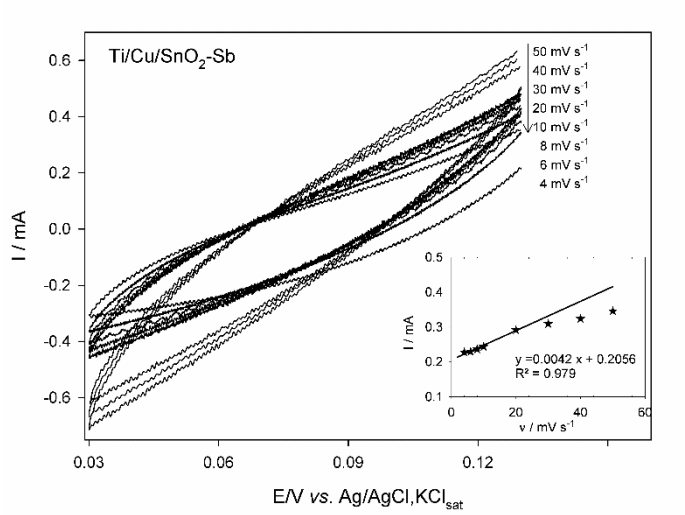

Figure 17. Cyclic voltammograms for Ti/Cu/SnO_2-Sb electrode material (10 cm^2) obtained at the double-layer region for scan rates from 2 to 50 mV s^{-1} in a 0.035 M Na_2SO_4 solution. Inset: Linear regression of I *vs.* υ with theoretical equation adjusted to the linear zone, with I measured at: 0.07 V.

3.7 Discussion and conclusions

Looking at the structural characterization, when Sn and Sb electrodepositions were carried out simultaneously the predominant phase was the SnO_2, assigned according to the file PDF#41-1445 from the JCPDS ICDS database. In the materials prepared with a Pt or Cu electrodeposited interlayer, Pt or Cu diffraction lines were, respectively, identified. When the Sn and Sb electrodepositions were alternated, the formation of distinct Sn or Sb oxide phases was observed: SnO_2 (PDF#41-1445) and Sb_2O_4 (PDF#11-0694) or Sb_2O_3 (PDF#43-1071). This fact is in agreement with what was previously observed in the cases of Ti/SnO_2-Sb_2O_4 [Ciríaco *et al.*, 2011], with a different electrodeposition time from the one prepared in this work, and Ti/Pt/SnO_2-Sb_2O_4 [Santos *et al.*, 2013], although antimony presents a different oxidation state when copper is the interlayer, possibly due to competition between copper and antimony for the oxygen. An SbSn intermetallic phase (PDF#33-0118) can be detected in almost all of the diffractograms. The simultaneous or alternated electrodeposition form of Sn and Sb produce different results: when Sn and Sb electrodeposition is simultaneous, Sb may substitute Sn in the lattice, and only one oxide phase, SnO_2, is obtained in addition to the intermetallic SbSn phase; when the Sn and Sb electrodeposition is alternated, the two oxide phases are obtained. In the films prepared by the simultaneous electrodeposition method, some diffraction lines, not assigned to the previous discussed phases, can be assigned to the Sn,Sb-P_2O_7 phases [Chernaya *et al.*, 2005; Xu *et al.*, 2012; Hibino and Kobayashi, 2013] because pyrophosphate is used in the simultaneous electrodeposition preparation method.

Regarding the SEM results, it can be observed that the introduction of a Pt or Cu interlayer increases the roughness of the surface, particularly in the case of the Pt layer. Ti/SnO_2-Sb and Ti/Cu/SnO_2-Sb present similar morphologies, with homogeneous Sn-Sb oxide crystallites with a globular form consisting of 5-10 μm agglomerates of smaller crystallites. The structure is highly porous. The introduction of a Pt metallic interlayer reduces the porosity of the film and

presents a more compact coating similar to cauliflower. However, the number of agglomerates is higher and presents lower dimensions, leading to a higher surface area.

In Ti/SnO_2-Sb_2O_4, prepared with a shorter deposition time than the one presented in Ciríaco *et al.* (2011), shows a different morphology from the cracked mud view that characterizes these films [Andrade *et al.*, 2004; Montilla *et al.*, 2004]. This fact is related to the higher homogeneity obtained in the films prepared with shorter deposition times that prevents a higher separation of the two phases, with different thermal expansion coefficients. In Ti/Cu/SnO_2-Sb_2O_3, two distinct morphologies are presented, evidencing the two oxide phases identified by X-ray diffraction: one with a sea sponge look, attributed to tin oxide, and another with a branched tree form, attributed to antimony oxide.

Considering the relative roughness the highest roughness factor was found for Ti/Pt/SnO_2-Sb. Comparing Ti/Pt/SnO_2-Sb (R_f =201) prepared with simultaneous metal electrodeposition, with Ti/Pt/SnO_2-Sb_2O_4 (R_f =41), prepared in a previous work by alternating metal electrodeposition [Santos *et al.*, 2013], it may be concluded that, for this platinized material, simultaneous electrodeposition produces higher roughness factors, as shown by the SEM results (Figure 13 a and b, and [Santos *et al.*, 2013]). The explanation for this fact is that the roughness of the platinized titanium is very high (see Figure 2 b) and can influence the roughness of the posterior SnO_2-Sb layer, whose thickness is low, because it is prepared with only one simultaneous Sn,Sb electrodeposition. On the other hand, the Ti/Pt/SnO_2-Sb_2O_4 electrode is prepared with 4 alternating electrodepositions of each metal, leading to a higher thickness that can minimize roughness. Comparing the Ti/SnO_2-Sb_2O_4 (R_f =18), prepared in this work, with Ti/SnO_2-Sb_2O_4 (R_f =777), prepared in a previous work [Ciríaco *et al.*, 2011], both by alternating metal electrodeposition but different electrodeposition durations, it can be concluded that a fourfold increasing in the electrodeposition time increases the roughness. The main differences found in the roughness factors for the Sn-Sb oxide films prepared on Ti/Pt or Ti/Cu must be due to the interlayers of Pt or Cu that present completely different aspects (see Figure 2 b and 6). From the observed roughness factors obtained for the films prepared in this work, it seems that they depend on the substrate morphology, as well as on the electrodeposition process and probably also on the film thickness. It is difficult to show a linear behavior for the roughness from the experimental details.

4. Environmental applications of tin and antimony mixed oxides

This chapter presents different environmental applications of tin and antimony mixed oxides. It starts with a description of the materials and methods utilized in the studies performed with the different electrode materials.

The results of the thermodynamic study of the oxygen evolution reaction for all the tin and antimony mixed oxides, whose preparation and characterization was described in the previous chapter, are then presented and discussed.

The utilization of Ti/Pt/SnO_2-Sb as anode in the degradation of a pharmaceutical compound, diclofenac, is also presented in this chapter.

Due to its mechanical, chemical and electrochemical stabilities and extended lifetime, Ti/Pt/SnO_2-Sb_2O_4 was chosen as anode for the electrodegradation of complex mixtures, namely:

- biologically pretreated sanitary landfill leachate and simulated samples, having in their composition only different N-containing compounds, without organic matter;
- raw sanitary landfill leachate and synthetic samples, containing humic acid and inorganic salts, with COD and ammonium ion contents similar to that of the real leachate.

The results and the main conclusions obtained in these two studies are also presented in this chapter.

4.1 Materials and Methods

4.1.1 Reagents

The following reagents were used as purchased in the preparation of synthetic samples:

Ammonium nitrate, calcium chloride, magnesium chloride, sodium chloride, humic acid, ammonium sulfate, ammonium chloride and potassium chloride.

The chemicals used as model pollutants and electrolyte were sodium diclofenac salt (DIC) and sodium sulfate, respectively.

The reagents were analytical grade and were purchased from Sigma Aldrich and used without additional purification.

4.1.2 Samples characterization techniques

Several parameters were used to characterize samples and to follow the electrochemical experiments, namely chemical oxygen demand (COD), 5-day biochemical oxygen demand BOD_5, dissolved organic carbon (DOC), total nitrogen (TN), total kjedahl nitrogen (TKN), ammonia nitrogen (AN), pH, conductivity (Cond.), suspended solids (SS), dissolved solids (DS) and UV-visible (UV-vis) absorption spectrophotometry. Also, chloride, nitrate, nitrite and ammonium concentrations were determined by ion chromatography. In subsections below, a brief description of the analytical methods and equipment's used to determine each parameter is presented.

4.1.2.1 Chemical oxygen demand

The COD is commonly used to indirectly measure the amount of organic matter in samples and to evaluate the performance of the oxidation treatment in these samples. It is defined as the amount of a specified oxidant that reacts with the sample under controlled conditions. The quantity of oxidant consumed is expressed in terms of its oxygen equivalence. The basis for the COD determination methods is that nearly all carbon content of the organic compounds can be fully oxidized to carbon dioxide with a strong oxidizing agent under acidic conditions.

In this work, COD was determined by closed reflux titrimetric method, following the procedure described in Section 5220C of the Standard Methods [Eaton *et al.*, 2005]. Dichromate ion is the oxidant used in this method, being reduced to the chromic ion. In COD determinations, digestion of the samples occurred in strongly acid solution with a known quantity of potassium dichromate that has to be in excess, and containing also a silver catalyst to oxidize resistant organic compounds and mercury sulphate to reduce interferences from the oxidation of chloride ions. The samples closed reflux digestion was performed, using a thermoreactor Merck Spectroquant TR 420, during 2 h at 150 ºC. After digestion, the remaining unreduced $K_2Cr_2O_7$ was titrated with ferrous ammonium sulphate, using ferroine as indicator, to determine the amount of $K_2Cr_2O_7$ consumed. The titration was performed using an automatic titrator Metrohm 876 Dosimat Plus. The dichromate consumed by the sample is equivalent to the amount of oxygen required to oxidize the organic matter.

4.1.2.2 Biochemical oxygen demand

The BOD is defined as the amount of oxygen required for microbial metabolism of organic matter dissolved in samples. Its function is similar to that of COD, since both measure the amount of organic compounds present in waters and wastewaters. However, COD is less specific, since it measures everything that can be chemically oxidized, and the BOD evaluate biologically active organic matter. Biochemical oxygen demand determination occurs over some variable period of time depending on temperature, nutrient concentrations, and the enzymes

available to indigenous microbial populations. This is not a precise quantitative test, although it is widely used as an index of the biodegradable organic matter present in a wastewater, being an important parameter to evaluate the quality of wastewaters' treatment results.

BOD determination is a slow process that theoretically requires an infinite time to be completed. To overcome this drawback, it is determined the BOD_5, which corresponds to an incubation period of 5 days at which about 60-70% of the reaction has occurred. It is also used the BOD_{20}, that corresponds to an incubation period of 20 days in which 95-99% of organic matter has already been degraded.

In this work, BOD_5 was determined by the respirometric method, following the procedure described in Section 5210D of the Standard Methods [Eaton *et al.*, 2005], which provided the direct measurement of the oxygen consumed by microorganisms from an air enriched environment, in a closed vessel, under conditions of constant temperature (20±1 ºC) and stirring. Manometric respirometers were used, which relate oxygen uptake to the change in pressure caused by oxygen consumption while maintaining a constant volume. The assays were performed in a WTW Oxitop IS 12 with Inductive Stirring System, in a WTW TS 606-G/2-i Thermostat Cabinet, using lyophilized biomass PolySeed, commercially available.

4.1.2.3 Dissolved organic carbon

The total organic carbon is the amount of organic carbon in the samples, expressed in concentration of carbon. Unlike COD or BOD_5, TOC is independent of the oxidation state of the organic matter. It is a global parameter that allows the evaluation of the mineralization efficiency of the leachate sample treatment. In the present work, it was measured DOC, which is the fraction of TOC that passes through a 0.45 µm pore-diameter filter.

DOC was determined by the high-temperature combustion method, following the procedure described in Section 5310B of the Standard Methods [Eaton *et al.*, 2005]. Its value is not achieved by direct measurement, the method used in this work analyses separately the dissolved fractions of total carbon (DC) and inorganic carbon (DIC), and DOC is then determined by subtracting DIC from DC.

The DOC determinations were performed in a Shimadzu TOC-VCPH analyser, which combines combustion catalytic oxidation at 680°C and non-dispersive infrared (NDIR) detection method. The samples were filtered through a glass fiber filter, from Whatman (GF/F filter, 0.45 µm). For the DC determinations, an automated process injected the sample into the combustion furnace, where it undergoes combustion through heating at 680 ºC, with a platinum catalyst in an oxygen rich atmosphere. The water is vaporized and the organic and inorganic carbons are oxidized to CO_2 and H_2O. The gas phase, containing the CO_2, is transported by the carrier gas through a moisture trap and halide scrubbers, to remove water vapour and halides from the gas

stream before it reaches the detector. The CO_2 concentration is then measured with non-dispersive infrared detector. DIC is measured separately by injecting the sample into a reaction chamber where it is acidified, and all inorganic carbon is converted to CO_2, which is carried to the detector and measured. The obtained DIC or DC values are the average of, at least, two measurements. Regularly, calibration curves are performed.

4.1.2.4 Total nitrogen

The total nitrogen determination accounts for all forms of organic and inorganic nitrogen present in the leachate sample. Since before TN determinations samples are filtered through a GF/F Whatman filter, 0.45 µm, it is assumed that, in complex matrix samples as sanitary landfill leachates, TN stands for total dissolved nitrogen.

TN was measured in a Shimadzu TNM-1 unit coupled with the TOC-VCPH analyser. All nitrogen present in samples is first converted to nitrogen monoxide and nitrogen dioxide by catalytic combustion in the furnace. Then, the nitrogen species react with ozone, to form an excited state of nitrogen dioxide. Upon returning to ground state, the emitted light energy is measured, using a chemiluminescence detector, and converted to TN.

4.1.2.5 Total Kjeldahl nitrogen and ammonia nitrogen

TKN measures the sum of organic nitrogen, ammonia and ammonium. It is determined using the Kjeldahl method that determines all the nitrogen in the trinegative state present in the samples. This method fails to account for nitrogen in the form of azide, azine, azo, hydrazine, nitrate, nitrite, etc.

TKN determinations followed the procedure described in Section 4500-Norg B of the Standard Methods [Eaton *et al.*, 2005], and as equipment it was used a Kjeldatherm block-digestion-system and a Vapodest 20 s distillation system, both from Gerhardt, and an automatic titrator Metrohm 876 Dosimat Plus.

The method to determine TKN consists of heating the sample with sulfuric acid, which decomposes the organic substance by oxidation to liberate the reduced nitrogen as ammonium sulfate. In this step, potassium sulfate is added to increase the boiling point of the medium and cupric sulfate is used as catalyst. After samples digestion, a small quantity of sodium hydroxide is added and the resulting ammonia solution is distilled from an alkaline medium, after adding a boric acid solution in the presence of a mixture of indicators (methyl red and methylene blue). The ammonia present in the sample, corresponding to the amount of nitrogen contained in the initial sample, reacts with the boric acid, and is determined indirectly by the titration of the borate ion formed with a H_2SO_4 standard solution.

The determination of ammonia nitrogen followed the procedure described in Section 4500-NH_3 B and Section 4500-NH_3 C of the Standard Methods [Eaton *et al.*, 2005], using the same distillation and titration systems used to determine TKN. The determination of ammonia nitrogen is similar to the determination of Kjeldahl nitrogen, although in this case the sample does not undergo digestion. For AN determinations, samples were buffered at pH 9.5 using a borate buffer to decrease hydrolysis of cyanates and organic nitrogen compounds. Then, they were distilled into a boric acid solution, containing the mixture of indicators used in TKN determination, and titrated with a standard H_2SO_4 0.1 M solution.

4.1.2.6 Ion chromatography

Ion chromatography is a process that allows the separation of ions based on their affinity to the ion exchanger. The basic process of ion chromatography can be represented in four steps: eluent loading to equilibrate the column, sample injection, separation of sample, and elution of the analyte. Elution is the process by which the compound of interest is moved through the column. This happens because the eluent is constantly pumped through the column. Ion chromatography retains the analyte ions on the column based on coulombic interactions. The stationary phase surface displays ionic functional groups that interact with analyte ions of opposite charge. As the sample elutes through the column, the analyte ions interact differently with the stationary phase. The affinity of the ions present in the sample with the stationary phase depends primarily on the ion charge and radius.

In section 4.3, ion exclusion chromatography was used in the determination of carboxylic acids. It was performed using a Shimadzu 10Avp HPLC apparatus coupled with a Shimadzu SPD M20A diode array detector. Acids were separated using an Aminex HPX – 87H of Bio-Rad (7.8 mm ID × 300 mm) column at 35 ºC. The elution was performed in isocratic mode using an aqueous solution of 4 mM of sulfuric acid as a mobile phase at a flow rate of 0.6 mL min^{-1}. The sample volume injected was 100 µL. The detection wavelength was 210 nm. The concentrations of the different ions were determined using calibration curves, prepared with standard solutions.

In section 4.4 and 4.5, ion chromatography was used in the determination of Cl^-, NO_3^-, NO_2^- and NH_4^+ ions. It was performed using a Shimadzu 10Avp HPLC apparatus coupled with a Shimadzu CDD 10Avp conductivity detector. Anions were separated using an IC I-524A Shodex (4.6 mm ID × 100 mm) column at 40 ºC. The elution was performed in isocratic mode using an aqueous solution of 2.5 mM of phthalic acid and 2.3 mM of tris(hydroxymethyl)aminomethane as a mobile phase at a flow rate of 1.5 mL min^{-1}. For the determination of the NH_4^+, an IC YK-A Shodex (4.6 mm ID × 100 mm) column at 40 ºC was used. The isocratic elution mode was used and the mobile phase was a 5.0 mM tartaric acid, 1.0 mM dipicolinic acid and 24 mM boric acid aqueous solution at a flow rate of 1.0 mL min^{-1}. For both analyses, the sample volume injected was 20 µL. The retention time of the ions determined were the following: Cl^- - 2.32 min;

NO_3^- - 3.89 min, NO_2^- - 2.78 min and NH_4^+ - 5.13 min. The concentrations of the different ions were determined using calibration curves, prepared with standard solutions.

4.1.2.7 Voltammetric studies

The cyclic voltammetric measurements were performed with a potentiostat/galvanostat VoltaLab PGZ 301, in a one-compartment cell, with a 10 cm^2 anode prepared as the working electrode, a 5 cm^2 (per side) platinum plate as the counter electrode and a commercial saturated Ag/AgCl, KCl_{sat} electrode as the reference electrode. Voltammograms were recorded at scan rate 0.5 50 mV s^{-1} in 1 M KOH aqueous solution.

4.1.2.8 Other parameters

- pH

In this work, the pH of the samples, thermostatised at 20 ºC, was measured using a pH meter HANNA (HI 931400).

- Conductivity

Conductivity is a measure of the ability of an aqueous solution to carry an electric current. This ability depends on the presence of ions, on their total concentration and mobility, and on the temperature. In this work, samples conductivity was measured using a conductivity meter Mettler Toledo (SevenEasy S30K). Before measurement samples were kept at 20 ºC.

- UV-Vis absorption spectrophotometry

UV-vis absorption spectrophotometry uses light in the visible and ultraviolet ranges. The absorption or reflectance in the visible range directly affects the perceived colour of the chemicals involved. In this region of the electromagnetic spectrum, molecules undergo electronic transitions. According to Beer-Lambert law, the absorbance of a solution is directly proportional to the concentration of the absorbing species in the solution and the pathlength. Thus, for a fixed pathlength, UV-vis absorption spectrophotometry can be used to determine the concentration of the absorber in a solution.

In this work, UV–Vis absorbance was measured from 200 to 800 nm using a Shimatzu UV-1800 spectrophotometer. The method was used to determine the variation in the absorbance of the samples, as well as in the content of aromatic compounds during the electrodegradation assays.

4.2 The oxygen evolution reaction at Sn-Sb oxide anodes

The oxygen evolution reaction is one of the most intensively studied electrochemical reactions due to its importance in practical applications such as water electrolysis, chloralkali cells, fuel cells, and secondary metal air batteries.

The OER is a very interesting process because of its high activation overpotentials in aqueous solutions [Wu *et al.*, 2011].

The anodic activity of an electrode material depends on the oxygen evolution overpotential. If the material is to be used in the production of oxygen from the water electrooxidation reaction, there are advantages in choosing materials with a low overpotential for oxygen evolution so that the energy consumption becomes lower. Additionally, at these materials, the direct anodic oxidation of pollutants occurs with high efficiency for low current densities [Armenta-Armenta and Diaz, 2005] because if the current density is high, a significant decrease in the current efficiency is expected due to oxygen evolution. However, it was demonstrated that the electrochemical combustion of most of the organic compounds only occurs without the loss of electrode activity at anode materials with high overpotential for oxygen evolution [Comninellis, 1994].

In this study, the apparent activation energy for the water oxidation at the different materials was determined. The electrode materials utilized were the following:

Ti/SnO_2-Sb_2O_4 (described in Ciríaco *et al.*, 2011); Ti/Pt/SnO_2-Sb_2O_4 (described in section 3.2); Ti/Cu/SnO_2-Sb_2O_3 (described in section 3.3; Ti/SnO_2-Sb (described in section 3.4; Ti/Pt/SnO_2-Sb (described in section 3.5 and Ti/Cu/SnO_2-Sb (described in section 3.6).

4.2.1 Experimental results

Figure 18, presents the voltammograms of the anodic currents obtained with one set of the five new electrode materials prepared in this work, as well as with one electrode material prepared according to literature [Santos *et al.*, 2013], for five different temperatures, up to the oxygen evolution region. Regarding the type of Sn and Sb electrodeposition, simultaneous or alternate, and the existence or absence of a Pt or Cu interlayer, the following conclusions can be obtained: the introduction of a Pt or a Cu metallic interlayer leads to an increase in the current intensity values due to the increase in the conductivity of the substrates Ti/Pt and Ti/Cu relative to the Ti. When the metallic interlayer is the same, the electrodes of the composite material of Sn and Sb oxides present lower current intensity for equal applied potential, indicating that the presence of only one predominant phase increases the current intensity. The presence of two distinct phases introduces more resistance in the grain boundaries; however, the real surface area has also an important role in the current intensity. In Figure 18, c and d, it can be observed that, simultaneously to the oxygen evolution, Pt can be oxidized, leading to distinct behaviors in the voltammogram profiles of the platinized and not-platinized electrodes [Wiberg and

Arenz, 2012]. In the voltammograms presented in Figure 18, e and f, before oxygen evolution, an anodic peak can be observed, which can be attributed to the copper oxidation.

To better visualize the potential window and the relative intensities at the same applied potential for the different Sn-Sb materials, a comparison of the obtained voltammograms for different temperatures are 25 and 65 ºC is depicted in Figure 19. The highest potential window is presented by the electrode materials prepared without a metallic interlayer, followed by that with a Pt interlayer and finally that with a Cu interlayer. Regarding the preparation mode, the simultaneous electrodeposition of Sn and Sb slightly decreases the potential window.

To study the mechanism of the oxygen evolution reaction on the surface of the different prepared anodes, steady-state polarization curves were conducted at temperatures ranging from 25 to 65 ºC in aqueous 1 M KOH solutions at the anodic potential limit of the electrochemical window. This reaction at the Sn-Sb anodes' surfaces (MOx) can be represented by the following mechanism [Lyons and Brandon, 2008]:

$MOx + OH^- \leftrightarrows MOx\text{-}OH + e^-$ (3)

$MOx\text{-}OH + OH^- \rightarrow MOx\text{-}O^- + H_2O$ (4)

$MOx\text{-}O^- \rightarrow MOx\text{-}O + e^-$ (5)

$2\ MOx\text{-}O \leftrightarrows 2\ MOx + O_2$ (6)

where equation (3) is the rate determining step.

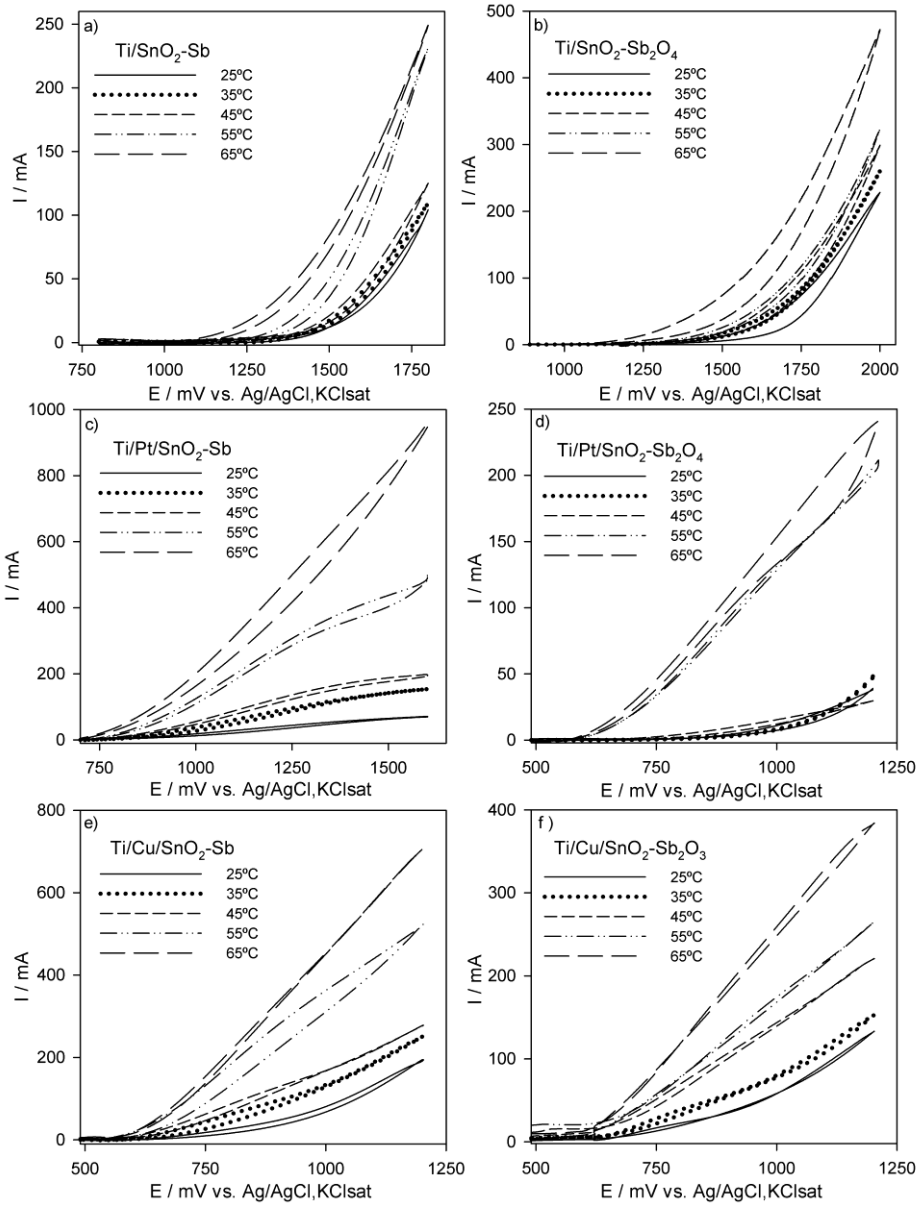

Figure 18. Cyclic voltammograms performed with 1 M KOH solutions at temperatures ranging from 25 to 65 ºC using different electrode materials: (a) Ti/SnO_2-Sb; (b) Ti/SnO_2-Sb_2O_4; (c) Ti/Pt/SnO_2-Sb; (d) Ti/Pt/SnO_2-Sb_2O_4; (e) Ti/Cu/SnO_2-Sb; (f) Ti/Cu/SnO_2-Sb_2O_3. Scan rate 0.5 mV s^{-1}.

Because the Tafel plots of log j, where j is the current density, versus the overpotential, η, presented two different slopes, one for low overpotential and another for high overpotential, all of the calculations were made at two different ranges of current density for all of the tested materials and for temperatures ranging from 25 to 65 ºC. The corresponding overpotentials for the different anode materials, used for the three sets of electrode materials, are presented in Table 1. This table also contains Tafel slopes and exchange current densities, j_0, determined from the Tafel plots for one set of freshly prepared materials at all experimental conditions. From Table 1, it can be seen that j_0 and the Tafel slopes are higher for the highest overpotential region and for higher temperatures. According to Montilla *et al.* (2004), the existence of two different Tafel slopes, for low and high overpotentials, may be related with the change in the valence state of the active sites of the anode materials. Thus, the active sites partially

inactivated for low overpotential or lower temperatures can be activated in the high overpotential region and at higher temperatures [Kibria and Tarafdar, 2002].

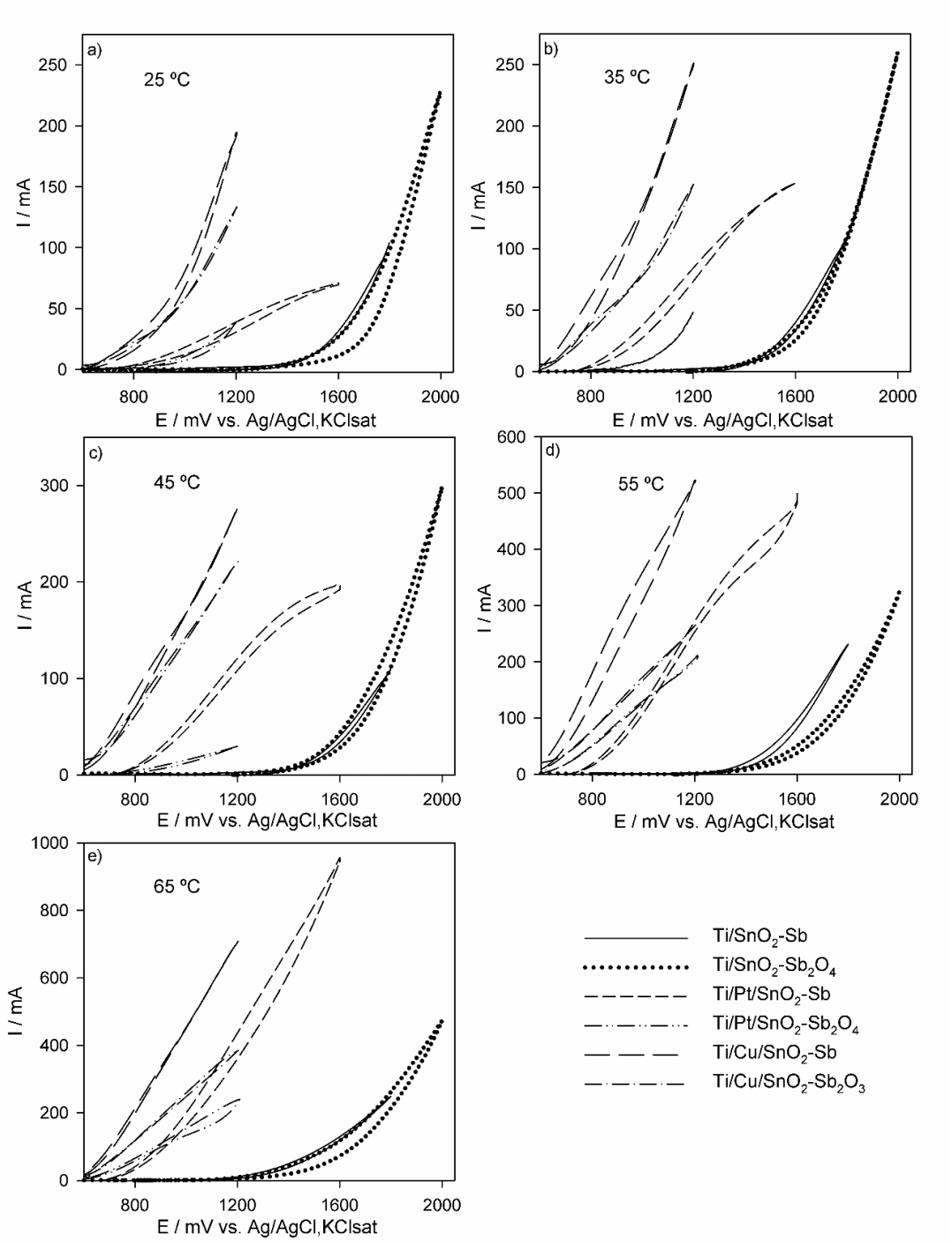

Figure 19. Cyclic voltammograms performed with 1 M KOH solutions at different temperatures, for different electrode materials. Scan rate 0.5 mV s^{-1}.

The anodes that present higher catalytic properties for the oxygen evolution reaction are those that present lower overpotential and higher j_0. From Figure 19, it can be seen that the anodes with better electrocatalytic properties for this reaction are those with a copper interlayer, followed by those with a platinum interlayer. The anodes without a metallic interlayer have

the poorest electrocatalytic activity for oxygen evolution. However, the latter are the most efficient for the oxidation of organic pollutants, with lower energy loss in water electrolysis.

The Tafel slope depends on the electrodes' surface characteristics and on the reaction mechanism. The materials that present higher increases in the Tafel slope between low and high overpotential are those having antimony in the form of Sb(III) and that can be partially oxidized to Sb(V) at higher overpotential, increasing the adsorption of OH^-. However, this is not the only factor that can affect the Tafel slope because for high roughness factors, an increase in the active sites can decrease the Tafel slope. When similar anodes prepared by the two different methods are compared, those presenting higher roughness have lower Tafel slopes.

To determine the apparent activation energy, log j_0 was plotted versus 1/T(K) for the three sets of the different anode materials at low and high overpotentials. These Arrhenius plots are presented in Figure 20 for one set of freshly prepared materials. From these Arrhenius plots, apparent activation energies for the oxygen evolution reaction at the Sn-Sb materials, for low and high overpotentials, were attained and are presented as mean values in Table 2. The apparent activation energies standard errors presented are mainly due to differences between the Tafel slopes and the j_0 obtained for the two sets of the freshly prepared materials. The apparent activation energies values are distributed into two groups: one that presents values similar to the value reported for the oxygen evolution reaction on Pt in acid medium, 47 kJ mol^{-1} [Chernaya *et al.*, 2005], and the other with values higher than 160 kJ mol^{-1}, suggesting that adsorption on the surface of these latter materials is more difficult to attain. Values higher than 47 kJ mol^{-1} were also obtained by Suffredii *et al.* (2004) for this reaction at boron-doped diamond anodes in acidic media.

Table 1. Tafel slopes and exchange current densities for the oxygen evolution reaction obtained from steady-state polarization curves with one set of freshly prepared electrode materials at different temperatures and two different overpotential ranges.

Material	Parameters	Low η					High η				
		Temperature / °C									
		25	35	45	55	65	25	35	45	55	65
Ti/SnO_2-Sb	η / mV	1200 - 1250					1400 - 1450				
	Tafel slope / mV	212	217	260	324	375	312	338	392	423	489
	j_0 / 10^{-3} mA cm^{-2}	0.001	0.002	0.019	0.374	2.822	0.099	0.270	1.151	4.491	16.66
Ti/SnO_2-Sb_2O_4	η / mV	1200 - 1250					1400 - 1450				
	Tafel slope / mV	282	298	355	393	396	302	330	370	410	445
	j_0 / 10^{-3} mA cm^{-2}	0.022	0.064	0.286	0.967	2.724	0.052	0.177	0.604	1.781	6.711
Ti/Pt/SnO_2-Sb	η / mV	600 - 650					800 - 850				
	Tafel slope/mV	162	166	178	174	190	488	463	491	481	491
	j_0 /10^{-3} mA cm^{-2}	0.065	0.113	0.358	0.662	2.676	35.58	73.53	137.3	282.1	440.8
Ti/Pt/SnO_2-Sb_2O_4	η / mV	600 - 650					800 - 850				
	Tafel slop /mV	204	284	306	419	463	198	300	496	755	1590
	j_0 /10^{-3} mA cm^{-2}	0.404	5.938	15.93	369.2	720.7	0.075	1.843	33.81	1138	4715
Ti/Cu/SnO_2-Sb	η / mV	500 - 550					800 - 850				
	Tafel slope /mV	198	200	228	239	253	468	622	845	762	895
	j_0 /10^{-3} mA cm^{-2}	3.362	6.698	21.94	57.38	103.4	199.8	687.1	1912	3004	5842
Ti/Cu/SnO_2-Sb_2O_3	η / mV	500 - 550					800 - 850				
	Tafel slope/mV	211	220	241	261	267	526	675	867	951	1035
	j_0 /10^{-3} mA cm^{-2}	3.981	8.294	24.07	46.23	78.37	179.7	521.2	1698	2498	4338

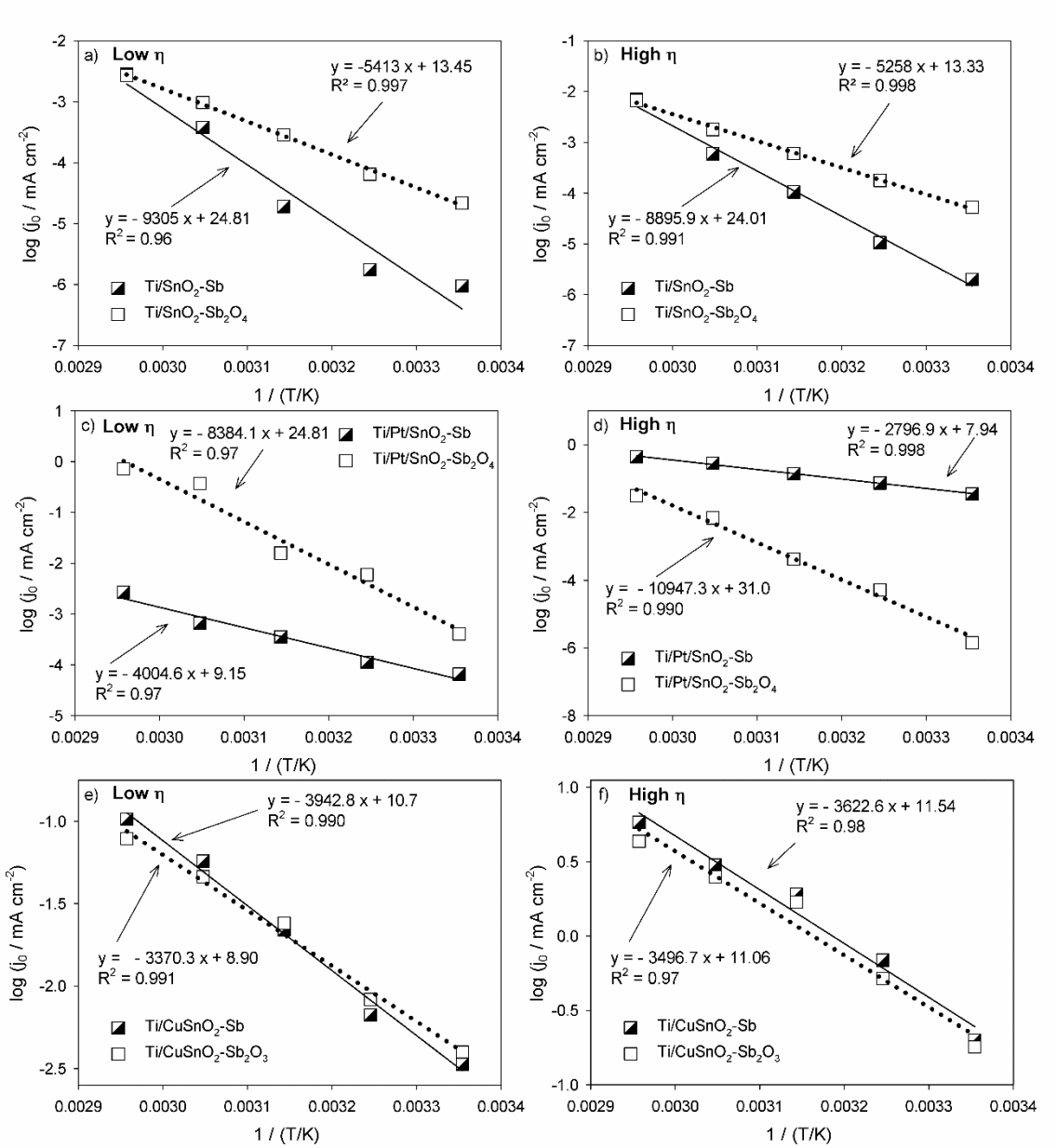

Figure 20. Plots of the exchange current density *vs.* the reciprocal temperature for the oxygen evolution reaction in 1 M KOH solutions, for low and high overpotential, at the different materials tested: (a,b) Ti/SnO_2-Sb and Ti/SnO_2-Sb_2O_4; (c,d) Ti/Pt/SnO_2-Sb and Ti/Pt/SnO_2-Sb_2O_4; (e,f) Ti/Cu/SnO_2-Sb and Ti/Cu/SnO_2-Sb_2O_3.

From the data collected in Tables 1 and 2, the following conclusions can be drawn: the values of 73 and 51 kJ mol^{-1} presented by Ti/Pt/SnO_2-Sb are similar to that presented by a Pt electrode because the Sn-Sb film is very thin, as shown in Figure 12, where the lines attributed to Pt are very intense, showing a poor coverage of the Pt interlayer; for equal substrate and interlayer, the material with higher roughness factor presents lower apparent activation energy because a higher specific surface area favors adsorption; the highest difference in apparent activation energy observed for low and high η for Ti/SnO_2-Sb and Ti/Pt/SnO_2-Sb_2O_4 is related with the Ti or Pt oxidations, respectively, which may occur simultaneously with the oxygen evolution; the materials prepared with a copper interlayer are those that present the lowest differences in

apparent activation energy among them, probably because the influence of the interlayer is a dominant factor, and Cu oxidation must have a lower activation energy than Ti or Pt oxidations.

Table 2. Mean apparent activation energy, with standard errors, determined for the oxygen evolution reaction for the study performed with the three sets of the six different electrode materials.

Material	ΔG / kJ mol^{-1}	
	Low η	High η
Ti/SnO_2-Sb	179 ± 1	107 ± 2
Ti/SnO_2-Sb_2O_4	101 ± 3	99 ± 2
Ti/Pt/SnO_2-Sb	73 ± 4	51 ± 3
Ti/Pt/SnO_2-Sb_2O_4	149 ± 12	221 ± 19
Ti/Cu/SnO_2-Sb	74 ± 2	76 ± 3
Ti/Cu/SnO_2-Sb_2O_3	63 ± 2	64 ± 3

4.2.2 Conclusions

Several electrode materials based on tin and antimony oxides were prepared by two different methods and with different substrates/interlayers. Depending on the preparation method, different phases were identified by XRD: when the Sn and Sb electrodepositions were alternated, the formation of distinct SnO_2 and Sb_2O_4 or Sb_2O_3 phases was observed; for simultaneous Sn and Sb electrodepositions, the main phase observed was SnO_2. The roughness of the prepared materials strongly depends on the roughness of the substrate/interlayer and on the thickness of the deposited layer, more than on the deposition method. The material that presented the highest roughness was Ti/Pt/SnO_2-Sb prepared over a Pt interlayer with very high roughness. The roughness deeply influences the oxygen evolution reaction because for equal substrate and interlayer, the material with higher roughness factor presents lower apparent activation energy, probably because the higher specific surface favors adsorption and facilitates the rate determining step. For some of the prepared materials, namely Ti/SnO_2-Sb and Ti/Pt/SnO_2-Sb_2O_4, a large difference was observed between the apparent activation energies calculated for low and high overpotentials, which is related to the Ti or Pt oxidation that can occur simultaneously with oxygen evolution. The lowest apparent activation energy for oxygen evolution was observed for Ti/Pt/SnO_2-Sb, the material that presented the highest roughness factor. The materials containing a copper interlayer presented very similar apparent activation energy for the oxygen evolution reaction. These materials also presented the lowest potentials for oxygen evolution, in particular the oxide prepared over a Cu interlayer with simultaneous Sn,Sb electrodepositions. Thus, for the tested materials, the most appropriate for oxygen evolution is Ti/Cu/SnO_2-Sb.

4.3 Anodic oxidation of diclofenac

This subchapter presents the results obtained in a study performed to test Ti/Pt/SnO_2-Sb as anode in the electrochemical degradation of a pharmaceutical compound - diclofenac.

4.3.1 Introduction

Over the last 15 years, pharmaceuticals have received increasing attention as potential bioactive chemicals in the environment. They are considered as emerging pollutants in waterbodies because they still remain unregulated or are currently undergoing a regularization process, although the directives and legal frameworks are not yet set-up [Sirés and Brillas, 2012].

Drugs are reaching the aquatic environment and, despite their very low concentrations, up to $\mu g\ L^{-1}$, presenting a potential hazard for human health, such as the increase of antibiotic-resistant bacterial infections, especially in locations where advanced wastewater treatments are not used [Boxall *et al.*, 2003; Chopra *et al.*, 2001; Martinez, 2009]. In fact, there are studies concerning the presence of pharmaceutical compounds in the effluents of municipal sewage treatment plants [Hirsch *et al.*, 1999; Kolpin *et al.*, 2002; Kümmerer , 2009].

Thousands of tons of pharmaceutical drugs are consumed yearly worldwide in human and veterinary medicine and agricultural and consumer products. An important part of these compounds enters into the environment from excretion after drug administration to humans and animals, production sites, direct disposal of excess of drugs in households and treatments throughout the water in fish and other animal farms [Brillas *et al.*, 2010].

Diclofenac (2-[2-(2,6-dichlorophenyl)aminophenyl]acetate ion), commercialized as sodium salt, is one of the most common non-steroidal anti-inflammatory drugs. It is extensively used for controlling renal colic and protecting against recurrent urinary calculi, also being present in numerous pharmaceutical formulations to treat various diseases. As a result of its resistance to biodegradation, it is one of the most frequently pollutants detected in ground waters, influents and effluents of sewage treatment plants, rivers and lakes around the world up to contents of 4.4 $\mu g\ L^{-1}$ [Brillas *et al.*, 2010].

Electrochemical oxidation treatment is a potential alternative method for eliminating pollutants with good efficiency. However, for the elimination of organic pollutants, it requires an anode with a high oxygen overpotential, high electrical conductivity and suitable mechanical and electrochemical stability.

The main advantage of the electrochemical technologies is their environmental compatibility because the main reagent, the electron, is a clean reagent. Other advantages include their versatility, high energy efficiency, amenability to automation, easy handling because of the simple equipment required and safety because they operate under mild conditions [Sirés and

Brillas, 2012]. Brillas *et al*. (2010), studied degradation of diclofenac in aqueous medium by anodic oxidation using an undivided cell with a Pt or BDD anode. It was demonstrated that diclofenac was completely depleted by AO with BDD even at the very high concentrations assessed (175 mg L^{-1}). Only some carboxylic acids were accumulated in low concentrations and oxalic and oxamic were found to be the most persistent acids.
In a previous work [Santos *et al*., 2013], our group studied the anodic degradation of Diclofenac with a Ti/Pt/SnO_2-Sb_2O_4 anode. After an 8 h assay, about 50% of COD and TOC removals were observed, with a combustion efficiency of 85% at an applied current density of 30 mA cm^{-2}.

4.3.2 Electrodegradation assays

Electrodegradation experiments were conducted in a 250 mL undivided cell using batch mode with stirring. The anode was a Ti/Pt/SnO_2-Sb electrode and the cathode a stainless steel foil, both electrodes being 10 cm^2 in area and having a 2 cm gap between them. Ti/Pt/SnO_2-Sb electrode was prepared as described in the section 3.5. All anodic oxidation assays were performed under galvanostatic conditions with an imposed current density of 30 mA cm^{-2}. The processed solution volume was 200 mL with a diclofenac concentration of 100 mg L^{-1}. Sodium sulfate aqueous solutions (0.035 M) were used as the supporting electrolyte in all experiments. Assays were run for 6 h, and data were collected at 1 h intervals.
Diclofenac degradation was followed by UV-Visible absorption spectrophotometry, with absorbance measurements between 200 and 800 nm, and COD and TOC determinations. The products formed during the electrodegradation assays were followed by ion exclusion chromatography, for the determination of the low molecular carboxilic acids determination. Assays were also followed by pH and conductivity measurements.
All of the assays were repeated twice, and COD and TOC values presented are mean values.

4.3.3 Results and discussion

Figure 21 presents the results obtained for the diclofenac electro-oxidation at a Ti/Pt/SnO_2-Sb anode. After a 6-h assay, the COD and TOC removals were almost 50% (Figure 21 a and b). The similar reductions in COD and TOC point towards a degradation mechanism of mainly combustion rather than conversion. The decay in absorbance, measured at 276 nm (Figure 21 c), where a maximum in the UV-Vis spectrum is observed (Figure 21 d), is slightly lower than COD and TOC decays, showing that some of the formed products may present absorbance at that wavelength. However, these products must be in low concentration, since the decay in the absorbance spectra seems very regular and do not show the formation of new absorbance bands.

There is also a decay in the pH (Figure 21 e), which is probably due to the formation of some carboxylic acids, well documented in the literature during this type of degradations [Panizza and Cerisola, 2009]. The slight reduction in the conductivity (Figure 21 e) must be due to the formation of some polymeric substances that precipitate when the samples are thermostated at the measuring temperature.

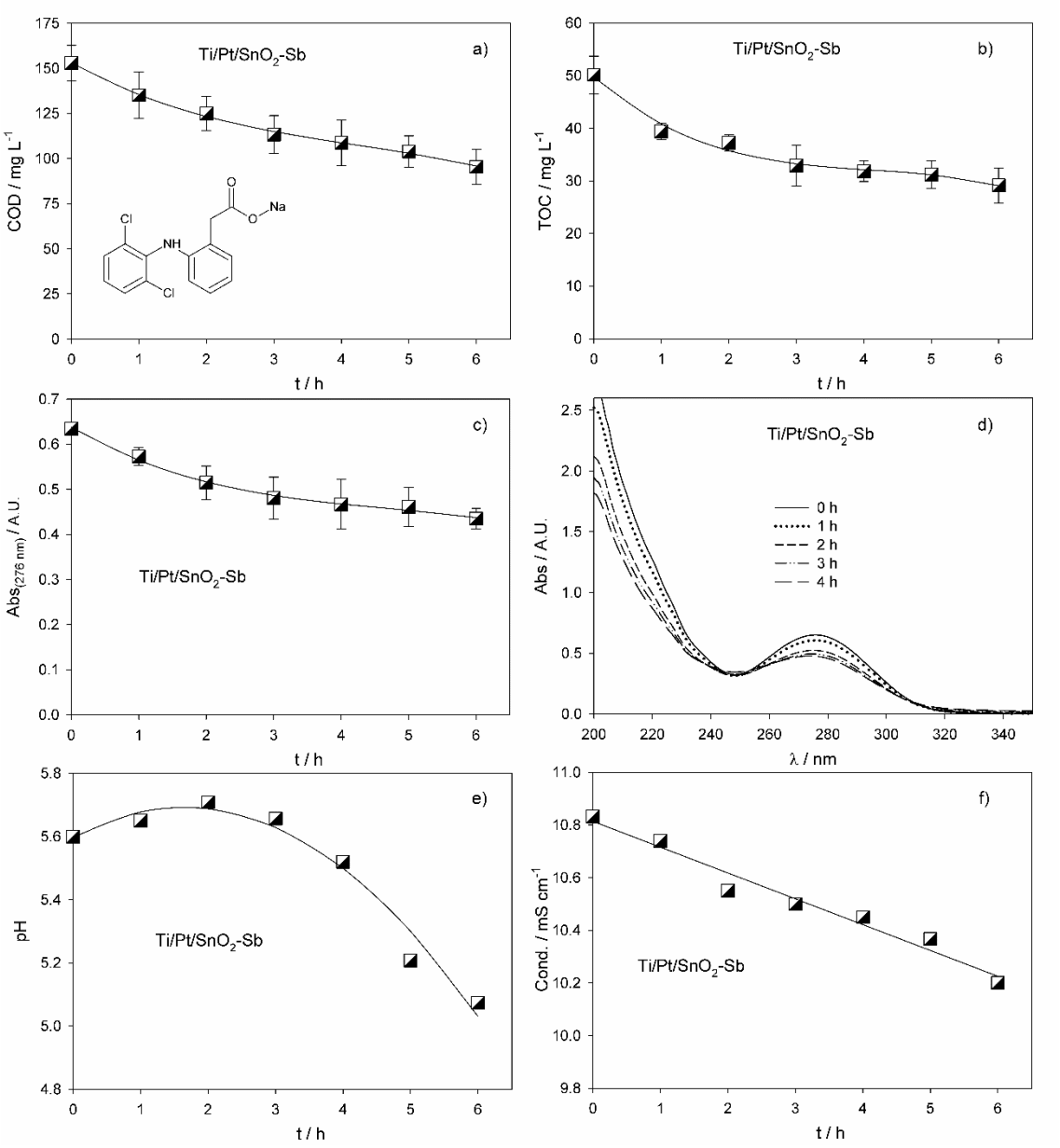

Figure 21. Evolution in time of (a) COD, (b) TOC, (c) Absorbance, measured at 276 nm, (d) UV-Vis spectra, (e) pH and (f) conductivity for the assays performed with Ti/Pt/SnO_2-Sb electrode at an applied current density of 30 mA cm^{-2}, using a diclofenac concentration – 100 mg L^{-1} in sodium sulfate aqueous solutions, 0.035 M. Inset of (a) – Diclofenac molecule.

To analyze the variation of the mineralization degree during the assays, a plot of TOC *vs.* COD is depicted in Figure 22 [Pacheco at al., 2007]. It can be observed that after the first hour there is a reduction in the ΔTOC/ΔCOD slope, showing that the mineralization degree decreases,

probably due to the formation of some products less easily mineralized than diclofenac. Thus, the existence of new products with lower mineralization degree reduces the referred slope.

To investigate the formation of carboxylic acids, samples collected during the assay were analyzed by ion exclusion chromatography, and the results are presented in Figure 23. To better visualize in the same figure the plots collected at different times, the HPLC spectrum baseline was gradually increased with assay time. In fact, the formation of several different carboxylic acids can be observed, namely oxamic acid formed from the amino group of the diclofenac molecule. Since the carboxylic acid concentrations did not vary significantly during the assay, it may be concluded that the diclofenac molecule is first broken into small very oxidized metabolites, the acids that are then mineralized, keeping acids concentration almost constant.

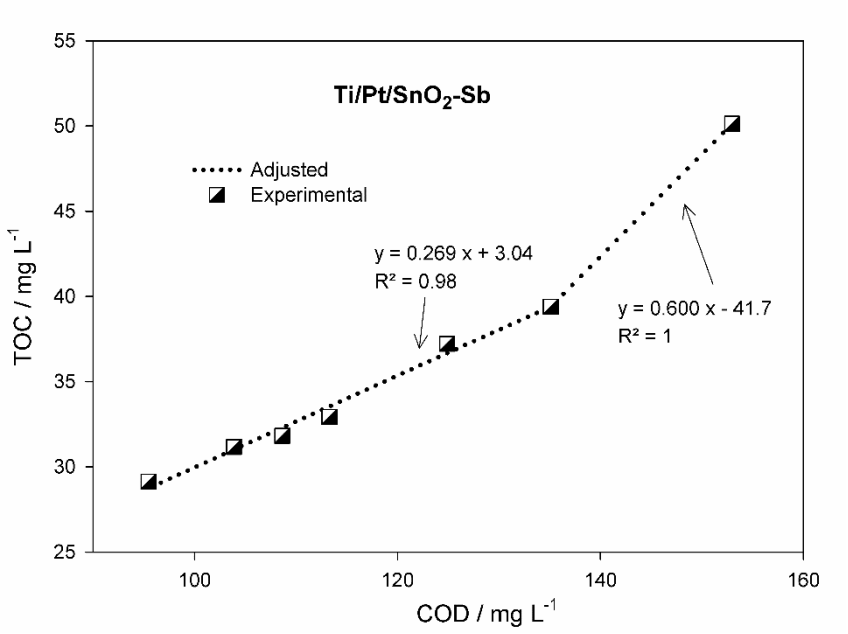

Figure 22. Variation of TOC with COD for the assays performed with Ti/Pt/SnO_2-Sb electrode at an applied current density of 30 mA cm^{-2}. Diclofenac concentration – 100 mg L^{-1}. Electrolyte - Sodium sulfate aqueous solutions, 0.035 M.

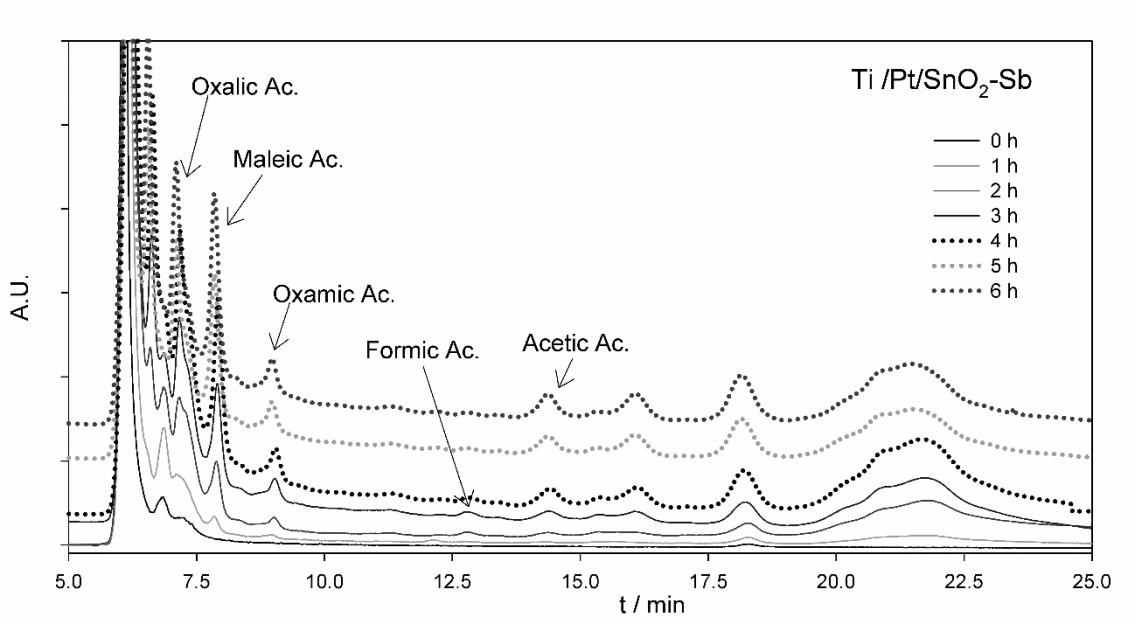

Figure 23. Ion exclusion chromatography qualitative results obtained for the samples collected during the assays performed with Ti/Pt/SnO_2-Sb electrode at an applied current density of 30 mA cm^{-2}. Diclofenac concentration – 100 mg L^{-1}. Electrolyte - Sodium sulfate aqueous solutions, 0.035 M.

4.3.4 Conclusions

Ti/Pt/SnO_2-Sb electrode has proved to be a suitable material for the electro-oxidation of organic compounds. In fact, the diclofenac anodic oxidation was successfully attained at this anode material. After more than 200 working hours, the material presented reproducible results, showing that this is a material with potentialities for environmental applications.

Medium COD and TOC removals, close to 50%, were obtained after 6 h assay. However, in similar experimental conditions, COD and TOC removals obtained at a BDD electrode were higher [Santos *et al.*, 2014b].

The similarity between COD and TOC removal rates points to a high degree of mineralization of the diclofenac molecule that is corroborated by the gradual decay of the UV-Visible spectra along the time. The main by-products identified by ion exclusion chromatography were oxalic, maleic and oxamic acids, the last one formed from the amino group of the diclofenac molecule. Vestigial quantities of formic and acetic acids were also found.

4.4 Nitrogen and organic load removal from sanitary landfill leachates by anodic oxidation at Ti/Pt/SnO_2-Sb_2O_4 anodes

In this subchapter, the oxidation ability of Ti/Pt/SnO_2-Sb_2O_4 anodes for the treatment of a biologically pretreated sanitary landfill leachate is accessed. To understand the elimination of the different forms of nitrogen present in the leachate samples, assays were also performed with simulated samples, having only different N-containing compounds, without organic matter. This work was already published in a scientific journal [Fernandes *et al.*, 2014].

4.4.1 Introduction

Recently, several studies have been reported the application of advanced oxidation technologies for the treatment of sanitary landfill leachates. Landfill leachate is one of the major environmental problems concerning water pollution, and conventional treatments have been inefficient in the treatment of this type of wastewater [Abbas *et al.*, 2009; Eggen *et al.*, 2010; Öman *et al.*, 2008]. Due to its effectiveness and ease of operation, the application of electrochemical oxidation to treat these effluents has been studied, with promising results. The effect of several operating factors and different types of anode material, in particular boron-doped diamond (BDD), have been assessed [Anglada *et al.*, 2009; Zhao *et al.*, 2010].
Anglada and co-workers [Anglada *et al.*, 2009; Anglada *et al.*, 2011], reported several studies concerning the electrochemical oxidation of landfill leachate using BDD anodes. In these studies, the effect of the applied current density, the initial concentration of chloride ions, the treatment time and the initial pH were analyzed. They reported that the electro-oxidation process of landfill leachate with BDD anodes is an efficient technology that is able to completely oxidize the organic matter and almost all ammonia under appropriate conditions. Their results showed that organic matter and ammonia oxidation are highly influenced by the applied current density, indicating a change in the mechanism of the organic matter oxidation when high current densities are applied. Moreover, the concentration of chloride has an effect on the oxidation of ammonia, and chloride ions compete with organic matter to be oxidized at the anode. Similar conclusions were reported by Cabeza *et al.* (2007 a and b) and Urtiaga *et al.* (2012). These authors observed that ammonium oxidation occurs at a slower rate than chemical oxygen demand (COD) decay and that chlorine evolution is enhanced at lower COD values, causing the indirect oxidation of ammonium. These authors also observed that when additional chloride ions were provided, the treatment efficiency increased.
The formation of inorganic oxidation by-products during the electrocatalytic treatment of ammonium from landfill leachates with BDD anodes was assessed by Pérez and co-workers [Pérez et al., 2012]. It was found that ammonium oxidation leads to the formation of nitrogen gas and nitrate as the main oxidation products. Higher chloride concentrations have a positive

influence on the formation of nitrogen as the main oxidation product. When high chloride concentrations (5-20 g L^{-1}) were used in the presence of ammonium, chloride remained almost constant because it was regenerated during the indirect oxidation reactions.

Other studies performed with BDD anodes [Fernandes *et al.*, 2012; Fernandes *et al.*, 2013; Urtiaga *et al.*, 2009; Urtiaga *et al.*, 2012] confirm that the anodic oxidation can be an efficient alternative/complement to treat sanitary landfill leachates. However, despite these good results, BDD anodes present a significant disadvantage: they are expensive. Thus, the use of different electrode materials that are less costly than BDD for the electrochemical oxidation of sanitary landfill leachates has been reported by several authors. Cossu *et al.* (1998) described the electrochemical oxidation of a landfill leachate with two different anode materials, Ti/PbO_2 and Ti/SnO_2. No significant differences were found in the behaviors of the two anode materials. An average current efficiency of 30% was measured for a decrease of COD from 1200 to 150 mg L^{-1}. The results indicated that the organic load was removed by both direct and indirect oxidation. Indirect oxidation by chlorine or hypochlorite originated from chloride oxidation was believed to be responsible for the nitrogen removal.

The indirect oxidation effect in the electrochemical oxidation treatment of landfill leachate using different anode materials was also studied by Chiang et al. (1995). These authors observed that the electrocatalytic behavior of the anode material strongly affects the chlorine/hypochlorite production efficiency. Moreover, there is a correlation between the COD removal efficiency and chlorine/hypochlorite production, and because COD and ammonium were removed simultaneously by the indirect oxidation effect during electrolysis, there is a competition between the removal of COD and ammonium.

Panizza *et al.* (2010) reported the anodic oxidation of a real leachate using a lead dioxide anode. The results indicated that the organic compounds were mainly removed by indirect oxidation by the active chlorine generated from chloride oxidation.

A comparative study between different anode materials, including Ti–Ru–Sn ternary oxide, PbO_2 and BDD, for the electrochemical oxidation of a landfill leachate was also performed [Panizza and Martinez-Huitle, 2013]. The experimental results indicated that after 8 h of electrolysis, the Ti-Ru-SnO_2 anode yields only 35% COD, 52% color and 65% ammonium removal. Using PbO_2, ammonium and color were completely removed, but residual COD was present. On the contrary, BDD enables complete COD, color and ammonium removal and also exhibits greater current efficiency along with a significantly lower energy cost compared to the other electrodes.

Most of the PbO_2 and SnO_2 electrodes implemented in previous studies used a titanium foil substrate that may oxidize during the anodic oxidation of the leachates, leading to the formation of an insulating titanium oxides layer that inactivates the electrode [Montilla *et al.*, 2004; Río *et al.*, 2009]. This insulating layer may be avoided by depositing a Pt layer over the titanium foil prior to deposition of the metallic oxide [Andrade *et al.*, 2007]. The anode materials thus obtained, Ti/Pt/PbO_2 and Ti/Pt/SnO_2-Sb_2O_4, have been successfully prepared and used by our research group in the electrochemical degradation of several pharmaceutical drugs [Ciríaco *et al.*, 2009; Santos *et al.*, 2013].

4.4.2 Experimental details

4.4.2.1 Samples preparation and characterization

The landfill leachate used in this study was collected from the intermunicipal sanitary landfill facility of Cova da Beira, Portugal. This site, which serves a population of over 220,000 inhabitants in 13 municipalities, has an onsite facility capable of treating up to 50 m^3 of leachate daily. The raw leachate was initially treated on site by an activated sludge process. The characteristics of the biologically pretreated leachate are presented in Table 3.

Simulated samples were prepared as follows: NH_4NO_3 - 0.232 g, NH_4Cl - 1.605 g, $CaCl_2$ - 0.7 g, $MgCl_2.6H_2O$ - 1.42 g, NaCl - 2.472 g and KCl - 2.0986 g and distilled water up to 1 L.

Table 3. Physicochemical characteristics of the biologically pre-treated leachate studied.

Property	Mean value (±SD*)
COD / g L^{-1}	6.2 ± 0.4
BOD_5 / g L^{-1}	0.80 ± 0.09
BOD_5/COD	0.13 ± 0.02
DOC / g L^{-1}	2.06 ± 0.02
TN / g L^{-1}	0.82 ± 0.09
TKN / g L^{-1}	0.78 ± 0.06
AN / g L^{-1}	0.48 ± 0.08
Nitrate / g L^{-1}	0.08 ± 0.01
Nitrite / g L^{-1}	0.30 ± 0.07
Chloride / g L^{-1}	4.7 ± 0.2
pH	9.0 ± 0.1
Conductivity / mS cm^{-1}	22.0 ± 1.2

*SD – Standard deviation

4.4.2.2 Electrodegradation experiments

Experiments were conducted in batch mode, with stirring, using 200 mL of solution. A 10 cm^2 Ti/Pt/SnO_2-Sb_2O_4 electrode was used as anode, and 10 cm^2 stainless steel foil was used as cathode, being the gap between them 2.0 cm. Ti/Pt/SnO_2-Sb_2O_4 electrode was prepared as described in the section 3.2 [Santos *et al.*, 2013]. Experiments were conducted at an applied current intensity of 0.3 A, at room temperature (22-25 ºC) without the addition of a background electrolyte. A Multimetrix XA 3033 unit was used as the power supply.

Simulated samples were prepared as follows: NH_4NO_3 - 0.232 g, NH_4Cl - 1.605 g, $CaCl_2$ - 0.7 g, $MgCl_2.6H_2O$ - 1.42 g, NaCl - 2.472 g and KCl - 2.0986 g and distilled water up to 1 L.

All the electrochemical tests were performed at least in triplicate. The mean values are presented for the parameters used to follow the assays: COD, DOC, TN, TKN, AN, and chloride, nitrate and nitrite concentrations.

4.4.3 Results and discussion

Figure 24, a and b, presents the results for the variation with time of the normalized COD and DOC obtained from the experiments performed with Ti/Pt/SnO_2-Sb_2O_4 anode. The variation of the normalized COD with electrical energy consumption is also presented (Figure 24 d). It can be observed that DOC removal was lower than COD removal. This behavior has been reported previously in the literature and has been explained by the formation of low molecular weight organic compounds with high degrees of oxidation that resist to further oxidation [Anglada *et al.*, 2009; Fernandes *et al.*, 2012]. The conversion of the organic matter into more oxidized by-products rather than resulting in mineralization promoted by Ti/Pt/SnO_2-Sb_2O_4 anodes must be due to the fact that hydroxyl radicals are expected to be strongly adsorbed on the electrode's surface.

When experimental COD evolution with time (Figure 24 c) is compared with the theoretical trend Eq. (7) according to the model previously proposed in the literature for electrolysis under current limited control [Panizza *et al.*, 2001], where I is the current intensity in A, F is the Faraday constant and V is the volume in m^3, it can be seen that the experimental results obtained for Ti/Pt/SnO_2-Sb_2O_4 are slightly better. This result is due to the electrocatalytic effect of the platinum because despite being covered by the metal oxides, platinum peaks are always detected by X-ray diffraction [Ciríaco *et al.*, 2009; Santos *et al.*, 2013], probably due to the porosity of the oxide film.

$$\mathrm{COD}(t) = \mathrm{COD}_0 - \frac{I}{4\,F\,V}\,t \qquad (7)$$

When the normalized COD is plotted against the electrical energy consumption (Figure 24 d) calculated based on the potential difference mean values, which was 6.2 V, an increase in the energy consumption with COD decay can be observed. This happens for two main reasons: the easier degradable compounds goes first, and as the assay proceeds, the effect of mass transportation becomes more important, reducing COD removal rate.

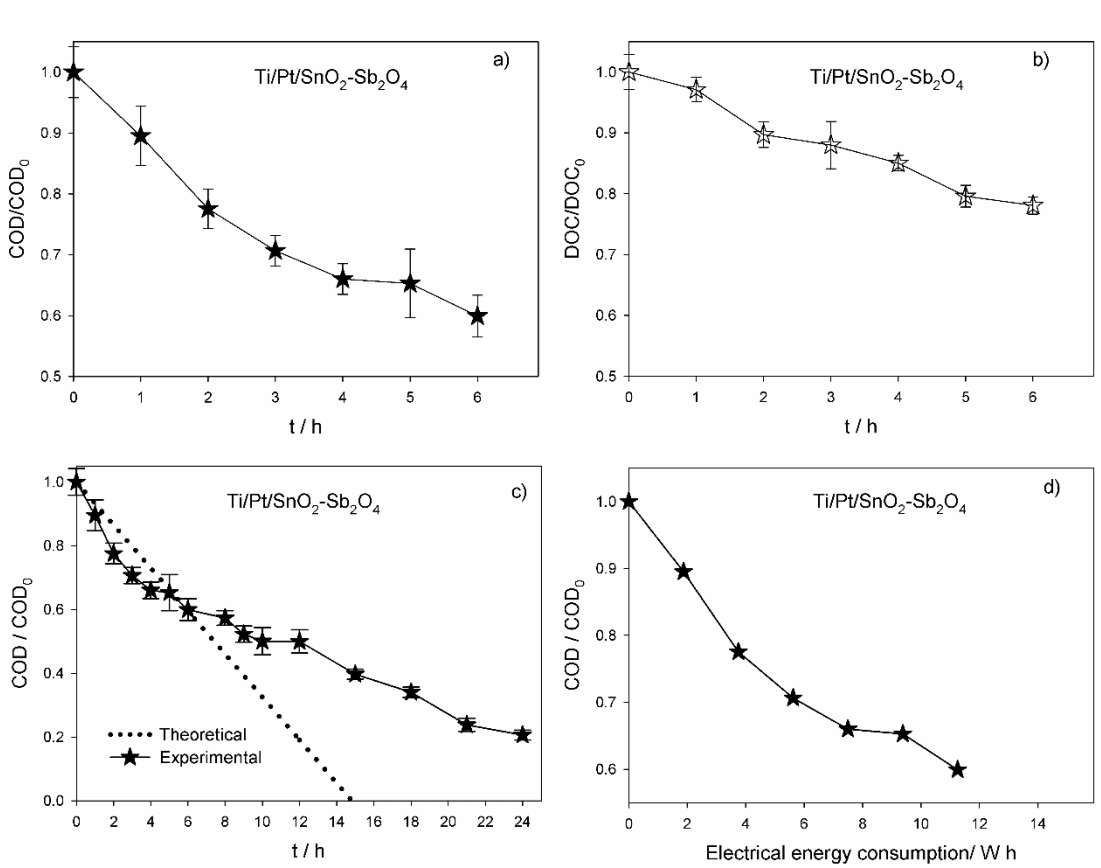

Figure 24. Variation with time of the normalized (a) COD and (b) DOC for the anodic oxidation experiments performed with real leachate using a Ti/Pt/SnO_2-Sb_2O_4 anode, (c) comparison of real and theoretical COD decays with time for a 24 h assay and (d) variation of the normalized COD with electrical energy consumption. Error bars refer to the standard deviation of the normalized mean values.

Figure 25 shows the results obtained for the nitrogen removal in the experiments performed with real leachate, where similar TN and TKN decays can be observed. AN removal is more pronounced, especially in the last hours of the assays, showing that Ti/Pt/SnO_2-Sb_2O_4 anodes are more effective in the removal of the ammonium nitrogen.

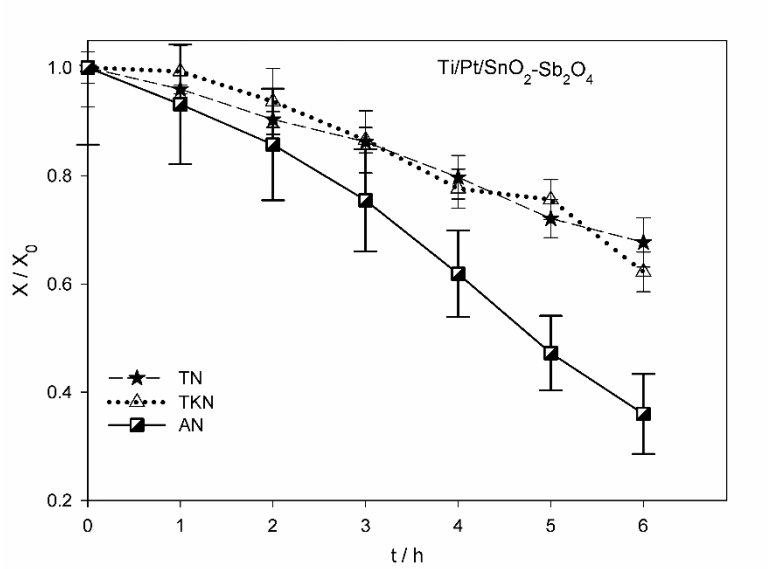

Figure 25. Variation with time of the normalized TN, TKN and AN for the anodic oxidation experiments performed with real leachate using Ti/Pt/SnO_2-Sb_2O_4 anodes. Error bars refer to the standard deviation of the normalized mean values.

Comparing the COD (Figure 24 a) and AN (Figure 25) profiles during the anodic oxidation runs, AN removal occurs at a slower rate than that of COD during the first 3 hours of the assays. However, when the COD value decreases to approximately 70% of the initial concentration, the AN removal rate increases. Similar results can be found in the literature. Cossu *et al.* (1998), using a Ti/Pt anode, reported that the removal rate of AN was lower than that of COD at the initial stage of electro-oxidation and that AN was substantially removed in the subsequent electrochemical oxidation stage when indirect oxidation became prevalent. This increase in indirect oxidation may be enhanced by the formation of HClO or chlorine from chloride [Anglada *et al.*, 2009; Chiang *et al.*, 1995]. According to Chiang *et al.* (1995) ammonium reacts with HClO through the following ''breakpoint reactions'' that regenerate chloride ions:

$HClO + NH_4^+ \rightarrow NH_2Cl + H_2O + H^+$ (8)

$HClO + NH_2Cl \rightarrow NHCl_2 + H_2O$ (9)

$NHCl_2 + H_2O \rightarrow NOH + 2H^+ + 2Cl^-$ (10)

$NHCl_2 + NOH \rightarrow N_2 + HClO + H^+ + Cl^-$ (11)

In fact, chloride concentration, determined by ionic chromatography, is always higher for the assays performed with Ti/Pt/SnO_2-Sb_2O_4 anode (Figure 26 a), indicating that this ion may be involved in the oxidation of ammonium and may be regenerated after that process. Additionally, this metal oxide anode is very effective in total nitrogen removal, showing that nitrogen gas is being formed at a high rate, being very effective at partially oxidizing ammonia to nitrate (Figure 26 b) [Cabeza *et al.*, 2007a]. Regarding nitrites (Figure 26 c), they are completely eliminated during the anodic oxidation.

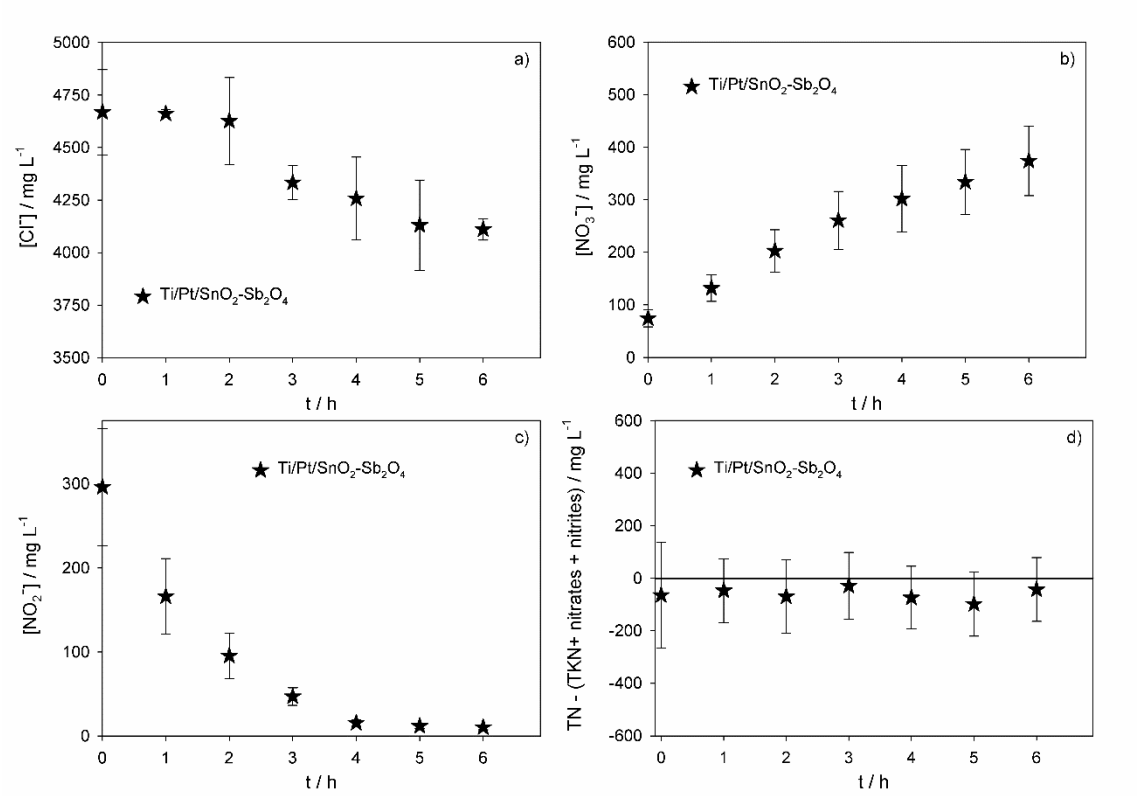

Figure 26. Variation with time of (a) Cl^-, (b) NO_3^- and (c) NO_2^- concentrations, determined by ionic chromatography, for the anodic oxidation experiments performed with real leachate using a Ti/Pt/SnO_2-Sb_2O_4 anode. (d) Mass balance of the different forms of nitrogen determined in solution during the assays. Error bars refer to the standard deviation of the mean values.

The mass balance to all nitrogen forms determined during the assays performed with the different electrode materials is presented in Figure 26 d. A discrepancy is observed only for the final period of the assays, although the zero value is always contained in the interval of the value±SD.

Biochemical oxygen demand after 5 days of incubation was determined for samples obtained after 6 h of electrochemical treatment with Ti/Pt/SnO_2-Sb_2O_4 anodes, and a value of 0.40 ± 0.05 g L^{-1} was obtained. This value led to BOD_5/COD ratio of 0.11 ± 0.02, indicating that the biodegradability of the samples after 6 h of anodic oxidation did not improve, and was even slightly worse. This issue occurs because matter that is more difficult to electrolyze is also less biodegradable and because the presence of chlorine/hypochlorite may also alter the BOD_5 results, since these species can deactivate microorganisms responsible for the biodegradation. After the electrochemical treatment, there were reductions of 42% in the absorbance measured at 275 nm and reductions of 8.6% in the conductivity for the assays performed with Ti/Pt/SnO_2-Sb_2O_4 anodes. The reduction in the absorbance is due to the removal/degradation of aromatic structures by anodic oxidation in materials with high oxygen evolution potentials that produce high concentrations of hydroxyl radicals [Panizza *et al.*, 2001], whereas the decrease in conductivity is due to metal deposition over the cathode, caused by the cathodic reduction of the metal ions present in the leachate samples, and also due to the elimination of other ions,

like ammonium to give nitrogen gas [Fernandes *et al.*, 2014b]. Regarding the pH variation during the assays, it was almost constant, within an acceptable range for experimental error.

To understand the effect of organic matter on the elimination of ammonium nitrogen, assays were run using simulated solutions containing chloride, nitrates and ammonium in concentrations similar to those encountered in the leachate samples. The results are presented in Figure 27. The elimination rate of chloride is enhanced because there is no competition with the organic matter for oxidation. In contrast, hydroxyl radicals are free to convert ammonium, which does not participate in equations (8) to (11) and which does regenerate chloride ions. Also, removals in ammonium and total nitrogen are increased and nitrate formation rate is decreased, showing that this metal oxide is effective in the complete elimination of nitrogen from solution via the partial oxidation of ammonium to nitrogen.

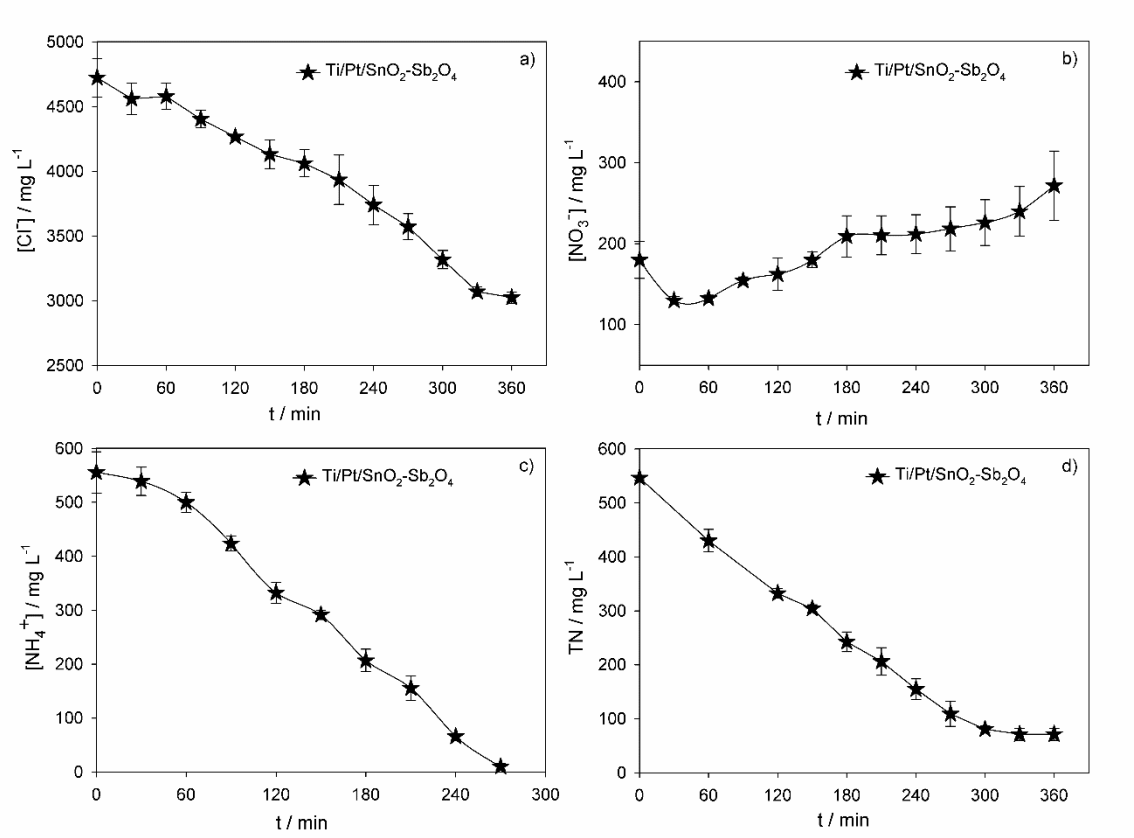

Figure 27. Variation with time of (a) Cl^-, (b) NO_3^-, (c) NH_4^+ and (d) TN concentrations for the anodic oxidation experiments performed with the simulated sample using a $Ti/Pt/SnO_2$-Sb_2O_4 anode. Error bars refer to the standard deviation of the mean values.

After the electrochemical treatment performed with this simulated solution, there were reductions in conductivity of approximately 20% for the assays performed, due to the oxidation of species with high conductivity, such as ammonium and chloride, and the formation of nitrate, which has lower conductivity than ammonium. The increase in pH (from 6.1 ± 0.1 to 7.5 ± 0.1) also contributed to the decrease in conductivity.

4.4.4 Conclusions

Ti/Pt/SnO_2-Sb_2O_4 anodes, which had already been used with good results in the degradation of pharmaceutical compounds [Ciríaco *et al.*, 2011], prove to be also very effective in the degradation of very complex mixtures, such as leachates from sanitary landfills. Its effectiveness was proved with COD removal rates higher than the theoretical one. Also, it can be a good material for the elimination of N-containing compounds, with a good TN removal, which means that part of the nitrogen is eliminated as nitrogen forms. It also promotes elimination of the organic load by indirect oxidation with chlorine oxidizing species. Although a Pt layer makes the material more expensive than a Ti/SnO_2-Sb_2O_4 anode, and a less efficient in the COD removal [Santos *et al.*, 2013], it can strategically increase the electrode lifetime; the electrodes used in this work were tested for more than 1000 h.

When the results of the oxidation ability to remove nitrogen and organic load from biologically pretreated sanitary landfill leachates obtained with Ti/Pt/SnO_2-Sb_2O_4 anodes are compared with those from Ti/Pt/PbO_2, and BDD [Fernandes *et al.*, 2014a; Fernandes, 2014] the following conclusions can be drawn:

- They all present similar COD removal kinetics, although BDD anode promotes the highest DOC removal, leading to a higher mineralization degree. This must be due to its inert surface where hydroxyl radicals, responsible for the indirect oxidation, are less strongly adsorbed than at the metal oxides surfaces.
- Ti/Pt/SnO_2-Sb_2O_4 promotes TN and AN removals higher than BDD and lower than Ti/Pt/PbO_2. This effect occurs because at metallic oxides, the partial oxidation of ammonium to nitrogen gas occurs, whereas for BDD, ammonium is oxidized to nitrate. On the other hand, it shows lower appetency than BDD shows for TKN removal.
- Metallic oxide anodes demonstrate low energy consumption because they are more conductive than BDD and also due to the electrocatalytic effect of the oxides.

Thus, Ti/Pt/SnO_2-Sb_2O_4 can be a good alternative as anode materials for the treatment of sanitary landfill leachates.

4.5 Electrochemical oxidation of humic acid and sanitary landfill leachate: Influence of anode material, chloride concentration and current density

Following the study presented in section 4.4 of this thesis, Ti/Pt/SnO_2-Sb_2O_4 electrode was utilized to study the influence of the applied current density and of the chloride ion concentration on the oxidation of a raw sanitary landfill leachate and, to better understand the influence of the experimental conditions on the elimination of organic matter and nitrogen in the presence of recalcitrant compounds, synthetic samples containing humic acid and inorganic salts, with COD and ammonium ion contents similar to that of the real leachate, were also prepared and subjected to electro-oxidation. Humic acid was chosen to prepare the synthetic samples because it has recalcitrant properties and, according to the literature, sanitary landfill leachates present a high content in humic substances [Bhalla *et al.*, 2013; Foo and Hameed, 2009; Kang *et al.*, 2002]. Besides humic acid, synthetic samples contained as nitrogen and chloride sources ammonium sulfate and ammonium chloride.
This study was already published in specialized literature [Fernandes *et al.*, 2016].

4.5.1 Introduction

Electrochemical oxidation is the most popular electrochemical procedure for removing organic pollutants from wastewaters (Brillas and Martínez-Huitle, 2015) and its application in the treatment of complex effluents, such as sanitary landfill leachates, has been reported by numerous authors with promising results (Anglada *et al.*, 2009, 2010a, 2010b, 2011; Fernandes *et al.*, 2012, 2014a, 2014b, 2015; Panizza and Martinez-Huitle, 2013; Panizza *et al.*, 2010; Pérez *et al.*, 2012; Turro *et al.*, 2011; Urtiaga *et al.*, 2012). Since the anode material strongly influences the selectivity and the efficiency of the EO process (Brillas and Martínez-Huitle, 2015), different anode materials have been investigated, being the highest organic oxidation rates and the highest current efficiencies attained with boron-doped diamond electrodes (Anglada *et al.*, 2009; Fernandes *et al.*, 2015). This is due to the chemical, physical and electrochemical outstanding properties of this anode material, when compared with other conventional electrode materials (Fryda *et al.*, 1999; Panizza and Cerisola, 2005). Removals of 100% in chemical oxygen demand and ammonium nitrogen contents have been achieved for the EO of sanitary landfill leachates using BDD anodes (Anglada *et al.*, 2010b; Cabeza *et al.*, 2007a, 2007b). However, despite the BDD electrodes exceptional properties and the good results obtained when this electrode is used, the most common BDD electrodes are Si-supported, which present difficulties related to their industrial transposition, due to the fragility and the relatively low conductivity of the Si substrate (Brillas and Martínez-Huitle, 2015). BDD films synthesized on Nb, Ta and W have also shown promising results, but their large-scale utilization is impossible due to the unacceptably high costs of these metal substrates (Brillas and Martínez-

Huitle, 2015). Therefore, it is necessary to study the application of new electrode materials that can successfully remove the pollutants with lower capital and operational costs. Among the different electrode materials studied for the EO process, metal oxides have shown promising results, even when used to treat complex effluents such as sanitary landfill leachates (Chiang *et al.*, 1995; Cossu *et al.*, 1998; Feki *et al.*, 2009; Fernandes *et al.*, 2014a; Panizza *et al.*, 2010; Panizza and Martinez-Huitle, 2013). A study comparing BDD and two different metallic oxides anodes, Ti/Pt/PbO_2 and Ti/Pt/SnO_2-Sb_2O_4, in the EO of a sanitary landfill leachate showed that metal oxides anodes promoted COD removals similar to that of BDD and lower energy consumptions, although the difference between the COD and dissolved organic carbon removals for BDD was less pronounced than for the other anodes, suggesting that BDD promotes more easily the complete combustion of the organic matter (Fernandes *et al.*, 2014a). Also, regarding nitrogen removal, metal oxide anodes were found to be more effective in the ammonium removal, whereas BDD was more efficient in the organic nitrogen removal (Fernandes *et al.*, 2014b). In a similar study, Panizza and Martinez-Huitle (2013) compared the performance of BDD, PbO_2 and Ti-Ru-SnO_2 and different results were achieved, since BDD yielded complete COD, color and AN removal, whereas with PbO_2 a residual COD remained and, when Ti-Ru-SnO_2 was used, the organic pollutants were only partially oxidized. Also, faster oxidation rate, higher current efficiency and lower specific energy consumption were achieved using the BDD anode, resulting, consequently, in lower treatment costs (Panizza and Martinez-Huitle, 2013). Although the results presented by Fernandes *et al.* (2014a) and Panizza and Martinez-Huitle (2013) were different, it must be noticed that whereas the leachate samples used by the first authors presented COD/AN/chloride concentrations of 6200/480/4700 mg L^{-1}, the leachate samples used by the second authors only had 780/266/1800 mg L^{-1}. Also, the lead and stannous electrodes used by Fernandes *et al.* (2014a) had a Pt layer between the titanium foil and the metallic oxide, which was not the case of the electrode used in the other study.

Besides the anode material, applied current density and chloride ion concentration also have shown to play an important role in the EO performance. Several authors reported an increase in COD and AN removals by increasing the applied current density or the chloride ion concentration (Anglada *et al.*, 2009, 2011; Bashir *et al.*, 2009; Cabeza *et al.*, 2007a, 2007b; Chiang *et al.*, 1995; Cossu *et al.*, 1998; Feki *et al.*, 2009; Moraes and Bertazzoli, 2005; Pérez *et al.*, 2012; Turro *et al.*, 2011; Zhang *et al.*, 2010, 2011). In a study performed by Anglada *et al.* (2009), it was observed that an increase in the current density from 300 to 450 A m^{-2} scarcely affected the removal rate of the organic matter, but at higher current densities the oxidation levels increased with current density, which suggested a change in the oxidation mechanism of the organic matter, since at high current densities mediated electrochemical oxidation processes, such as indirect oxidation by hydroxyl radicals and by other electrogenerated oxidants, had a strong influence. Also, the influence of the applied current density was much more significant in the ammonium oxidation than in the COD removal, even if ammonium removal occurred at a slower rate than that of COD. Different results were achieved by Zhang *et al.* (2010 and 2011) that reported an increase in the COD removal with increasing current

density, but only up to a certain value of current density, from which a further increase would lead to a decrease in the COD removal rate. This behavior was explained by the authors taken into account that, at lower current densities, organic matter anodic oxidation with hydroxyl radicals was favored against chlorine evolution at the anode, and thus the increase in current density would lead to the increase in COD removal rate. However, a further increase in the current density would enhance chlorine generation and hence the anodic oxidation with hydroxyl radicals would be depressed. In the meantime, the AN removal would be dominant in the competition between AN and COD removal by the indirect oxidation, via active chlorine, and, consequently, COD removal rate would decrease with current density (Zhang *et al.*, 2010 and 2011). The effect of the indirect oxidation through chlorine/hypochlorite species in the EO treatment of landfill leachates had already been studied by Chiang *et al.* (1995) that provided additional chloride ions to the leachate as supporting electrolyte during the electrolysis. The experimental results showed that when 2.5 g L^{-1} chloride was added, both COD and AN removal rates increased, being the AN removal rate much higher than that of COD.

Pérez *et al.* (2012) identified nitrogen and nitrate as the main ammonium oxidation products obtained in the EO of a landfill leachate with a BDD anode: for high chloride concentration, nitrogen gas was the main product, having the percentage of ammonium transformed into nitrogen gas increased from 74 to 85%, after 4 hours, when the chloride content was increased from 5 to 20 g L^{-1}, while the percentage of ammonium converted into nitrate varied from 26% to 15%. Also, the formation of chloramines, chlorate and perchlorate was hindered by increasing the initial concentration of chloride ions.

Since the difficulties in treating complex effluents such as landfill leachates is associated to the presence of persistent organic pollutants, the oxidation of synthetic wastewaters with different test substances has been investigated. The electrochemical oxidation of synthetic solutions, containing glucose and humic acid using BDD anodes was performed by Woisetschläger *et al.* (2013) and the results showed that the degradation process was increasingly inhibited by the increase in the amount of humic acid. According to these authors, during the electrochemical oxidation, hydroxyl radicals primarily react with organic substances to form partially oxidized intermediate products and carbon dioxide. Retardation and inhibition of these reactions due to mass transport limitations or because of the low reactivity of constituents will preferably lead to the decomposition of hydroxyl radicals as gaseous oxygen. As a consequence, the dissolved oxygen content increases, leading to low current efficiency and COD removal.

4.5.2 Experimental details

4.5.2.1 Sanitary landfill leachate and humic acid synthetic samples

The landfill leachate samples (L) used in this study were collected from an intermunicipal sanitary landfill facility in Portugal. This site, with an area of approximately 7 ha, is sealed since 2003. The leachate samples were collected in the stabilization lagoon, before any kind of

treatment, and were kept refrigerated until their use, in order to maintain their initial characteristics. L samples characterization was performed just after the collection and just before their use in experiments and no significant differences on the parameter values were found. The characteristics of the landfill leachate are presented in Table 4. No nitrite or nitrate were detected in the L samples.

In the electrodegradation assays, besides the raw leachate samples, L samples with added chloride (2 g L^{-1}) were also assayed.

The synthetic samples (S), were prepared as aqueous solutions of humic acid and inorganic salts presented COD and NH_4^+ contents similar to the real landfill leachate samples. The inorganic salts utilized were ammonium sulfate, ammonium chloride and potassium chloride, to provide the necessary amounts of ammonium and chloride. Different Cl^- contents were tested, from 0 to 4.5 g L^{-1}. Table 5 summarizes the composition of the different S samples used in the experiments and Table 4 presents the physicochemical characteristics of the S samples before the chloride addition.

All the reagents used were of analytical grade and were purchased from Sigma Aldrich and used without additional purification.

Table 4. Physicochemical characteristics of humic acid and landfill leachate samples used in the study.

Parameter	Mean value (±SD*)	
	Humic acid (S)	Leachate
COD / g L^{-1}	3.7 ± 0.2	3.5 ± 0.2
BOD_5 / g L^{-1}	[a]	0.96 ± 0.08
BOD_5/COD	[a]	0.27 ± 0.04
DOC / g L^{-1}	1.2 ± 0.2	1.0 ± 0.2
TN / g L^{-1}	2.3 ± 0.1	2.0 ± 0.2
TKN / g L^{-1}	[a]	1.9 ± 0.1
[NH_4^+] / g L^{-1}	2.8 ± 0.2	2.5 ± 0.4
[Cl^-] / g L^{-1}	0.08 ± 0.02	2.5 ± 0.2
[Humic acid] / g L^{-1}	3.30 ± 0.01	0.26 ± 0.01
pH	8.4 ± 0.2	8.0 ± 0.1
Conductivity / mS cm^{-1}	16.1 ± 0.2	22.0 ± 0.4

*SD – Standard deviation; [a] Not determined.

Table 5. Composition of the humic acid aqueous synthetic samples (S) used in the experiments.

$[Cl^-]_{added}$ / g L^{-1}	S samples composition / g L^{-1}
0	Humic acid – 3.300 $(NH_4)_2SO_4$ – 10.278
2.5	Humic acid – 3.300 $(NH_4)_2SO_4$ – 5.618 NH_4Cl – 3.768
4.5	Humic acid – 3.300 $(NH_4)_2SO_4$ – 5.618 NH_4Cl – 3.768 KCl – 4.206

4.5.2.2 Electrodegradation experiments

Experiments were conducted in batch mode, with stirring, using 200 mL of solution. A 10 cm^2 Ti/Pt/SnO_2-Sb_2O_4 plate was used as anode, and 10 cm^2 stainless steel plate was used as cathode, with a 2.0 cm gap between them. Assays were performed with synthetic and real leachate samples at applied current densities of 300 and 700 A m^{-2}, using a GW, Lab DC, model GPS-3030D (0–30 V, 0–3 A) as power supply. Synthetic and leachate samples with different chloride concentrations were assayed.

All the electrochemical tests were performed at least in duplicate. The mean values are presented for the parameters used to follow the assays: COD, DOC, TN, TKN, AN, and chloride, nitrate and nitrite concentrations.

4.5.3 Results and discussion

Figure 28 present the results for the variation with time of COD and DOC for the experiments performed with synthetic and sanitary landfill leachate samples, with different initial Cl^- concentrations and for the different applied current densities, utilizing as anode material Ti/Pt/SnO_2-Sb_2O_4. For L samples, the chloride concentration of 2.5 g L^{-1} corresponds to samples where no chloride was added, since this was the chloride concentration in the raw leachate (Table 4).

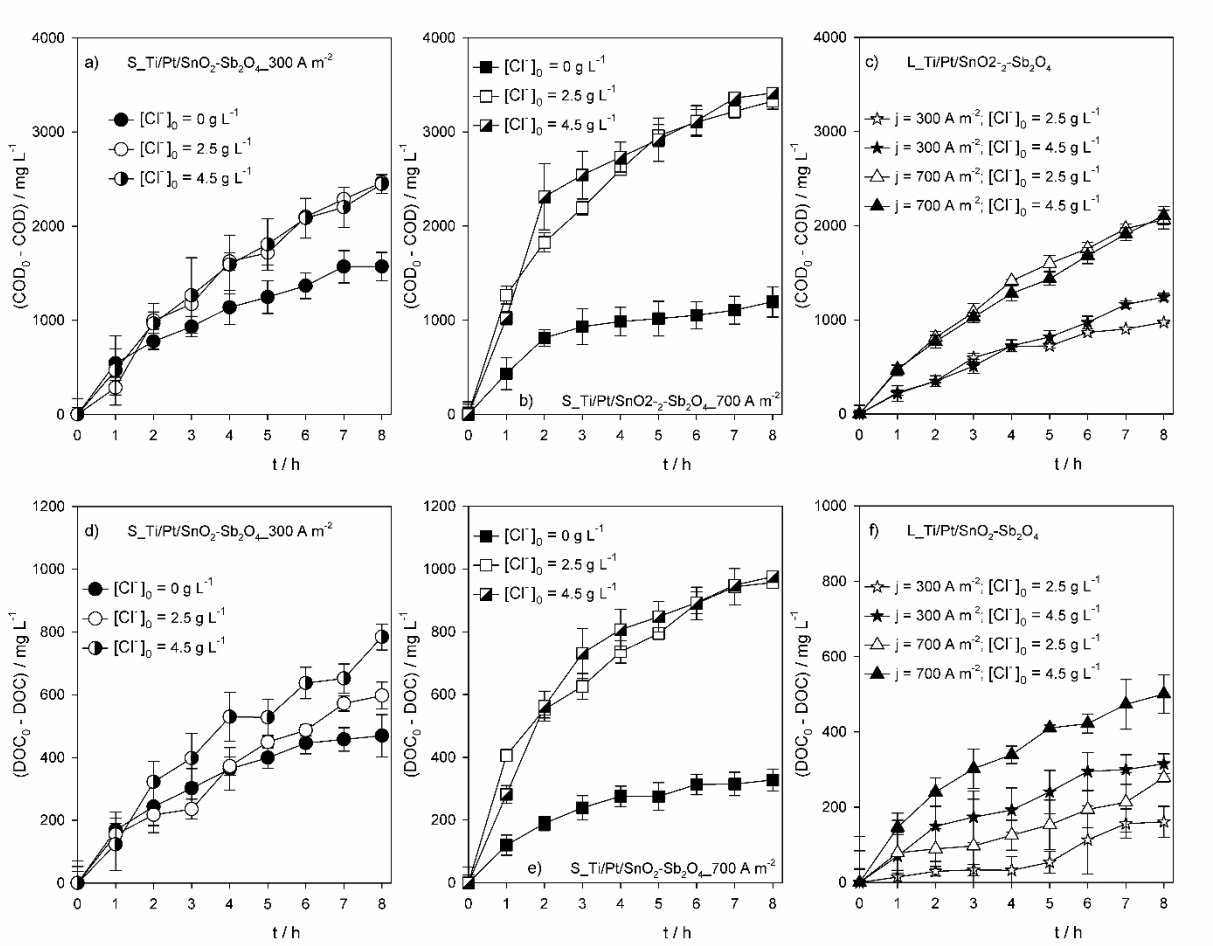

Figure 28. Variation with time of the COD (a,b,c) and DOC (d,e,f) removed in the electrodegradation experiments performed with synthetic (S) and leachate (L) samples using Ti/Pt/SnO_2-Sb_2O_4 anode, at two applied current densities, 300 and 700 A m^{-2}, and different initial chloride contents.

Figure 28, a to c, shows that when S samples were used, for both applied current densities studied, the presence of Cl^- influenced the COD removal, since in the assays without chloride COD removal rate was much lower than for the assays performed with the addition of chloride. However, the increase in chloride initial concentration from 2.5 to 4.5 g L^{-1} did not introduce meaningful changes in the COD removal rates, at both applied current densities, meaning that the increment on the chloride concentration did not significantly increase the indirect oxidation through chlorine/hypochlorite. This fact must be related with an optimum COD/[Cl^-] ratio, and an extra addition of chloride does not result in an increase in COD removal rate, because part of the applied current is spent in the chloride oxidation and intermediate compounds more resistant to oxidation may also be formed, in particular at low j. In fact, according to the medium mass transfer coefficients presented in the literature for leachate samples (Anglada *et al.*, 2011; Fernandes *et al.*, 2012), the current densities used are lower than the limiting current density for the initial COD value (738 A m^{-2} < j_{lim} < 1156 A m^{-2}). Thus, the process is under kinetic control most of the time, and only when COD removals are high the process becomes diffusion controlled.

The inexistence of a positive effect due to the increase in [Cl^-] from 2.5 ad 4.5 g L^{-1} was also observed for the L samples, where the effect of the current density was much more significant

than the increase in chloride concentration. Regarding the influence of the current density, for the assay performed with S samples without chloride, COD removal rate decreased with j. This behavior has been reported in the literature and has been explained by the increased production in oxidizing species with the operating current density (Chiang *et al.*, 1995). The existence of such species is determinant due to the growing relevance of the diffusional step with j. Thus, for $[Cl^-]$ = 0 g L^{-1}, the decrease in COD removal with the increase in j may be related with an enhanced oxygen evolution at higher j that may hinder the mass transfer process and the adsorption of the reacting species on the electrode surface. In fact, due to the influence of the platinum interlayer and to the higher porosity of this material, the hydroxyl radicals, with more expression at higher j, are more strongly adsorbed at the anode surface, enhancing their decomposition as gaseous oxygen. Regarding the slightly lower COD removal rate obtained with this material in the treatment of L samples, a similar behavior was also observed by Zhang *et al.* (2010 and 2011), due to an enhancement in the active chlorine generation that reduces the anodic oxidation with hydroxyl radicals.

Concerning DOC removal for S samples, for j = 300 A m^{-2} (Figure 28d) there is a regular influence of the chloride initial concentration. This fact is due to the organic matter random oxidation in the bulk of the solution promoted by the active chlorine, formed by the chloride oxidation, that leads to low mineralization when the chloride initial concentration is low, being more oriented to COD removal. At higher initial chloride concentration, the excess in active chlorine promotes the compounds complete oxidation, leading to higher mineralization degree. The increase in the formation of the active chlorine with chloride initial concentration can be observed by the chloride concentration decay during the electrolysis (Figure 29), which increases with chloride initial concentration and with applied current density. Although for 700 A m^{-2} the differences in the chloride concentration decay still exists, chloride concentration of 2.5 g L^{-1} must be enough to indirectly oxidize most of the organic matter present in the S samples, being the effect of the chloride initial concentration in DOC removal (Figure 28, d to f) similar to what was observed for the COD removal rate.

In the DOC removals in time, for most of the S samples, there are sudden changes in the curves' slope. This is due to the formation of a precipitate, associated with a sharp drop in the pH of the solution (Figure 30), observed for the assays performed with S samples containing chloride. The formation of the precipitate interferes with DOC determination because the samples are filtered before analysis. The precipitation occurrence was enhanced by the increase in the Cl^- initial concentration and applied current density. The reason why the pH drop was only observed in the S samples could be the buffer effect caused by carbonate in the leachate samples (Chiang *et al.*, 1995).

Regarding DOC removals for L samples (Figure 28, f), it can be observed that the increase in chloride initial concentration leads to an increase in the mineralization degree, since the effect of the increase in chloride initial concentration was obvious in the DOC removal and was insignificant in the COD removal.

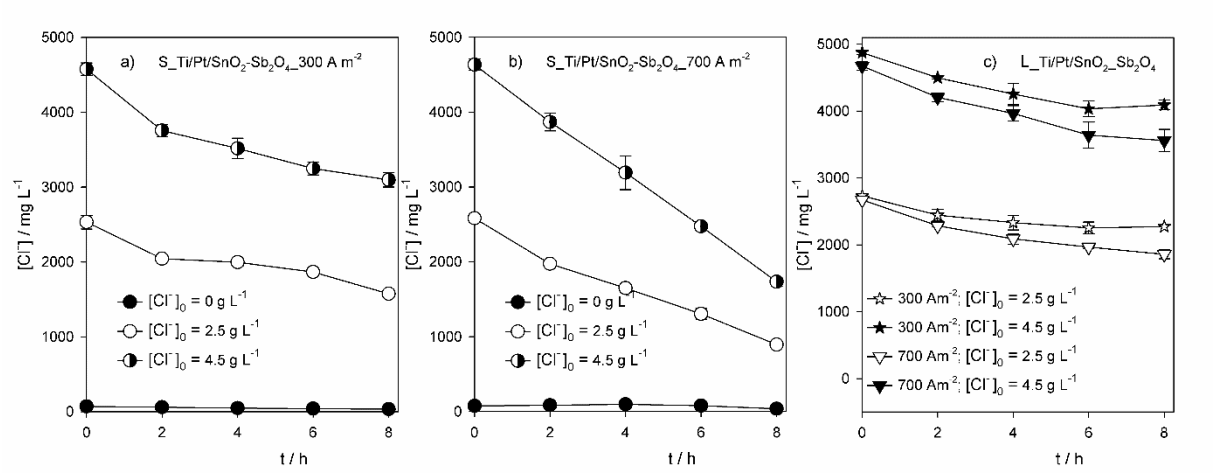

Figure 29. Variation with time of the chloride concentration during the electrodegradation experiments performed with synthetic (S) and leachate (L) samples using Ti/Pt/SnO_2-Sb_2O_4 anode, at two applied current densities, 300 and 700 A m^{-2}, and different initial chloride contents.

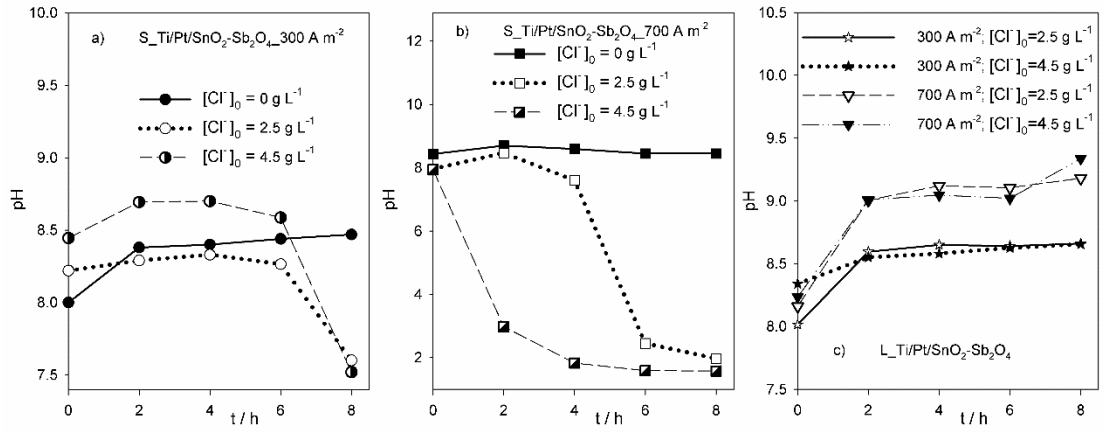

Figure 30. Variation with time of the pH value during the electrodegradation experiments performed with synthetic (S) and leachate (L) samples using Ti/Pt/SnO_2-Sb_2O_4 anode, at two applied current densities, 300 and 700 A m^{-2}, and different initial chloride contents.

When the variation of ammonia and total nitrogen forms present in the samples is analyzed (Figure 31, a to f), at any applied current density, it can be seen that, for S samples without added Cl^-, no significant removal of the ammonium ion was observed, showing that NH_4^+ removal takes place mainly by indirect oxidation through chlorine/hypochlorite species. Another possible explanation is the formation of small amounts of AN from the oxidation of the low organic nitrogen content, simultaneously with its consumption to give nitrates (Figure 32). This balance could also explain the ammonium ion irregular removal for S samples without added chloride (Figure 31 a and b). Similar results were found for total nitrogen (Figure 31, d to f), indicating that TN removal happens also by the indirect oxidation mediated by chlorine/hypochlorite species.

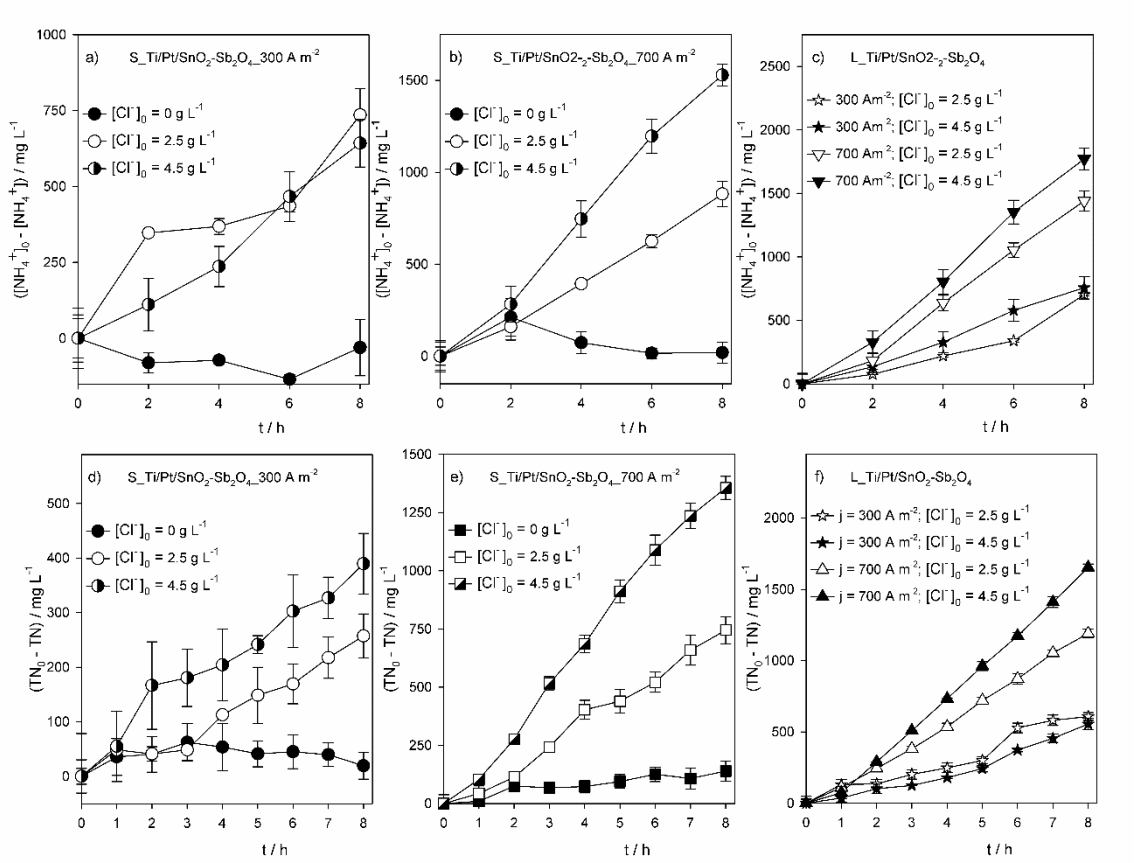

Figure 31. Variation with time of the ammonium ion (a,b,c) and total nitrogen (d,e,f) removed in the electrodegradation experiments performed with synthetic (S) and leachate (L) samples using Ti/Pt/SnO_2-Sb_2O_4 anode, at two applied current densities, 300 and 700 A m^{-2}, and different initial chloride contents.

For the S samples with initial addition of chloride and j=300 A m^{-2}, the influence of the initial amount of added chloride, 2.5 or 4.5 g L^{-1}, is very small in the ammonium ion removal (Figure 31 a) and on the nitrate formation (Figure 32 a), but significant on the TN removal (Figure 31 d). High TN removal was also described by Pérez *et al.* (2012), using a BDD anode, during the electrochemical oxidation of a landfill leachate. According to these authors, ammonium degradation takes place mainly due to the indirect oxidation through chlorine/hypochlorite, according to Eq. 12 and 13, being nitrogen gas the main ammonium oxidation product, leading to a removal in the TN content.

$$2/3\ NH_4^+ + HOCl \rightarrow 1/3\ N_2 + H_2O + 5/3\ H^+ + Cl^- \quad (12)$$

$$NH_4^+ + 4\ HOCl \rightarrow NO_3^- + H_2O + 6\ H^+ + 4\ Cl^- \quad (13)$$

Regarding the assays performed with L samples, an increase in j increases ammonium ion removal (Figure 31 c), TN removal (Figure 31 f) and nitrate formation (Figure 32 c). The effect of the increase in the chloride content is not so linear, being very small for nitrate formation and presenting a marked influence in the ammonium ion removal, in particular for the highest applied j, showing the effect of the indirect oxidation. On the other hand, in TN removal at higher j, an increase in the chloride content presents a very clear impact, showing the

importance of Eq. 12 in the process. For the lowest applied j, however, the increase in chloride content leads to a decrease in TN removal, probably due to lower active chlorine production at lower electrical current, or due to a competition with the organic matter, since at low j the increase in chloride content deeply influences the DOC removal rate (Figure 28 f).

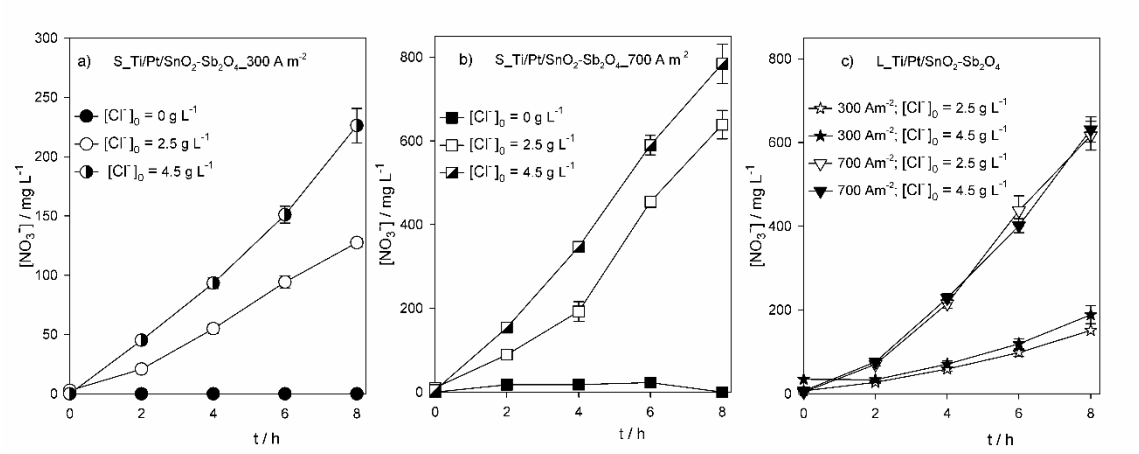

Figure 32. Variation with time of the nitrate concentration during the electrodegradation experiments performed with (a,b) synthetic, S, and (c) leachate, L, samples using Ti/Pt/SnO_2-Sb_2O_4 anode, at two applied current densities, 300 and 700 A m^{-2}, and different initial chloride contents.

In general, comparing the results obtained for L and S samples, it can be seen that the highest organic load removals were achieved with S samples, while the highest nitrogen removals were attained for L samples. These dissimilar results are probably due to the different composition of the samples, since in the S samples the humic acid was the single source of organic matter, whereas L samples contain a lot of different organic compounds, being some of them complex structures of humic substances and inorganic ions (Kang *et al.*, 2002), more resistant to oxidation than the humic acid itself.

To analyze the influence of the chloride concentration on the COD and ammonium ion removals, the variations of the COD removed *vs.* $[Cl^-]$/COD ratio and NH_4^+ removed *vs.* $[Cl^-]/[NH_4^+]$ (Figure 33) were plotted for the different experimental conditions tested. Regarding the influence of chloride concentration on the COD removal, it can be seen that the $[Cl^-]$/COD ratio remains almost constant, especially for the first hours of the assays, meaning that chlorine/hypochlorite resulting from the chloride ion oxidation is being consumed proportionally to the oxidation of the organic load and indirect oxidation through chlorine/hypochlorite is dominant. A different behavior is observed for the NH_4^+ removal, since in L samples an increase of the $[Cl^-]/[NH_4^+]$ ratio with time is found, whereas in S samples the plots show a general tendency for a decrease in time of this ratio. This behavior is consistent with the fact that NH_4^+ removal rate is higher for L samples than for S samples, being the COD removal rate depressed for L samples and NH_4^+ removal rate improved. This shows that indirect oxidation with chlorine/hypochlorite is even more important in the NH_4^+ elimination than in the COD removal and that increasing Cl^- initial concentration without using an adequate j may lead to higher $[Cl^-]$ in the final samples with only a small increase in the NH_4^+ removal.

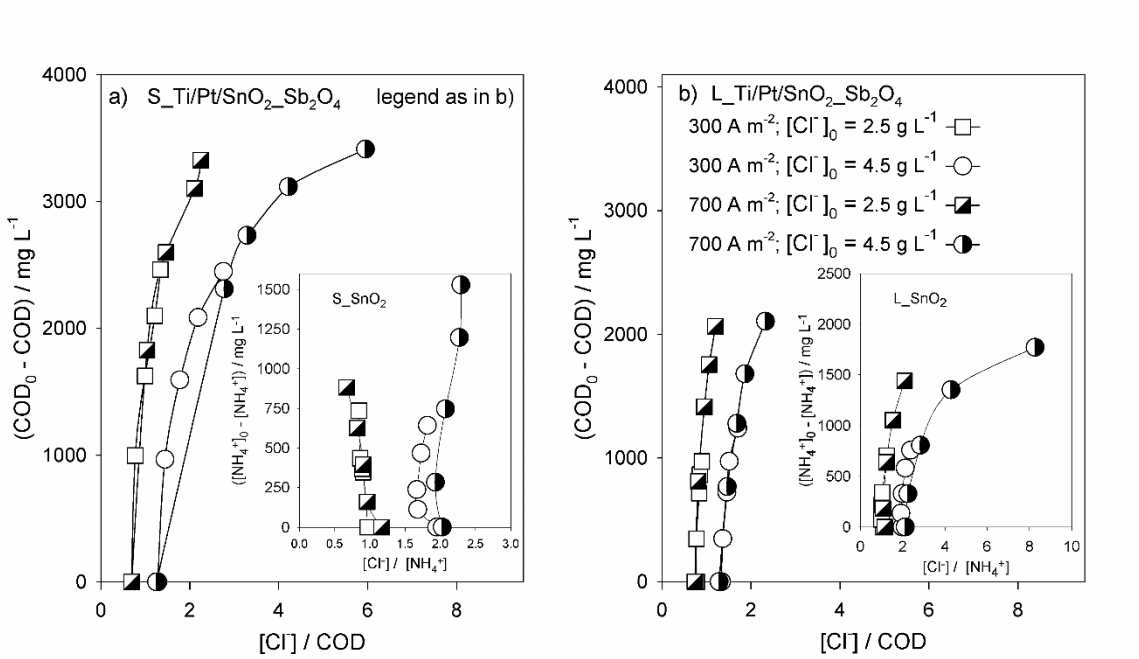

Figure 33. Variation of the removed COD *vs.* $[Cl^-]$/COD ratio (main plots) and of the removed ammonium ion *vs.* $[Cl^-]/[NH_4^+]$ ratio (insets), during the electrodegradation assays performed with (a) synthetic, S, and leachate, L, samples using Ti/Pt/SnO_2-Sb_2O_4 anode, at two applied current densities, 300 and 700 A m^{-2}, and different initial chloride contents.

To analyse the influence of the applied current density and chloride ion concentration on the leachate treatment energetic costs, the specific energy consumptions, E_{sp}, in W h $(g\ COD)^{-1}$, for the different assays performed with leachate samples were calculated, by means of Eq. 14, and are presented in Table 6. This Table also contains values from the literature for other two materials utilized with the same samples as those described in Table 4, and at identical experimental conditions.

$$E_{sp} = \frac{U\ I\ \Delta t}{3.6\ V\ \Delta COD} \quad (14)$$

where U is the cell voltage, in V, resulting from the applied current intensity I, in A, Δt is the duration of the electrolysis, in s, V is the volume of the solution in L and ΔCOD is the removed COD, in mg L^{-1}, during Δt. The lowest energy consumptions were achieved in assays performed at j = 300 A m^{-2} with $[Cl^-]_0$ = 4.5 g L^{-1}, and the highest consumptions were attained for j = 700 A m^{-2} and $[Cl^-]_0$ = 2.5 g L^{-1}. These results were expected since the increase in chloride ion concentration increases the electric conductivity of the sample, and consequently the cell voltage decreases. On the other hand, an increase in j leads to a decrease in current efficiency. Among the anode materials studied, PbO_2 showed the lowest energy consumptions for j = 300 A m^{-2} and $[Cl^-]_0$ = 4.5 g L^{-1}.

Regarding the possible leaching of heavy metals from the anode material, when metal oxide anodes are used, results from previous studies have shown that metal content in the electrolyzed solutions is negligible, either because anodes are mechanically stable (Ciríaco *et al.*, 2009) or the metal ions in samples are removed by cathodic reduction, during the electrodegradation assays (Fernandes *et al.*, 2014b).

Table 6. Values of the specific energy consumptions, E_{sp}, obtained for the leachate degradation assays, performed at different experimental conditions, and comparison with data from literature.

Current density / A m^{-2}	300		700		
$[Cl^-]_0$ / g L^{-1}	2.5	4.5	2.5	4.5	Ref.
Anode material	E_{sp} / Wh (g COD)$^{-1}$				
BDD	82	61	110	110	Fernandes *et al.*, 2016
Ti/Pt/PbO_2	77	52	125	89	Fernandes et al, 2016
Ti/Pt/SnO_2-Sb_2O_4	88	60	143	118	This work

4.5.4 Conclusions

Ti/Pt/SnO_2-Sb_2O_4 anode proved to be very effective in the electrooxidation of humic acid and sanitary landfill leachates, with a performance similar to that of BDD [Fernandes *et al.*, 2016]. Regarding the influence of chloride ion, both organic load and nitrogen removal rates increase with chloride ion concentration, although there is an optimum ratio between initial COD and chloride contents below which there is no further increase in the COD removal. The increase of current density has also a positive effect on the COD removal rate. The indirect oxidation through chlorine/hypochlorite is dominant on the electrooxidation process, being more relevant in leachate samples and for NH_4^+ elimination. However, depending on the applied current density, an increase in the Cl^- initial concentration may lead to higher $[Cl^-]$ in the final samples, without a significant increase in the COD and NH_4^+ removal.

The results obtained for L and S samples, regarding the removals of organic load and nitrogen, are not coincident, probably due to the different recalcitrance of both samples.

5. Conclusions

The main goal of this thesis was to search for an efficient tin and antimony mixed oxide to be utilized as anode and to find suitable and low-cost electrochemical solutions for oxygen evolution and degradation of organic pollutants, and refractory wastewaters. The above presented results show that this objective was achieved. In the next paragraphs this subject will be discussed in more detail.

Concluding remarks

To attain the main objectives, secondary goals were established and experimental work was developed to achieve the proposed objectives. In the presentation of the experimental results the main conclusions were already drawn for each of the different studies performed. Based on those conclusions, an evaluation of the obtained results according to the proposed objectives is presented in this chapter.

First objective: To prepare tin and antimony mixed oxides materials that are structural, chemical, mechanical and electrochemically stables.

This goal was accomplished, and five different new materials were prepared by two different preparation methods. Two different Sn-Sb mixed oxides were prepared, over a Ti/Pt and Ti/Cu ,substrate, by the alternate electrodeposition technique, Ti/Pt/SnO_2-Sb_2O_4 and Ti/Cu/SnO_2-Sb_2O_3. To obtain thinner and uniform films, Sn-Sb oxide materials were prepared using the simultaneous deposition of the metals over several different substrates, namely Ti, Ti/Pt and Ti/Cu, to obtain the anodes Ti/SnO_2-Sb, Ti/Pt/SnO_2-Sb and Ti/Cu/SnO_2-Sb. All the mixed oxides prepared were structural, morphological and electrochemically characterized by, respectively, XRD, SEM and CV.
In the simultaneous electrodeposition only one oxide phase was identified, SnO_2, being the antimony present in an intermetallic SbSn phase; in the alternate deposition, two oxide phases are obtained, SnO_2 and Sb_2O_4 or Sb_2O_3.
The introduction of a Pt or Cu interlayer increased surface's roughness, particularly in the case of the Pt layer, being the highest relative roughness presented by Ti/Pt/SnO_2-Sb. Apparently, relative roughness depends on the substrate morphology, as well as on the electrodeposition process and probably also on the film thickness. However, it is difficult to show a linear correlation between preparation method and roughness.

Second objective: To obtain tin and antimony mixed oxides materials with extended lifetime, suitable to be used in the degradation of organic pollutants or in the oxygen evolution reactions.

This goal was accomplished. Regarding the lifetime of anodes, the electrodes with platinium interlayer have the best performance. The lifetime of the anodes prepared without interlayer is shorter when compared with that of Ti/Pt/SnO_2-Sb_2O_4 and Ti/Pt/SnO_2-Sb. However the materials without a Pt interlayer are the best for direct oxidation of pollutants, as they present the largest potential window for oxygen evolution.

From the prepared oxides, those with a copper interlayer presented the lowest potentials for oxygen evolution, being the most appropriate for oxygen production. On the other hand, they are less stable towards oxidative potentials, being unsuitable as anodes for the electrodegradation of organic pollutants. In fact, in the presence of sulfate, the copper layer oxidizes, resulting in the formation of copper sulfate.

The roughness deeply influences the oxygen evolution reaction since for equal substrate and interlayer, the material with higher roughness factor (Ti/Pt/SnO_2-Sb prepared over a Pt interlayer) presents lower apparent activation energy, probably because the higher specific surface favors adsorption and facilitates the rate determining step.

Third objective: To find correlations between the preparation method and the abilities of the prepared material for the different possible applications, namely degradation of organic pollutants or oxygen evolution reactions.

Apparently, the correlation between the preparation method and the oxidizing abilities of the prepared material lies essentially on the existence or not of an interlayer and on the type of interlayer, since:

- The inexistence of an interlayer between the titanium plate and the mixed oxide layer promotes the formation of a passivating TiO_2 film that deeply reduces the lifetime of the electrode;
- A copper interlayer is not appropriate for the utilization of the electrode at high potentials, since copper oxidizes and disables the electrode;
- A platinum interlayer confers extended lifetime to the electrode, but reduces the electrodegradation rate of organic compounds, due to the platinum catalytic effect that promotes the reaction at the electrode's surface, reducing the ability of the hydroxyl radicals for indirect oxidation.

Fourth objective: To find, among all the prepared materials which is the most appropriate to be used as anode in the degradation of different types of pollutants.

From the discussion presented above, the most suitable materials to be used as anode in the degradation of organic pollutants are those with a platinum interlayer. In fact, although they have a more expensive preparation, due to the platinization, they present an outstanding service lifetime, with oxidation abilities similar to those presented by boron-doped diamond and lead oxide. Moreover, this electrode material, along with Ti/Pt/PbO_2, presents higher ability for nitrogen elimination as gaseous forms and lower energy consumption than BDD, even in the treatment of sanitary landfill leachates and humic substances.

Future trends

Electrodes with platinium interlayer have proved to be electrochemical and mechanically stable. However, the introduction of a Pt layer increases their cost. Thus, to reduce the preparation costs, Pt must be substituted by a cheaper metal that also avoids the formation of an insulating TiO_2 interlayer. Thus, other substrates, such as titanium nanotubes, carbon nanotubes, niobium, should be tested.

References

Abbas, A.; Jingsong, G.; Ping, L.; Ya, P.; Al-Rebaki, W.; Review on Landfill Leachate Treatments; Journal of Applied Sciences Research (2009); 5; 534.

Amjoud, M.; Maury, F.; Soukane, S.; Duverneuil, P.; Making of specific electrodes by CVD; Surface and Coatings Technology (1998); 100-101; 169.

Andrade, L.; Rocha-Filho, R.; Bocchi, N.; Biaggio, S.; Study of the effect of precursor salts on the electrocatalytic properties of Ti-SnO_2/Sb electrodes prepared by thermal decomposition; Quimica Nova (2004); 27; 866.

Andrade, L.; Rutuolo, L.; Rocha-Filho, R.; Bocchi, N.; Biaggio, B.; Iniesta, J.; Garcia-Garcia, V.; Montiel, V.; On the performance of Fe and Fe, F doped Ti–Pt/PbO_2 electrodes in the electrooxidation of the Blue Reactive 19 dye in simulated textile wastewater; Chemosphere (2007); 66; 2035.

Anglada, A.; Urtiaga, A.; Ortiz, I.; Pilot scale performance of the electro-oxidation of landfill leachate at boron-doped diamond anodes; Environmental science and technology (2009); 43; 2035.

Anglada, A.; Ortiz, D.; Urtiaga, A.; Ortiz, I.; Electrochemical oxidation of landfill leachates at pilot scale: evaluation of energy needs; Water Science and Technology (2010a); 61; 2211.

Anglada, A.; Urtiaga, A.; Ortiz, I.; Laboratory and pilot plant scale study on the electrochemical oxidation of landfill leachate; Journal of Hazardous Materials (2010b); 181; 729.

Anglada, A.; Urtiaga, A.; Ortiz, I.; Mantzavinos, D.; Diamadopoulos, E.; Boron-doped diamond anodic treatment of landfill leachate: evaluation of operating variables and formation of oxidation by-products; Water Research (2011); 45; 828.

Armenta-Armenta, M. and Diaz, A.; Oxidation of benzoic acid by electrochemically generated Ce (IV); Environmental Science and Technology (2005); 39; 5872.

Barrocas, B.; Monteiro, O.; Melo Jorge, M. E.; Sério, S.; Photocatalytic activity and reusability study of nanocrystalline films TiO_2 prepared by sputtering technique; Applied Surface Science (2013); 264; 111.

Bartlett, P.; Dunford, T.; Ghanem, M.; Templated electrochemical deposition of nanostructured macroporous PbO_2; Journal of Materials Chemistry (2002); 12; 3130.

Bashir, M.; Isa, M.; Kutty, S.; Awang, Z.; Aziz, H.; Mohajeri, S.; Farooqi, I.; Landfill leachate treatment by electrochemical oxidation; Waste Management (2009); 29; 2534.

Berenguer, R.; Quijada, C.; Morallón, E.; Electrochemical characterization of SnO_2 electrodes doped with Ru and Pt; Electrochimica Acta (2009); 54; 5230.

Bhalla, B.; Saini, M. S.; Jha, M. K.; Effect of age and seasonal variations on leachate characteristics of municipal solid waste landfill; International Journal of Engineering Research and Technology (2013); 2; 223.

Boxall, A.; Kolpin, D.; Halling-Sorensen, B.; Tolls, J.; Peer reviewed: are veterinary medicines causing environmental risks? Environmental Science and Technology (2003); 37; 287A.

Brillas, E.; Garcia-Segura, S.; Skoumal, M.; Arias, C.; Electrochemical incineration of diclofenac in neutral aqueous medium by anodic oxidation using Pt and boron-doped diamond anodes; Chemosphere (2010); 79; 605.

Brillas, E.; Martínez-Huitle, C. A.; Decontamination of wastewaters containing synthetic organic dyes by electrochemical methods. An updated review; Applied Catalysis B: Environmental (2015); 166; 603.

Cabeza, A.; Urtiaga, A.; Rivero, M.; Ortiz, I.; Ammonium removal from landfill leachate by anodic oxidation; Journal of Hazardous Materials (2007a); 144; 715-719.

Cabeza, A.; Urtiaga, A.; Ortiz, I.; Electrochemical treatment of landfill leachates using a boron-doped diamond anode; Industrial & Engineering Chemistry Research (2007b); 46; 1439.

Canevari, T.; Vinhas, R.; Landers, R.; Gushikem, Y.; $SiO_2/SnO_2/Sb_2O_5$ microporous ceramic material for immobilization of Meldola's blue: Application as an electrochemical sensor for NADH; Biosensors and Bioelectronics (2011); 26; 2402.

Chaplin, B.; Critical review of electrochemical advanced oxidation processes for water treatment applications; Environmental Science: Processes and Impacts, (2014), 16, 1182.
Chen, G.; Electrochemical technologies in wastewater treatment; Separation and Purification Technology (2004) 38; 11.

Chen, X.; Chen, G.; Gao, F.; High-performance Ti/BDD electrodes for pollutant oxidation; Environmental Science and Technology (2003); 37; 5021.

Chen, X.; Gao, F.; Chen, G.; Comparison of Ti/BDD and Ti/SnO_2–Sb_2O_5 electrodes for pollutant oxidation; Journal of Applied Electrochemistry (2005); 35; 185.

Chen, Y.; Hong, L.; Xue, H.; Han, W.; Wang, L.; Sun, X.; Li, J.; Preparation and characterization of TiO_2-NTs/SnO_2-Sb electrodes by electrodeposition; Journal of Electroanalytical Chemistry (2010a); 648; 119.

Chen, X.; Liang, J.; Zhou, Z.; Duan, H.; Li, B.; Yang, Q.; The preparation of SnO_2 film by electrodeposition; Materials Research Bulletin (2010b); 45; 2006.

Chernaya, V.; Mitiaev, A.; Chizhov, P.; Dikarev, E.; Shpanchenko, R.; Antipov, E.; Korolenko, M.; Fabritchnyi, P.; Synthesis and investigation of Tin (II) pyrophosphate $Sn_2P_2O_7$; Chemistry of Materials (2005) 17; 284.

Chiang, L.; Chang, J.; Wen, T.; Indirect oxidation effect in electrochemical oxidation treatment of landfill leachate; Water Research (1995); 29; 671-678.

Chopra, I.; Roberts, M.; Tetracycline antibiotics: mode of action, applications, molecular biology, and epidemiology of bacterial resistance; Microbiology and Molecular Biology Reviews (2001) 65; 232.

Ciríaco, L.; Anjo, C.; Correia, J.; Pacheco, M. J.; Lopes, A.; Electrochemical degradation of ibuprofen on Ti/Pt/PbO_2 and Si/BDD electrodes Electrochimica Acta (2009) 54; 1464.

Ciríaco, L; Santos, D.; Pacheco, M. J.; Lopes, A.; Anodic oxidation of organic pollutants on a Ti/SnO_2–Sb_2O_4 anode; Journal of Applied Electrochemistry (2011); 41; 577.

Comninellis, C. and Chen,G.; "Electrochemistry for the environment";1st edition; Springer; London; 2010.

Comninellis, Ch. and Nerini, A.; Anodic oxidation of phenol in the presence of NaCl for wastewater treatment; Journal of Applied Electrochemistry (1995); 25; 23.

Comninellis, Ch. and Pulgarin, C.; Electrochemical oxidation of phenol for wastewater treatment using SnO_2 anodes; Journal of Applied Electrochemistry (1993); 23; 108.

Comninellis, Ch.; Electrocatalysis in the electrochemical conversion/combustion of organic pollutants for waste water treatment; Electrochimica Acta (1994); 39; 1857.

Comninellis, Ch.; Electrochemical treatment of waste water containing phenol; Institution of Chemical Engineers Symposium (1992); 70; 219.

Cossu, R.; Polcaro, A.; Lavagnolo, M.; Mascia, M.; Palmas, S.; Renoldi, F.; Electrochemical Treatment of Landfill Leachate: Oxidation at Ti/PbO_2 and Ti/SnO_2 anodes; Environmental Science and Technology (1998); 32; 3570.

Duverneuil, P.; Maury, F.; Pebere. N.; Senocq, F.; Vergnes H.; Chemical vapor deposition of SnO_2 coatings on Ti plates for the preparation of electrocatalytic anodes; Surface and Coatings Technology (2002); 151 –152; 9.

Eaton, A.; Clesceri, L.; Rice, E.; Greenberg, A.; Franson, M. A.; Standard Methods for Examination of Water and Wastewater, twenty-first ed., American Public Health Association, Washington, DC, 2005.

Eggen, T.; Moeder, M.; Arukwe, A.; Municipal landfill leachates: a significant source for new and emerging pollutants; Science of the Total Environment (2010); 408; 5147.

Feki, F.; Aloui, F.; Feki, M.; Sayadi, S.; Electrochemical oxidation post-treatment of landfill leachates treated with membrane bioreactor Chemosphere (2009); 75; 256.

Feng, Y.; Cui, Y.; Liu, J.; Logan, B.; Factors affecting the electro-catalytic characteristics of Eu doped SnO_2/Sb electrode; Journal of Hazardous Materials; (2010); 178; 29.

Fernandes, A.; Catalão, E.; Pacheco, M. J.; Ciríaco, L.; Lopes, A., Electrochemical treatment of leachates from sanitary landfills; Journal of Electrochemical Science and Engineering (2013) 3; 125.

Fernandes, A.; Pacheco, M. J.; Ciríaco, L.; Lopes, A.; Anodic oxidation of a biologically treated leachate on a boron-doped diamond anode; Journal of Hazardous Materials (2012); 199-200; 82.

Fernandes, A.; Electrochemical treatment of sanitary landfill leachates; Ph.D. thesis; UBI; Covilhã (2014).

Fernandes, A.; Santos, D.; Pacheco, M. J.; Ciríaco, L.; Lopes, A.; Nitrogen and organic load removal from sanitary landfill leachates by anodic oxidation at Ti/Pt/PbO_2, Ti/Pt/SnO_2-Sb_2O_4 and Si/BDD; Applied Catalysis B: Environmental (2014a); 148–149; 288.

Fernandes, A.; Spranger, P.; Fonseca, A. D.; Pacheco, M. J.; Ciríaco, L.; Lopes, A.; Effect of electrochemical treatments on the biodegradability of sanitary landfill leachates; Applied Catalysis B: Environmental (2014b); 144; 514.

Fernandes, A.; Pacheco, M. J.; Ciríaco, L.; Lopes, A.; Review on the electrochemical processes for the treatment of sanitary landfill leachates: Present and future; Applied Catalysis B: Environmental (2015); 176–177; 183.

Fernandes, A.; Santos, D.; Pacheco, M. J.; Ciríaco, L.; Lopes, A.; Electrochemical oxidation of humic acid and sanitary landfill leachate: Influence of anode material, chloride concentration and current density; Science of the Total Environment (2016); 541; 282.

Foo, K. Y.; Hameed, B. H.; An overview of landfill leachate treatment via activated carbon adsorption process; Journal of Hazard Materials (2009); 171; 54.

Fryda, M.; Herrmann, D.; Schäfer, L.; Klages, C. P.; Perret, A.; Haenni, W.; Comninellis, C.; Gandini, D.; Properties of diamond electrodes for wastewater treatment; New Diamond and Frontier Carbon Technology (1999); 9; 229.

Hibino, T. and Kobayashi, K.; Intermediate-temperature alkaline fuel cells with non-platinum electrodes; Journal of Materials Chemistry A (2013); 1; 7019.

Hirsch, R.; Ternes, T.; Haberer, K.; Kratz, K.; Occurrence of antibiotics in the aquatic environment; Science of The Total Environment (1999); 225; 109.

Huang, S.; Zhao, G.; Li, H.; High quality Sb-doped SnO_2 electrodes with high oxygen evolution potential prepared by in situ hydrothermal synthesis method; Chinese Chemical Letters (2007); 18; 997.

Johnson, D. C.; Feng, J.; Houk, L. L.; Direct electrochemical degradation of organic wastes in aqueous media; Electrochimica Acta (2000); 46; 323.

Kang, K. H.; Shin, H. S.; Park, H.; Characterization of humic substances present in landfill leachates with different landfill ages and its implications; Water Research (2002); 36; 4023.

Kelly, P. J.; Arnell, R. D.; Magnetron sputtering: a review of recent developments and applications; Vacuum (2000); 56; 159.

Kibria, A. and Tarafdar, S.; Electrochemical studies of a nickel–copper electrode for the oxygen evolution reaction (OER); International Journal of Hydrogen Energy (2002); 27; 879.

Kolpin, D.; Furlong, E.; Meyer, M.; Thurman, E.; Zaugg, S.; Barber, L.; Buxton, H.; Pharmaceuticals, hormones, and other organic wastewater contaminants in US streams, 1999-2000: A national reconnaissance; Environmental Science and Technology (2002); 36; 1202.

Kong, J.; Shi, S.; Zhu, X.; Ni, J.; Effect of Sb dopant amount on the structure and electrocatalytic capability of Ti/Sb-SnO_2 electrodes in the oxidation of 4-chlorophenol; Journal of Environmental Sciences (2007); 19; 1380.

Kümmerer, K.; The presence of pharmaceuticals in the environment due to human use–present knowledge and future challenges; Journal of Environmental Management (2009); 90; 2354.

Lan, Z.; Liu, L.; Huang, M.; Wu, J; Lin, J.; Preparation of nano-flower-like SnO2 particles and their applications in efficient CdS quantum dots sensitized solar cells; Journal of Materials Science: Materials in Electronics (2015); 26; 7914.

Lassali, T.; Boodts, J.; Bulhões, L.; Charging processes and electrocatalytic properties of $IrO_2/TiO_2/SnO_2$ oxide films investigated by in situ AC impedance measurements; Electrochimica Acta (1999); 44; 4203.

Liu, J. F.; Feng, Y. J.; Investigation on the electrocatalytic characteristics of SnO_2 electrodes with nanocoating prepared by electrodeposition method; Science in China Series E: Technological Sciences (2009); 52; 1799.

Lyons, M.; Brandon, M.; The oxygen evolution reaction on passive oxide covered transition metal electrodes in aqueous alkaline solution. Part 1-Nickel; International Journal of Electrochemical Science (2008); 3; 1386.

Maharana, D.; Xu, Z.; Niu, J.; Rao, N.; Electrochemical oxidation of 2,4,5-trichlorophenoxyacetic acid by metal-oxide-coated Ti electrodes; Chemosphere (2015); 136; 145.

Martinez, J. L.; Environmental pollution by antibiotics and by antibiotic resistance determinants; Environmental Pollution (2009); 157; 2893.

Martínez-Huitle, C. A.; Andrade, L. S.; Electrocatalysis in wastewater treatment: recent mechanism advances; Quimica Nova (2011); 34; 850.

Martínez-Huitle, C. A.; Ferro, S.; Battisti, A.; Electrochemical incineration of oxalic acid: Role of electrode material; Electrochimica Acta (2004); 49; 4027.

Montilla, F.; Morallón, E.; Battisti, A.; Vázquez, J.; Preparation and characterization of antimony-doped tin dioxide electrodes. Part 1. Electrochemical characterization; Journal of Physical Chemistry B (2004); 108; 5036.

Moraes, P.; Bertazzoli, R.; Electrodegradation of landfill leachate in a flow electrochemical reactor; Chemosphere (2005); 58; 41.

Mueller, F.; Bresser, D.; Chakravadhanula, V.; Passerini, S.; Fe-doped SnO_2 nanoparticles as new high capacity anode material for secondary lithium-ion batteries; Journal of Power Sources (2015); 299; 398.

Musiani, M.; Furlanetto, F.; Guerriero, P.; Electrochemical deposition and properties of $Pb0_2$ + $C0_3O_4$ composites; Journal of Electroanalytical Chemistry (1997); 440; 131.

Öman, C.; Junestedt, C.; Chemical characterization of landfill leachates–400 parameters and compounds; Waste Management (2008); 28; 1876.

Pacheco, M. J.; Morão, A.; Lopes, A.; Ciríaco, L.; Gonçalves, I.; Degradation of phenols using boron-doped diamond electrodes: a method for quantifying the extent of combustion; Electrochimica Acta (2007); 53; 629.

Panizza, M.; Michaud, P.; Cerisola, G.; Comninellis, C.; Anodic oxidation of 2-naphthol at boron-doped diamond electrodes; Journal of Electroanalytical Chemistry (2001); 507; 206.

Panizza, M. and Cerisola, G.; Influence of anode material on the electrochemical oxidation of 2-naphthol: Part 2. Bulk electrolysis experiments; Electrochimica Acta (2004); 49; 3221–3226.

Panizza, M. and Cerisola, G.; Application of diamond electrodes to electrochemical processes; Electrochimica Acta (2005); 51; 191.

Panizza, M. and Cerisola, G.; Direct and Mediated Anodic Oxidation of Organic Pollutants; Chemical Reviews (2009); 109; 6541.

Panizza, M.; Delucchi, M.; Sirés, I.; Electrochemical process for the treatment of landfill leachate; Journal of Applied Electrochemistry (2010); 40; 1721.

Panizza, M.; Martinez-Huitle, C.; Role of electrode materials for the anodic oxidation of a real landfill leachate–Comparison between Ti–Ru–Sn ternary oxide, PbO_2 and boron-doped diamond anode; Chemosphere (2013); 90; 1455.

Pérez, G.; Saiz, J.; Ibañez, R.; Urtiaga, A.; Ortiz, I.; Assessment of the formation of inorganic oxidation by-products during the electrocatalytic treatment of ammonium from landfill leachates; Water Research (2012); 46; 2579.

Polcaro, A. M.; Palmas, S.; Renoldi, F.; On the performance of Ti/SnO_2 and Ti/PbO_2 anodesin electrochemical degradation of 2-chlorophenolfor wastewater treatment; Journal of Applied Electrochemistry (1999); 29; 147.

Pulgarin, C.; Adler, N.; Péringer, P.; Electrochemical detoxification of a 1,4-benzoquinone solution in wastewater treatment; Water Research (1994); 28; 887.

Rao, A., Venkatarangaiah, V.; Metal oxide-coated anodes in wastewater treatment; Environmental Science and Pollution Research (2014); 21; 3197.

Río, A.; Molina, J.; Bonastre, J.; Cases, F.; Study of the electrochemical oxidation and reduction of CI Reactive Orange 4 in sodium sulphate alkaline solutions; Journal of Hazardous Materials (2009); 172; 187.

Rodgers, J. D.; Jedral, W.; Bunce, N. J.; Electrochemical oxidation of chlorinated phenols; Environmental Science and Technology (1999); 33; 1453.

Sakka, S.; "Handbook of sol-gel science and technology"; 1st edition; Springer; Osaka; 2005.

Santos, D.; Lopes, A.; Pacheco, M. J.; Gomes, A.; Ciríaco, L.; Preparation of Ti/Pt/SnO_2–Sb_2O_4 electrodes for anodic oxidation of pharmaceutical drugs; Journal of Applied Electrochemistry (2013); 43; 407.

Santos, D.; Lopes, A.; Pacheco, M. J.; Gomes, A.; Ciríaco, L.; The Oxygen Evolution Reaction at Sn-Sb Oxide Anodes: Influence of the Oxide Preparation Mode; Journal of The Electrochemical Society (2014a); 161; H564.

Santos, D.; Daniane, A.; Pacheco, M. J.; Ciríaco, L.; Lopes, A.; Environmental applications of Ti/Pt/SnO_2-Sb electrodes: Diclofenac anodic oxidation; Abstracts Book; Istanbul (2014b); EuCheMs.

Sirés, I.; Brillas, E.; Remediation of water pollution caused by pharmaceutical residues based on electrochemical separation and degradation technologies: a review; Environment International (2012); 40; 212.

Sirés, E.; Brillas, E.; Oturan, M.; Rodrigo, M; Panizza, M.; Electrochemical advanced oxidation processes: today and tomorrow. A review; Environmental Science and Pollution Research (2014); 21; 8336.

Song, S.; Zhan, L.; He, Z.; Mechanism of the anodic oxidation of 4-chloro-3-methyl phenol in aqueous solution using Ti/SnO_2–Sb/PbO_2 electrodes; Journal of Hazardous Materials (2010); 175; 14.

Stucki, S.; Kötz, R., Carcer, B.; Electrochemical waste water treatment using high overvoltage anodes. Part I: Physical and electrochemical properties of SnO_2 anodes; Journal of Applied Electrochemistry (1991a); 21; 99.

Stucki, S.; Kötz, R.; Carcer, B.; Electrochemical waste water treatment using high overvoltage anodes Part II: Anode performance and applications; Journal of Applied Electrochemistry (1991b); 21; 14.

Suffredini, H.; Machado, S.; Avaca, L.; The water decomposition reactions on boron-doped diamond electrodes; Journal of the Brazilian Chemical Society (2004); 15; 16.

Turro, E.; Giannis, A.; Cossu, R.; Gidarakos, E.; Mantzavinos, D.; Katsaounis, A.; Electrochemical oxidation of stabilized landfill leachate on DSA electrodes; Journal of Hazardous Materials (2011); 190; 460.

Urtiaga, A.; Rueda, A.; Anglada, A.; Ortiz, I.; Integrated treatment of landfill leachates including electrooxidation at pilot plant scale; Journal of Hazardous Materials (2009); 166; 1530.

Urtiaga, A.; Ortiz, I.; Mantzavinos, D.; Diamadopoulos; Kinetic modeling of the electrochemical removal of ammonium and COD from landfill leachates; Journal of Applied Electrochemistry (2012); 42; 779.

Villullas, H.; Mattos-Costa, F.; Bulhões, L.; Oxygen evolution on platinum modified Ti/RuO_2 sol–gel films; Journal of Electroanalytical Chemistry (2003); 545; 89.

Watts, R.; Wyeth, M.; Finn, D.; Teel, A.; Optimization of Ti/SnO_2–Sb_2O_5 anode preparation for electrochemical oxidation of organic contaminants in water and wastewater; Journal of Applied Electrochemistry (2008); 38; 31.

Wiberg, G.; Arenz, M.; Establishing the potential dependent equilibrium oxide coverage on platinum in alkaline solution and its influence on the oxygen reduction; Journal of Power Sources (2012); 217; 262.

Woisetschläger, D.; Humpl, B.; Koncar, M.; Siebenhofer, M.; Electrochemical oxidation of wastewater – opportunities and drawbacks; Water Science & Technology (2013); 65; 1173.

Wu, H.; Ruan, Q.; Li, L.; Wang, B.; Characterization and electrocatalytic properties of titanium-based $Ru_{0.3}Co_{0.7-x}Ce_x$ mixed oxide electrodes for oxygen evolution in alkaline solution; Journal of Nanomaterials (2011); doi:10.1155/2011/439162.

Wu, M.; Zhang, L.; Wang, D.; Xiao, C.; Zhang, S.; Cathodic deposition and characterization of tin oxide coatings on graphite for electrochemical supercapacitors; Journal of Power Sources (2008); 175; 669.

Wu, W.; Huang, Z.; Lim, T.; Recent development of mixed metal oxide anodes for electrochemical oxidation of organic pollutants in water; Applied Catalysis A: General (2014); 480; 58.

Xu, J.; Li, Q.; Hansen, M.; Christensen, E.; García, A.; Liu, G.; Wanga, X.; Bjerrum, N.; Antimony doped tin oxides and their composites with tin pyrophosphates as catalyst supports for oxygen evolution reaction in proton exchange membrane water electrolysis; International Journal of Hydrogen Energy (2012); 37; 18629.

Yang, X.; Zou, R.; Huo, F.; Preparation and characterization of Ti/SnO_2–Sb_2O_3–Nb_2O_5/PbO_2 thin film as electrode material for the degradation of phenol; Journal of Hazardous Materials (2009); 164; 367.

Yao, P.; Chen, X.; Wu, H.; Wang, D.; Active Ti/SnO2 anodes for pollutants oxidation prepared using chemical vapor deposition; Surface and Coatings Technology (2008); 202; 3850.

Yusta, F.; Hitchman, M.; Shamlian, S.; CVD preparation and characterization of tin dioxide ®lms for electrochemical applications; Journal of Materials Chemistry (1997); 7; 1421.

Zanta, C.; Michaud, P. A.; Comninellis, Ch.; Andrade, A.; Boodts, J.; Electrochemical oxidation of p-chlorophenol on SnO_2–Sb_2O_5 based anodes for wastewater treatment; Journal of Applied Electrochemistry (2003); 33; 1211.

Zhang, H.; Li, Y.; Wu, X.; Zhang, Y.; Zhang, D.; Application of response surface methodology to the treatment landfill leachate in a three-dimensional electrochemical reactor. Waste Management (2010); 30; 2096.

Zhang, H.; Ran, X.; Wu; X.; Zhang, D.; Evaluation of electro-oxidation of biologically treated landfill leachate using response surface methodology; Journal of Hazardous Materials (2011); 188; 261.

Zhang, L.; Xu, L.; He, J.; Zhang, J.; Preparation of Ti/SnO_2-Sb electrodes modified by carbon nanotube for anodic oxidation of dye wastewater and combination with nanofiltration; Electrochimica Acta (2014); 117; 192.

Zhao, G.; Pang, Y.; Liu, L.; Gao, J.; Lv, B.; Highly efficient and energy-saving sectional treatment of landfill leachate with a synergistic system of biochemical treatment and electrochemical oxidation on a boron-doped diamond electrode; Journal of Hazardous Materials (2010); 179; 1078.

Zheng, Y.; Su, W.; Chen, S.; Wu, X.; Chen, X.; Ti/SnO_2–Sb_2O_5–RuO_2/α-PbO_2/ß-PbO_2 electrodes for pollutants degradation; Chemical Engineering Journal (2011); 174; 304.